Department of Cell Biology, Utrecht University

Critical regulation of microtubule density by CLASP during interphase

Depleting microtubules: How low can we go?

Misko Bobeldijk

Major research internship report

Master's Program 'Molecular and Cellular Life Sciences'

Supervisor:
Prof. Dr. A.S. Akhmanova

Daily Supervisor:
Dipti Rai

November 2021

Abstract

Microtubules are indispensable components of the cellular cytoskeleton, responsible for maintaining cellular integrity. They are polar structures that form through the polymerization of αβ-tubulin heterodimers. On its own, spontaneous nucleation of microtubules is energetically unfavorable. Despite this, molecular factors like the gamma-tubulin ring complex (γ-TuRC) can promote nucleation. Following their nucleation, microtubules are inherently unstable, constantly fluctuating between phases of growth and shrinkage, termed dynamic instability. An extensive group of regulatory proteins modulates this dynamic instability and collectively form the microtubule-associated proteins (MAPs). This regulation is required for an array of microtubule-based processes, such as, microtubule-based transport, cell division, and the organization of intracellular machinery throughout the cytosol. One such regulatory MAP, Cytoplasmic-linker-associated proteins (CLASPs) inhibit catastrophe and stabilize microtubules at their growing ends, tether and stabilize free microtubule ends at the Golgi, promote microtubule nucleation at the Golgi, and repair damaged microtubules by incorporating new tubulin heterodimers at damaged-sites. Here, we present CLASP as a more robust regulator of the microtubule network in cells than a microtubule polymerase like chTOG. We show that retinal pigment epithelial cells (RPE1) thoroughly depleted of CLASPs have severe reductions in microtubule density and organization. Microtubules in these cells grow slightly faster and have decreased catastrophe frequencies, likely owing to a higher pool of free tubulin and a stable remaining population of microtubules. Furthermore, we report that microtubule nucleation from the Golgi and cytosol are perturbed almost wholly, whereas centrosomal-based microtubule nucleation is reduced in the absence of CLASPs. Moreover, we show a substantial reduction in γ-TuRC, NEDD1, and Ninein, but not Pericentrin, CEP152, CEP192, and CDK5RAP2 localization to the centrosome, yet this does not translate to the robust decrease in microtubule density we observe in the absence of CLASPs. We also present a p53 knock-out based strategy that intriguingly improves the viability of microtubule scarce cells. Removing the centrosome in cells lacking CLASPs reduced the microtubule density even further, which to our knowledge has not been observed before, revealing a critical threshold of microtubule density required for the proper organization and distribution of organelles throughout the cell.

Introduction

Dynamic instability of microtubules

Eukaryotic cells depend on a complex interconnected network of biopolymers and regulatory proteins, called the cytoskeleton, for keeping their cellular integrity (Pegoraro *et al.*, 2017). The cytoskeleton structure helps cells keep their shape, transport intracellular cargo, resist mechanical stress, and allows cell division and movement. (Fletcher & Mullins, 2010; Pegoraro *et al.*, 2017; Logan & Menko, 2019). Microtubules are an indispensable part of this cytoskeleton (Fletcher & Mullins, 2010; Pegoraro *et al.*, 2017). These microtubules are hollow, cylindrical, and polarized structures that form through the polymerization of GTP-bound αβ-tubulin heterodimers (Logan & Menko, 2019; Akhmanova & Steinmetz, 2015). The hydrolyzation of these polymerized, GTP-bound tubulin dimers occurs with a delay, causing a stable GTP-cap to form on the microtubule growing end. Unlike the stabilized growing end, the microtubule lattice usually is GDP-bound, and therefore, it is fundamentally unstable (Wade, 2009; Akhmanova & Steinmetz, 2015; Koning, 2010). Consequently, loss of the stable GTP-cap would switch the microtubule into a state of rapid depolymerization, termed 'catastrophe.' Therefore, microtubules are inherently unstable, constantly fluctuating between phases of growth and shrinkage – a phenomenon termed dynamic instability (**Fig. 1**) (Desai & Mitchison, 1997; Lawrence & Zanic, 2019).

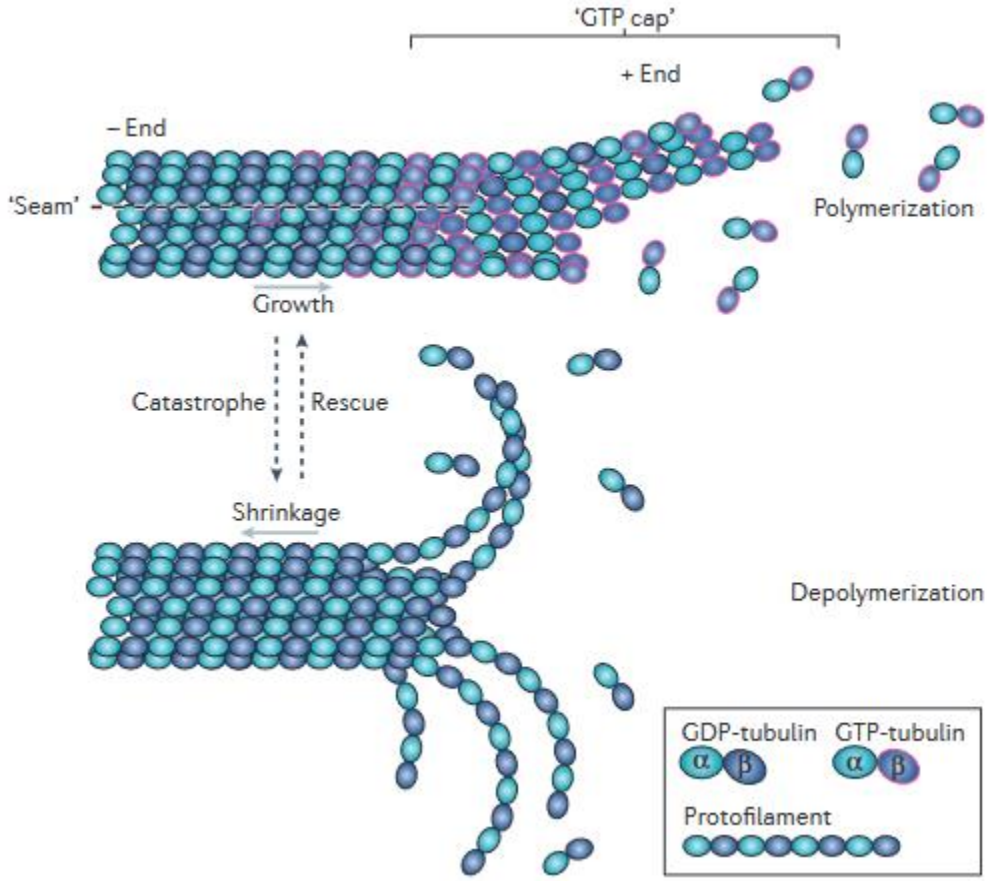

Figure 1. Microtubule dynamic instability. *Schematic overview of dynamic instability. Microtubules continuously fluctuate between events of growth and shrinkage. Microtubules grow by rapidly adding soluble αβ-tubulin dimers at the microtubule plus-end, which is stabilized by a stable GTP-cap. Loss of this stable cap would switch the microtubule into a state of rapid depolymerization, called catastrophe. Transitioning back from shrinkage to a phase of growth is called a rescue. Taken from Roostalu & Surrey, 2017.*

Microtubule nucleation in the cell

Microtubules are polar protein filaments due to the orientation of their αβ-tubulin heterodimers, where β-tubulin is exposed at the plus-end of the microtubule and α-tubulin is exposed at the minus-end of the microtubule (Roostalu & Surrey, 2017). Free tubulin heterodimers are quickly integrated at the plus-end of microtubules, whereas they are more slowly integrated at the minus-end (**Fig. 1**). Therefore, free minus-ends grow slower than plus-ends. Almost all the microtubules in mammalian cells have 13-protofilaments, suggesting an additional cellular control to regulate a unique geometry (Tilney *et al.,* 1973). This thirteen-fold geometry is probably favored as it is the only geometry where the protofilaments position straight along the length of the microtubule contrary to twisting around it, allowing for motor proteins to run continuously on the same face of the microtubule (Rice, Montabana & Agard, 2008; Kollman, Merdes, Mourey & Agard, 2011). *In vitro*, microtubules grow through smaller, early assembly intermediates, where disassembly is more energetically favored over the assembly, resulting in slower general growth (Rice, Montabana & Agard, 2008). After a sufficiently long microtubule assembles, microtubule growth becomes more energetically favored, resulting in more rapid incorporation of tubulin dimers and, therefore, growth. Interestingly, cells do not rely on spontaneous polymerization of microtubules; instead, they have evolved differentiated microtubule nucleation sites that avoid the slower, earlier growth phase (Rice, Montabana & Agard, 2008; Kollman, Merdes, Mourey & Agard, 2011). Generally, these specialized nucleation sites are found at microtubule organizing centers (MTOCs). Even though many cellular organelles and compartments are known to act as MTOCs, including the cell cortex and Golgi-apparatus, generally, the centrosome is the major MTOC.

Centrosomal-based microtubule organization

In dividing cells, the centrosome has a significant role in nucleating and anchoring microtubules, acting as a strong MTOC during interphase and mitosis (Azimzadeh & Marshall, 2010; Wu & Akhmanova, 2017). The centrosome contains two centrioles, namely the younger daughter centriole and the mature mother centriole. The centrioles are microtubule-based cylindrical structures consisting of nine triplet microtubule blades fundamentally connected to a cartwheel template, a central hub from which nine spokes radially emerge towards the microtubule wall (Reis & Gopalakrishan, 2013; LeGuennec *et al.,* 2021). In mammalian cells, the two centrioles can recruit an array of proteins, named the pericentriolar material (PCM), to form the centrosome that constitutes microtubule-nucleating activity (**Fig. 2**).

The PCM is an amorphous, electron-dense material, whose primary role is to anchor microtubules directly or through microtubule nucleating templates, like as the gamma-tubulin ring complex (γ-TuRC) (Menella, Agard, Bo & Pelletier, 2014; Kollman, Merdes, Mourey & Agard, 2011). In the PCM, proteins are positioned toroidal, where pericentrin (PCNT) acts as one of the significant organizing proteins of this structure. PCNT is a large, conserved coiled-coil protein targeted to the mother centriole through its PACT (pericentrin-AKAP450 centrosomal targeting) domain (Gillingham & Munro, 2000; Delaval & Doxsey, 2010). In interphase cells, PCNT forms fibrils spanning the width of the PCM that potentially follow the nine-fold symmetry of the centrioles (Mennella *et al.,* 2012; Lawo *et al.,* 2012) (**Fig. 2**). Here, PCNT facilitates the recruitment and the positioning of other essential PCM proteins, such as CDK5RAP2, CEP192, and its binding partner NEDD1, inside the PCM concentric layers. These proteins are crucial for centrosome maturation and the tethering and recruitment of γ-TuRC to the centrosome (Mennela *et al.,* 2014; Woodruff *et al.,* 2014; Woodruff *et al.,* 2015). Another PCM protein, CEP152, does not depend on PCNT for its disposition inside the concentric layers of the PCM. Still, it has an essential function where it regulates centriole duplication and PCM size, acting as a scaffold for the recruitment of polo-kinase 4 (Plk4) and CPAP (Cizmecioglu *et al.,* 2010).

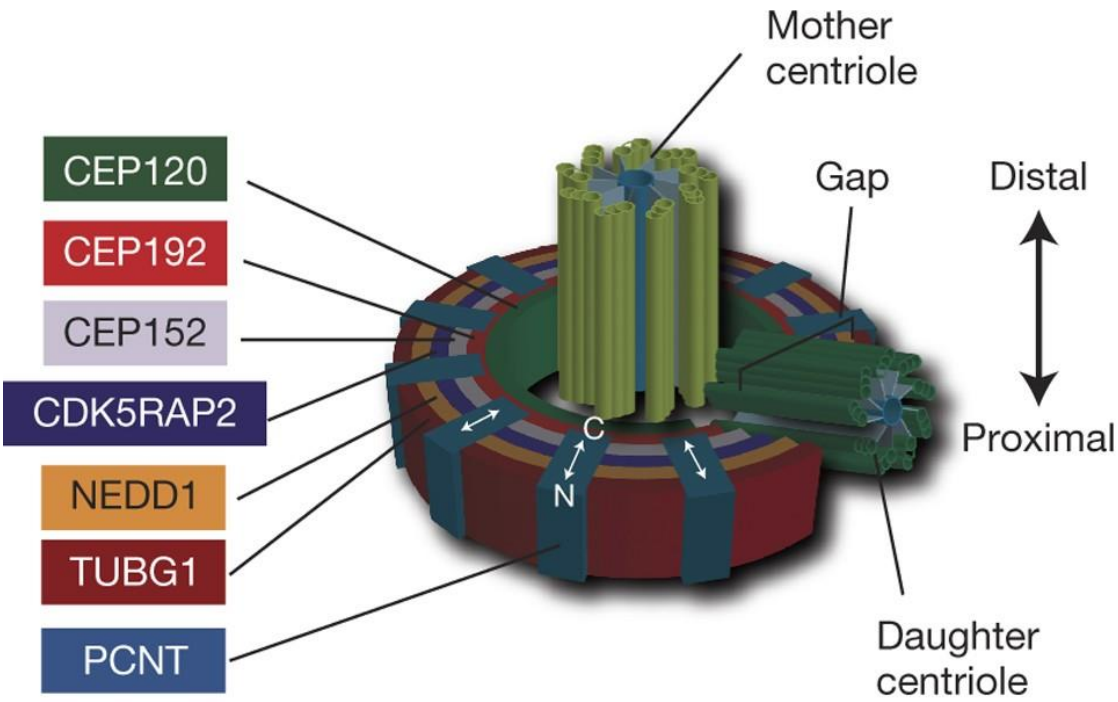

Figure 2. Schematic representation of the centrosome and the toroidal position of pericentriolar material proteins. *The centrosome is an amorphous, protein-dense PCM surrounding two orthogonal centrioles, namely the mother and daughter centriole. PCM components (CEP120, CEP192, CEP152, CDK5RAP2, NEDD1, γ-tubulin, and PCNT) assemble themselves in a highly-structured toroidal manner through their hierarchical deposition. PCNT is positioned perpendicular to the other PCM proteins, with its N-terminus outward and C-terminus inwards. Taken from Lawo et al., 2012.*

The reaction that occurs in the early stages of microtubule nucleation is energetically unfavorable and therefore prefers depolymerization. Thus, cells have evolved a macromolecular template to accelerate this energetically unfavored process, namely γ-TuRC, the primary microtubule nucleation template in mammalian cells (Kollman *et al.,* 2011; Roostalu & Surrey, 2017). The basic unit of γ-TuRC is the gamma-tubulin small complex (γ-TuSC), a heterotetramer comprised of a gamma-tubulin complex protein 2 (GCP2) molecule and a GCP3 molecule, that both bind two separate γ-tubulin molecules. GCP4, GCP5, and GCP6 can substitute GCP2 and GCP3 in the heterotetramer to form a variety of γ-TuSC. Multiple γ-TuSC heterotetramers can assemble into a γ-TuRC complex. In these complexes, γ-tubulin molecules are positioned in a single-turn helical pattern (Kollman *et al.,* 2011; Guillet *et al.,* 2011; Thawani *et al.,* 2018; Consolati *et al.,* 2020; Liu *et al.,* 2020; Wieczorek *et al.,* 2020; Zupa *et al.,* 2021). As γ-tubulin is known to bind to αβ-tubulin heterodimers, this end-on interaction is thought to assist the lateral association of αβ-tubulin heterodimers during their assembly into a microtubule (Roostalu & Surrey, 2017; Tovey & Conduit, 2018). This assembly promotes the otherwise energetically unfavorable conformation.

In mammalian cells, the assembly of γ-TuRC can occur in the cytoplasm (Lin *et al.,* 2016; Tovey & Conduit, 2018). However, to achieve efficient microtubule nucleation from the complex, it is recruited to an MTOC and activated there (Tovey & Conduit, 2018). One PCM-protein complex that can recruit γ-TuRC is that of CDK5RAP2, which interacts with γ-TuRC through its centrosomin motif 1 (CM1), and PCNT, which can bind γ-TuRC through its N-terminal domain. (Haren *et al.,* 2006; Choi *et al.,* 2010; Fong *et al.,* 2008; Lin *et al.,* 2014). Moreover, phosphorylation of NEDD1 by Plk1 and subsequent recruitment by CEP192 critically regulates γ-TuRC recruitment to the centrosome (Haren *et al.,* 2006; Johmura *et al.,* 2011). Intruigingly, there is an explicit functional distinction between the regions of CDK5RAP2 and NEDD1 that bind γ-TuRC. Here, the CM1 domain of CDK5RAP2 also activates γ-tubulin-mediated microtubule

nucleation from γ-TuRC (Choi *et al.,* 2010), whereas the binding region of NEDD1 is required to anchor microtubules directly at the centrosome (Muroyama *et al.,* 2016).
Following nucleation, microtubules can stay associated with the centrosome through microtubule anchoring. The mechanism of microtubule anchoring at the centrosome is thought to rely on the microtubule minus-end being capped by γ-TuRC, subsequently tethered by PCM proteins (reviewed in Wu & Akhmanova, 2017). Another major player in the anchoring of γ-TuRC is Ninein, a coiled-coil protein dependent on PCNT for its centrosomal recruitment (Chen *et al.,* 2014). Here, it localizes to the subdistal appendages of the mother centriole and participates in the tethering of γ-TuRC and microtubules (Delgehyr *et al.,* 2005). Consequently, overexpression of Ninein can lead to inhibition of microtubule release from the centrosome (Abal *et al.,* 2002).

Golgi-based microtubule organization

Despite being the major MTOC in mammalian cells, the centrosome is not the sole location of microtubule organization. Even in mammalian cells with a distinct radial microtubule array, other MTOCs can act as alternative organization sites. One example of a well-described MTOC is the Golgi-apparatus, the second major MTOC in mammalian cells (Chabin-Brion *et al.,* 2001). In a few mammalian cell types, such as retinal pigment epithelial (RPE) cells, almost half of the microtubules are organized at the Golgi apparatus (Efimov *et al.,* 2007). Microtubule organization at the Golgi-apparatus is dependent on AKAP450. Being similar in structure to PCNT, it also contains a PACT domain, through which it can interact with centrosomes and CDK5RAP2. While its role at the centrosome is minor, it firmly localizes to the *cis*-Golgi stacks by binding to GM130 through its N-terminal domain (Gillingham & Munro, 2000; Wang *et al.,* 2010). Here, AKAP450 can either recruit γ-TuRC directly or recruit one of the γ-TuRC binding proteins, namely CDK5RAP2 or its paralog Myomegalin (Wang *et al.,* 2014; Wu *et al.,* 2016) (**Fig. 3**). Due to its vitality, removal of AKAP450 perturbs microtubule nucleation from the Golgi-apparatus completely (Wu *et al.,* 2016).

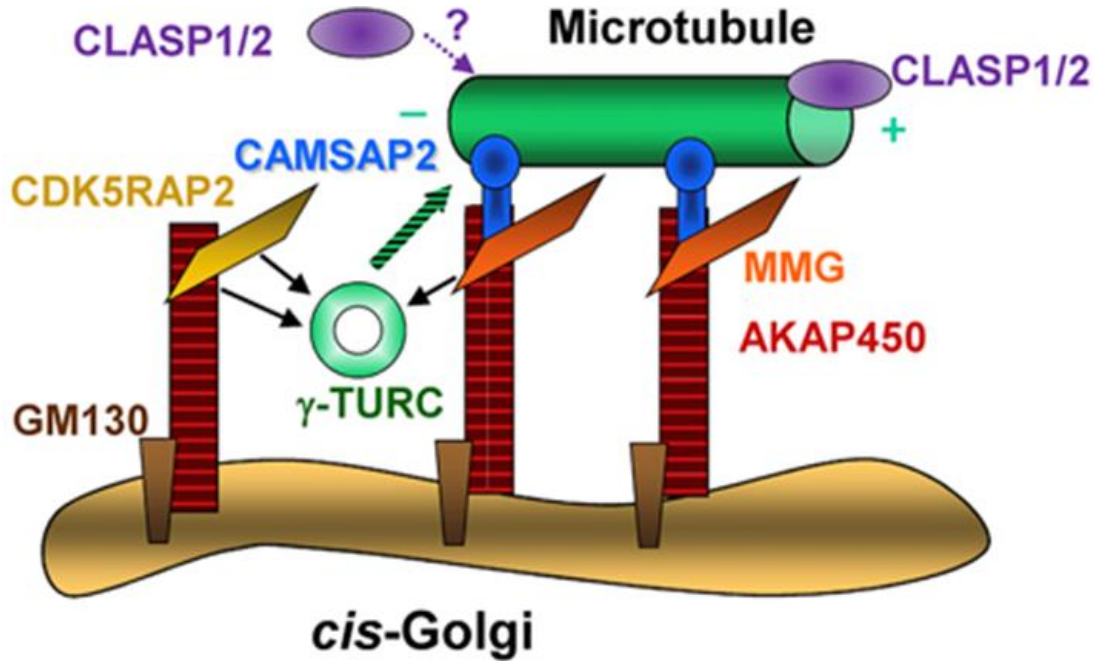

Figure 3. The Golgi-based microtubule nucleation pathway. *AKAP450 is directed to the cis-Golgi by GM130, where it controls microtubule nucleation by recruiting γ-TuRC complexes either directly or through CDK5RAP2 and Myomegalin (MMG). CAMSAP2 attaches microtubules to the Golgi through a complex of MMG and AKAP450. Moreover, CAMSAP2 can stabilize the microtubule minus-ends. CLASPs promote microtubule stability by stabilizing the microtubule plus-end and possibly also the minus-end. At the trans-Golgi, CLASPs tether microtubules by interacting with trans-Golgi-bound GCC185 (process not shown). Adapted from Wu et al., 2016.*

Interestingly, a complex of AKAP450 with either CDK5RAP2 or Myomegalin is not sufficient for microtubule anchoring at the Golgi (Wu *et al.,* 2016). Here, another essential protein is involved, namely, CAMSAP2, which stabilizes the free microtubule minus-ends (Jiang *et al.,* 2014). These stable CAMSAP2 stretches can be tethered to the Golgi through the Myomegalin and AKAP450 complex, whereas CDK5RAP2 is not involved (Wu *et al.,* 2016) (**Fig. 3**). Thus, microtubules that nucleated spontaneously or lost their γ-TuRC complex can be decorated by CAMSAP2 and get anchored at the Golgi.

Furthermore, it has been shown that cytoplasmic linker-associated proteins (CLASPs) are critical for Golgi-based microtubule organization (Efimov *et al.,* 2007). Here, CLASPs promote microtubule nucleation, possibly by lowering the kinetic barrier required for microtubule outgrowth from the Golgi (Grimaldi *et al.,* 2014; Sanders & Kaverina, 2015). Additionally, CLASPs can anchor microtubules to the Golgi by binding to the *trans*-Golgi protein GCC185 (Efimov *et al.,* 2007). Moreover, CLASPs stabilize CAMSAP2 decorated microtubule stretches (**Fig. 3**). As CLASPs are crucial for microtubule organization from the Golgi-apparatus, most noncentrosomal microtubules are lost upon their removal (Efimov *et al.,* 2007; Wu *et al.,* 2016).

Regulation of microtubule dynamics within the cell

Many factors in the intracellular environment contribute to microtubule dynamics. In cells, catastrophes are regularly induced by forces pushing on the growing microtubule tips, such as the cell cortex, which slows down microtubule growth, leading to loss of their stable GTP-cap, subsequently resulting in catastrophe (Janson *et al.,* 2003). It has also been shown that walking motor proteins can remove tubulin dimers from the lattice and, through that, rapidly destroy microtubules (Triclin *et al.,* 2021). Moreover, microtubules that grow for more prolonged periods have higher chances of undergoing catastrophe. This intrinsic 'ageing' property highlights the need for several molecular events to occur to induce depolymerization (Gardner *et al.,* 2011; Coombes *et al.,* 2013). Furthermore, different tubulin isoforms and post-translational modifications (PTMs) have been indicated to alter microtubule stability (reviewed in Aher & Akhmanova, 2018). Stable microtubules can possess an array of PTMs, including polyglutamylation, acetylation, detyrosination, and phosphorylation, which are generally characteristic of long-lived microtubules (Hammond *et al.,* 2008). Whereas most PTMs cover the lattice of microtubules, the acetylation of the lysine 40 residue (K40) of α-tubulin is positioned inside the lumen of microtubules (LeDizet & Piperno, 1987; Nogales *et al.,* 1998; Wloga *et al.,* 2017). The acetylation of K40 makes microtubules more resistant to microtubule depolymerizing drugs and is correlated with long-lived microtubules in almost all eukaryotic cell types (Piperno & Fuller, 1985; Piperno *et al.,* 1987; Wloga *et al.,* 2017). This correlation can be explained by particular elements limiting microtubule acetylation's velocity, such as the slow rate of αTAT1 diffusion inside the microtubule lumen and the slow enzymatic activity of αTAT1 (Howes *et al.,* 2014; Szyk *et al.,* 2014; Ly *et al.,* 2016). In turn, this suggests age-dependent microtubule acetylation, where long-lived microtubules progressively get acetylated as opposed to being long-lived through acetylation (Howes *et al.,* 2014; Szyk *et al.,* 2014; Ly *et al.,* 2016). Besides the direct modification of microtubules, cells have evolved a broad array of factors, collectively named microtubule-associated proteins (MAPs), that regulate the dynamic instability of microtubules and the connection between cellular structures and microtubules (Desai & Mitchison, 1997).

Microtubule-associated proteins

MAPs that influence microtubule dynamics can be categorized functionally as stabilizing, destabilizing, cross-linking, and end-capping proteins. Other MAPs encompass motor proteins that use the microtubule as a track instead of directly influencing their dynamics, or proteins which promote cell organization by anchoring organelles to microtubules. MAPs can dramatically affect microtubule dynamics during the cell cycle by directly or indirectly inducing depolymerization, polymerization, or microtubule pausing (Akhmanova & Steinmetz, 2015).

Examples of stabilizing MAPs can be found in proteins containing multiple tumor overexpressed gene (TOG) domains. One well-established TOG-domain containing protein, XMAP215 (chTOG in humans), accelerates microtubule growth speed by increasing the incorporation of free tubulin dimers at the growing plus-end (Brouhard *et al.,* 2008; Widlund *et al.,* 2011). Moreover, XMAP215 exhibits an additional regulatory function on microtubules, regulating their catastrophe rate (reviewed in Kinoshita *et al.,* 2002). Another multi-TOG-domain protein, CLASP, stabilizes microtubules at the plus-ends and is involved in microtubule repair at the damaged microtubule lattice (Yu *et al.,* 2016; Lawrence *et al.,* 2018; Aher *et al.,* 2018, Aher *et al.,* 2020). Furthermore, a thoroughly investigated, neuronally expressed MAP, tau, protects the microtubule from depolymerization by decreasing the disassociation of tubulin dimers from either end (reviewed in Barbier *et al.,* 2019).

In contrast to stabilization, specific MAPs induce depolymerization of microtubules. Depolymerization can be influenced either directly or indirectly. An example of a MAP indirectly influencing depolymerizing is stathmin, which sequesters tubulin dimers, preventing their incorporation at the growing end (reviewed in Cassimeris, 2002). MAPs from the kinesin-13 family, like MCAK, can directly attack microtubule plus-ends. Here, MCAK harnesses the energy of ATP hydrolysis to remove the terminal tubulin dimers from microtubule ends (Hunter *et al.,* 2003; Asenjo *et al.,* 2013). Furthermore, several MAPs can sever microtubules, such as katanin and spastin, which are microtubule stimulated ATPases, and use ATP hydrolysis to disassemble stable microtubules (reviewed in Roll-Mecak & McNally, 2010).

Other MAPs include molecular motor proteins. These motor proteins can bind either directly to microtubules or to adapter proteins that facilitate their recruitment to microtubules. Two superfamilies of motor proteins move on microtubules, namely kinesin and dynein, both responsible for the spatial organization and distribution of organelles in the cell (Sweeney & Holzbaur, 2018). The microtubule polarity plays a significant role in the motor protein-based spatial organization, as kinesins are plus-end directed, whereas dyneins are minus-end directed. Consequently, typical kinesin-motors transport exocytic vesicles towards the plasma membrane and distribute organelles around the cytoplasm (Grigoriev *et al.,* 2007; Akhmanova & Hammer, 2010). Contrarily, dynein-motors are accountable for the central positioning of organelles like the Golgi-apparatus and nucleus (Gundersen & Worman, 2012; Zhu & Kaverina, 2013). These motor proteins can be recruited to the microtubules by other MAPs as well, an example being MAP7 family proteins, which recruit kinesin-1 to the microtubule, regulating the transport of organelles like mitochondria (Tymanskyj *et al.,* 2018; Hooikaas *et al.,* 2019). Removal of MAP7 and its isoforms results in robust clustering of mitochondria around the nucleus, indicating perturbation of their transport (Hooikaas *et al.,* 2019). Interestingly, post-translational modifications in the C-terminal tails of αβ-tubulin heterodimers either promote or inhibit interactions of different motor proteins. An example is the detyrosination of the α-tubulin C-terminal tail, which promotes the processivity of kinesin-2 binding but inhibits the microtubule depolymerization activity of MCAK (Sirajuddin *et al.,* 2014). In neurons, it has been reported that microtubules with opposite orientations possess different modifications. (Tas *et al.,* 2017). Here, in dendrites, minus-end-out-oriented microtubules are more stable and acetylated; and, therefore, facilitate axon selectivity of kinesin-1. Contrarily, plus-end-out-orientated microtubules are more tyrosinated and dynamic, and facilitate kinesin-3-based transport in dendrites (Tas *et al.,* 2017). Thus, the modification of microtubules can strongly contribute to the spatial organization of motor proteins, and therefore, cargoes. Recent findings also suggest a 'MAP-code,' in which the major cargo transport motors, kinesin-1, kinesin-3, and dynein, all have MAPs promoting or inhibiting their recruitment. Thus, these motor proteins and their cargoes can be spatiotemporally controlled by inhibiting or promoting their recruitment with different adapter proteins (Monroy *et al.,* 2020).

End-capping MAPs bind to the plus- or minus-ends of microtubules and therefore can prevent both the association and disassociation of tubulin dimers. A well-established minus-end capping protein complex is γ-TuRC, which initially nucleates the microtubule, then caps its nucleated minus-end, stopping the exchange of tubulin dimers (Wiese & Zheng, 2000). Other minus-end capping proteins are the members of the CAMSAP family, which either inhibit the growth of minus-ends by tracking them (CAMSAP1) or slow-down but not block polymerization of the microtubule minus-end (CAMSAP2 and CAMSAP3) (Hendershot & Vale, 2014; Jiang *et al.,* 2014).

Furthermore, an extensive array of MAPs localize and interact with the plus-ends of microtubules. Collectively, these MAPs are referred to as plus-end tracking proteins (+TIPs). +TIP networks consist of complex protein-protein interactions where end-binding proteins (EBs) are the primary regulators (Akhmanova & Steinmetz, 2015; Goodson & Jonasson, 2018). Higher eukaryotic cells express three EB isoforms, namely EB1, EB2, and EB3. EBs bind autonomously to growing plus- and minus-ends, recruiting strategical regulatory factors (Slep *et al.,* 2007; Xia *et al.,* 2014). EBs localize to the growing ends with their N-terminal calponin homology (CH) domain and interact with numerous +TIP partners through their C-terminal domain (Hayashi *et al.,* 2003). An example of these +TIP binding partners are cytoskeleton-associated protein Gly-rich domain (CAP-Gly domain) family proteins, such as cytoplasmic linker protein of 170 kDa (CLIP170), which promotes rescues (Komorova *et al.,* 2002). Like EBs, CLIP170 can also bind microtubule plus-ends autonomously and, therefore, is considered a +TIP (Bieling *et al.,* 2008). Moreover, CLIP170 and another CAP-Gly domain-containing protein, $p150^{glued}$, can regulate organelle transport by docking membranes on the associated microtubule (Vaughan *et al.,* 2002; Lomakin *et al.,* 2009).

Collectively, the varied functions of this broad array of MAPs regulate the dynamic instability of microtubules.

Essential regulation of the microtubule network in interphase and mitosis by CLASPs

This research will focus on CLASP, an indispensable regulatory +TIP, that is highly conserved amongst eukaryotes. Initially, the two mammalian paralogs of CLASP, namely CLASP1 and CLASP2, were described to interact with CLIPs (Akhmanova *et al.,* 2001). The interest in CLASPs arose from *Xenopus*, *Drosophila*, and *Caenorhabditis elegans,* only having a single CLASP homolog that proved crucial for the organism's viability and mitosis (Pasqualone *et al.,* 1994; Lemos *et al.,* 2000; Inoue *et al.,* 2000; Hannak & Heald, 2006). Mammalian CLASPs are critical for the proper completion of mitosis by regulating microtubule dynamics and microtubule polymerization near kinetochores (Maiato *et al.,* 2003, Maiato *et al.,* 2006; Mimori-Kiyosue *et al.,* 2006). Severe mitotic defects such as monopolarity, multipolarity, and disorganized spindles are already observed upon the knock-out of either of the two CLASP homologs. Consequently, this leads to aberrant chromosome separation, causing other defects such as chromatin bridges and aneuploidy (Pereira *et al.,* 2006; Mimori-Kiyosue *et al.,* 2006; Liu *et al.,* 2009; Logarinho *et al.,* 2012). Cells lacking CLASP2 are still viable, and their mitotic defects can be rescued through the overexpression of either paralog; still, rescue with CLASP1 was not as successful (Pereira *et al.,* 2006). As CLASP1 was unable to relieve the mitotic defects observed in CLASP2 knock-out cells fully, it suggests that both CLASP homologs are partially but not fully redundant during mitosis. CLASPs decorate the kinetochores and spindle poles throughout the early phases of mitosis, promoting spindle organization and kinetochore-microtubule attachment (Maiato *et al.,* 2003; Mimori-Kiyosue *et al.,* 2006; Liu *et al.,* 2009). In late Anaphase-B, where the spindle poles start moving apart, CLASPs localize to the central spindle (Liu *et al.,* 2009; Vukušić & Tolić, 2021). Abrogating the interaction between CLASP and PRC1, an antiparallel-microtubules cross-linking protein, which recruits CLASPs to the central spindle, obstructs chromatid separation, highlighting the importance of correct localization of CLASPs by PRC1 during mitosis (Liu et al., 2009).

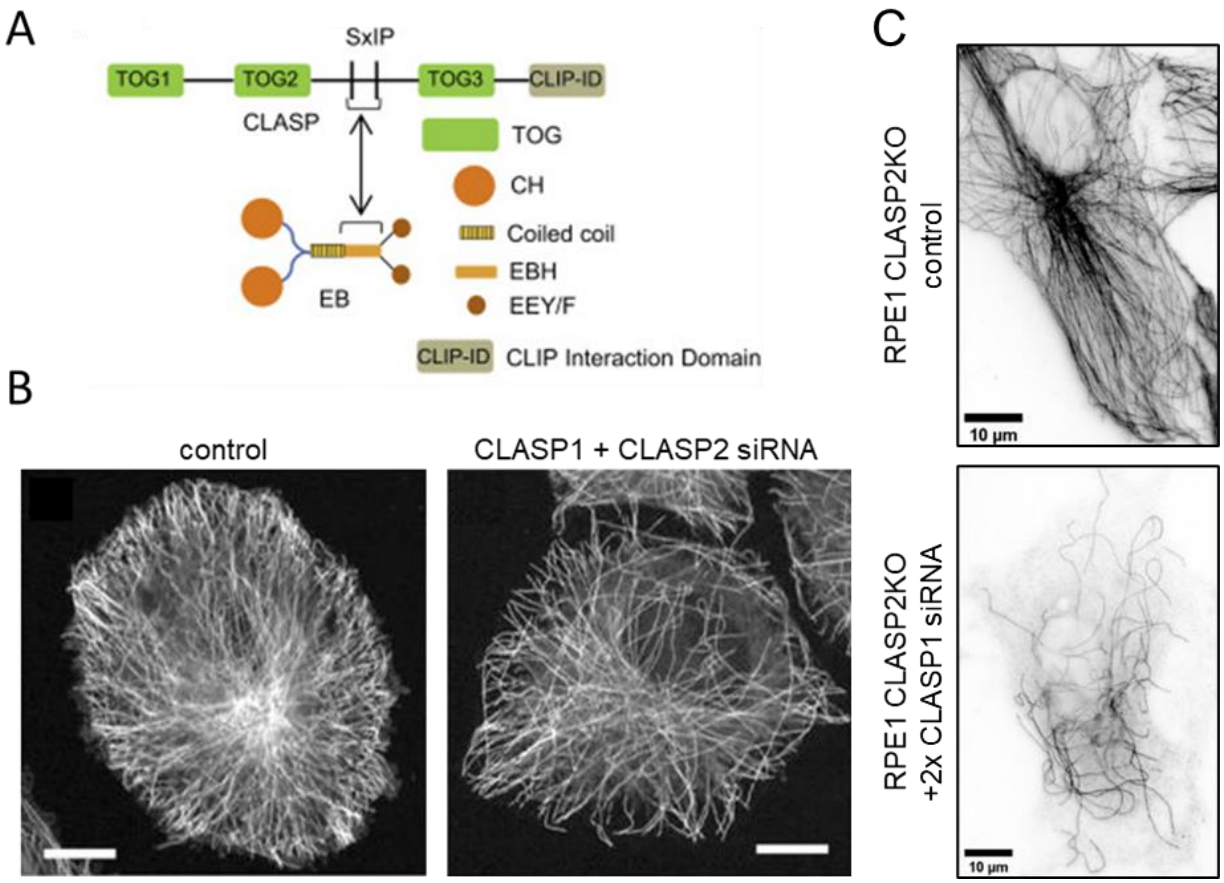

Figure 4. Knock-down of both CLASP homologs reduces the microtubule density in interphase. (A). *A simplified overview showing the architecture of CLASP. Herein it is depicted that CLASPs are build-out of three separate TOG-like domains, an SxIP motif that can interact with EBs directly, and a CLIP-interacting domain through which they can bind CLIPs (amongst others). Adapted from Aher et al., (2018).* ***(B).*** *HeLa wild-type cells treated with either control siRNA (left panel) or CLASP1 and CLASP2 siRNA (right panel), showing the reduction in microtubule density. Scale bars are 10 µm long. Adapted from Mimori-Kiyosue et al., (2005).* ***(C).*** *RPE1 C2KO cells were treated for two rounds with either control siRNA (top panel) or CLASP1 siRNA (bottom panel), showing the severe reduction in microtubule density. Taken from Robin Hoogenbeen, 2021, unpublished.*

CLASPs are part of the before-mentioned +TIP superfamily, localizing to various intracellular locations by binding EBs through their SxIP motif (Akhmanova *et al.,* 2001). Moreover, CLASPs can interact with numerous other partners through their CLIP-interacting domain (Akhmanova *et al.,* 2001) (**Fig. 4A**). Additionally, three TOG-like domains are dispositioned in the architecture of mammalian CLASPs (Aher *et al.,* 2018) **(Fig. 4A**). However, CLASPs do not function as a microtubule polymerase, unlike other TOG domain-containing proteins, such as chTOG/XMAP215, likely originating from the convex structure of TOG-like domains, making them incompatible with binding to free tubulin (Brouhard *et al.,* 2008; Maki *et al.,* 2015; Aher *et al.,* 2018). Instead, CLASPs do not alter microtubule growth speed; rather, they slow down the growth speed, if at all, and act as a microtubule-stabilizing factor at the plus-end (Yu *et al.,* 2016; Aher *et al.,* 2018; Lawrence *et al.,* 2018). *In vitro* reconstitution with the different TOG-like domains of mammalian CLASPs uncovered their separate functions. Mammalian CLASPs suppress catastrophes and promote rescues through their TOG2 domain, whereas the TOG3 domain mildly increases rescues (Aher *et al.,* 2018). Furthermore, their TOG1 domain has an autoregulatory role and relieves an autoinhibition imposed by their CLIP-interacting domain (Aher *et al.,* 2018).

CLASPs can stabilize microtubules through these domains by lowering catastrophe frequency and increasing rescue frequency at microtubule plus-ends. Additionally, CLASPs can stabilize microtubules by attaching distal microtubule ends to the cell cortex through interaction with LL5β (Lansbergen *et al.,* 2006). Recent *in vitro* work showed that mammalian CLASPs can also induce microtubule repair through their TOG2 domain by incorporating new tubulin dimers at damaged sites along the microtubule (Aher *et al.,* 2020). As previously stated, CLASPs are critical for microtubule organization at the Golgi-apparatus by possibly lowering the kinetic barrier required for microtubule outgrowth from γ-TuRC (Efimov *et al.,* 2007; Sanders & Kaverina, 2015). Interestingly, Aher *et al.* (2018) reported that CLASP on its own reduced the critical concentration of soluble tubulin required for templated outgrowth *in vitro*. Henceforth, CLASPs could also exhibit microtubule nucleating properties.
Consequentially, even the limited removal of both CLASP homologs already results in a significantly diminished microtubule density (**Fig. 4B**) (Mimori-Kiyosue *et al.,* 2005). As previously stated, knocking out a single mammalian CLASP homolog already shows severe mitotic defects, yet due to the partial redundancy of CLASPs, they are still viable (Pereira *et al.,* 2006; Mimori-Kiyosue *et al.,* 2006; Liu *et al.,* 2009; Logarinho *et al.,* 2012). However, a mitotic arrest is induced even by partially removing both CLASP homologs (Mimori-Kiyosue *et al.,* 2006), subsequently causing a p53 driven apoptosis (Orth *et al.,* 2012). Hence, the generation of a cell line knocked out of CLASP1 and CLASP2 would not be feasible.

Previously, Robin Hoogenbeen (2021, unpublished) managed to deplete the microtubule density severely through “2-times depletion” of CLASP1 in an RPE1 CLASP2 knock-out cell line (RPE1 C2KO, Pavlovič, 2018, unpublished) (**Fig. 4C**). Here, they further explored the phenotypes of cells with fewer remaining microtubules. In particular, they looked at the intracellular organization of different MAPs and organelles in cells with few microtubules. However, it is unclear how CLASPs functions owe to this substantial reduction in microtubule density upon their depletion. Thus, we aimed to investigate how CLASPs functions lead to the extreme decrease in microtubule density we observe upon their depletion.
In this study, we made advances to identify the mechanistic links between CLASP functions in microtubule nucleation and stabilization and the drastic reduction in microtubule density in interphase upon their depletion. Furthermore, our methodology reduced the microtubule density in cells to a level that has never been achieved before, revealing a potential critical threshold of microtubule number required for the proper distribution of organelles.

Results

CLASPs are more robust regulators of microtubule density than chTOG

TOG-domain containing family proteins, such as XMAP215 (chTOG in humans) and CLASPs, are critical for regulating microtubule dynamics in interphase and mitosis (Akhmanova *et al.,* 2001; Aher *et al.,* 2018; Brouhard *et al.,* 2008; Widlund *et al.,* 2011). However, there is an explicit functional difference between the TOG-domains of XMAP215 and CLASPs. While XMAP215 increases microtubule polymerization and regulates catastrophe frequency (Brouhard *et al.,* 2008; Widlund *et al.,* 2011), CLASPs slow down microtubule growth speed, suppress catastrophe, and promote pausing and rescue (Yu *et al.,* 2016; Aher *et al.,* 2018; Lawrence *et al.,* 2018). Another key difference is that, unlike the TOG-domains of XMAP215, the TOG-like domains of CLASPs are incompatible with binding free tubulin (Brouhard *et al.,* 2008; Maki *et al.,* 2015). Moreover, CLASPs have been implicated in stimulating microtubule nucleation at the Golgi (Efimov *et al.,* 2007), possibly lowering the kinetic barrier required for microtubule outgrowth from γ-TuRC (Sanders & Kaverina, 2015). Consistently, XMAP215 has been shown to assist microtubule nucleation from various templates (Wieczorek *et al.,* 2015) and synergizes with γ-TuRC templates, promoting microtubule nucleation (Thawani *et al.,* 2018). Robin Hoogenbeen (2021, unpublished) showed that through rigorous depletion of CLASPs from cells, a significant reduction

in microtubule density could be achieved (**Fig. 4C**). As XMAP215/chTOG, like CLASPs, strongly regulates microtubule dynamics and is implicated in promoting microtubule nucleation from γ-TuRC templates, we wondered whether its removal would result in a similar reduction in microtubule density as we observed upon CLASP-depletion.

Depletion of chTOG in RPE1 C2KO cells resulted in a substantial reduction in microtubule density compared to control cells, yet CLASP-depleted cells were more scarce in microtubules (**Fig. 5A**). To estimate the reduction in microtubule density, we drew three lines of 10 µm in length in acquired 2D images. Next, we averaged the number of microtubules that traversed these lines, giving the average microtubule density (for more details, read the materials & methods, imaging, and analysis of fixed cells section). Indeed, the microtubule density in CLASP-depleted cells was approximately 3.4-fold lower than that in chTOG-depleted cells (5.6 ± 1.0 microtubules/ 10 µm for CLASP-depleted cells and 19.1 ± 3.5 microtubules/ 10 µm for chTOG-depleted cells). In contrast, chTOG depletion resulted in a 1.5-fold reduction in microtubule density compared to control cells (19.1 ± 3.5 microtubules/ 10 µm for chTOG-depleted cells and 28.4 ± 3.7 for control cells) (**Fig. 5B**). It is important to note that the antibody used to stain for chTOG was unable to stain any chTOG localized to the lattice or plus-ends of microtubules (with faint exceptions, **Fig. 5A**), whereas it did stain the population at the centrosome (**Fig. 5A**). In cells depleted of chTOG, although the centrosomal signal of chTOG was lost, there could still be a chTOG population left associated with the microtubules, potentially responsible for a higher

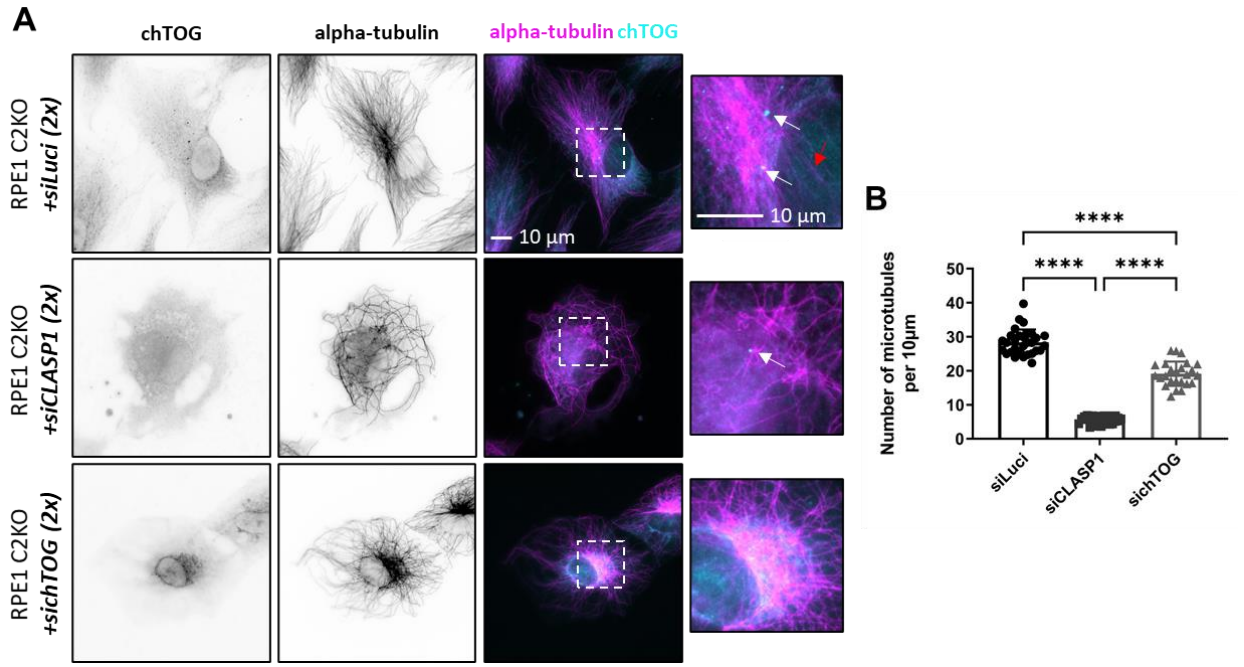

Figure 5. CLASPs are more robust regulators of microtubule density than chTOG. (A). *Immunofluorescence staining of RPE1 C2KO cells depleted with siCLASP1 (middle-panels), sichTOG (bottom-panels), or siLuciferase (top-panels) as a control. White arrows in the insets point at the centrosomal chTOG signal—red arrow points at faint chTOG microtubule decoration. Cells were stained for chTOG (cyan) and alpha-tubulin (magenta)* ***(B).*** *A quantitative comparison of the microtubule density in the cells as mentioned above. The following number of cells was used: 30 for siCLASP1, 30 for siLuciferase, and 25 for sichTOG. All cells were taken from at least two independent experimental repetitions. Using a One-way Anova gave a significance value of p < 0.0001, ****. The standard deviation is displayed through the error bars.*

microtubule density. A western blot is required to determine the level of chTOG left in these chTOG-depleted cells to confirm an efficient depletion. Nonetheless, these results indicate that CLASPs are more critical in regulating the microtubule density than chTOG.

The viability of CLASP-depleted cells increases upon knocking out p53

A mitotic arrest is already observed upon partial removal of both CLASP homologs (Mimori-Kiyosue *et al.,* 2006), often leading to cell death through a p53 induced apoptosis (Orth *et al.,* 2012; Hain *et al.,* 2016). Accordingly, we observed little to no growth and high lethality rates for our thoroughly CLASP-depleted cells. As we had perspectives of using various additional treatments on our CLASP-depleted cells, we set out to increase their viability. Chen *et al.* (2021, preprint) found that knocking-out p53 from cells depleted of proteins important for mitosis significantly increased the viability of those cells. We successfully knocked out p53 from our RPE1 C2KO backbone using the CRISPR/Cas9 system (see materials & methods section, Chen *et al.,* 2021, preprint) (**Fig. 6)**.

Western blot analysis showed no expression of p53 in the generated RPE1 C2p53KO cells (**Fig. 6D**). Comparing the microtubule density in RPE1 C2p53KO to RPE1 C2KO cells depleted with

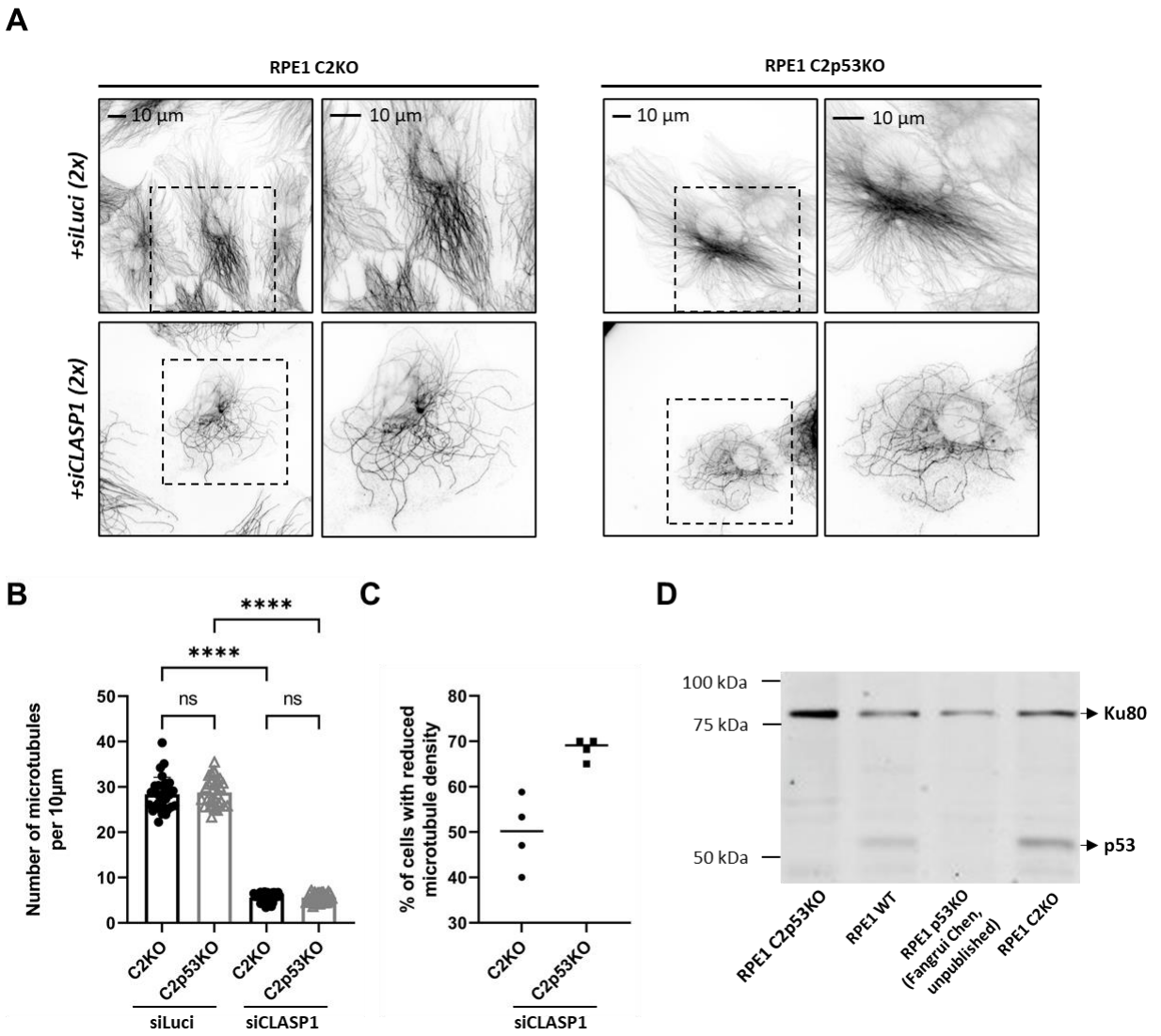

Figure 6. The viability of CLASP-depleted cells increases upon knocking out p53. (A). *Immunofluorescence staining of alpha-tubulin in RPE1 C2KO and RPE1 C2p53KO cells depleted with either siCLASP1 (bottom panels) or siLuciferase (top panels) as a control.* ***(B).*** *Quantitative comparison of the microtubule density in the cells as mentioned above. Per condition, 30 cells were used that were imaged from at least three independent experimental repetitions. Using a One-way Anova gave significance values of $p < 0.0001$, ****; $p = 0.9186$ for ns siLuci; and $p > 0.9999$ for ns siCLASP1. The standard deviation is displayed through the error bars.* ***(C).*** *Quantitative comparison of the number of surviving cells with a reduced microtubule density after depletion with siCLASP1 in RPE1 C2KO and RPE1 C2p53KO cells. Each dot represents an independent repetition.* ***(D).*** *Western blot confirming the knock-out of p53 in the RPE1 C2p53KO cells. RPE1 WT and RPE1 C2KO were used as negative controls, whereas RPE1 p53KO cells (Fangrui Chen, unpublished) were used as positive controls.*

both control siRNA (28.4 ± 3.7 microtubules/ 10 µm for RPE1 C2KO cells and 28.8 ± 3.1 microtubules/ 10 µm for RPE1 C2p53KO cells) and CLASP1 siRNA (5.59 ± 0.98 microtubules/10 µm for RPE1 C2KO cells and 5.59 ± 1.0 microtubules/ 10 µm for RPE1 C2p53KO cells) did not show any difference in microtubule density upon knocking out p53 (**Fig. 6A, B**). Interestingly, depleting RPE1 C2p53KO cells with CLASP1 siRNA yielded a higher percentage of cells with reduced microtubule density when compared to RPE1 C2KO cells depleted of CLASPs; indicating an increase in cell viability (**Fig. 6C**).

Moreover, previously generated U2OS C2KO cells (Tonja Pavlovič 2018, unpublished) were highly susceptible to our sequential CLASP-depletion method, leading to a high lethality rate (data not shown). Due to the increase in viability in RPE1 C2KO cells upon knocking out p53, we also knocked out p53 in U2OS C2KO cells. These U2OS C2p53KO cells showed a 5.0-fold reduction in microtubule density upon CLASP-depletion (25.8 ± 3.1 microtubules/ 10 µm in control cells and 5.2 ± 1.7 microtubules/ 10 µm in CLASP-depleted cells) (**Fig. S1**). However, as the method optimized for RPE1 cells led to a high lethality rate, even for U2OS C2p53KO cells, only a few cells were found with reduced microtubule densities. Therefore, we focussed our study on RPE1 cells, but the U2OS C2p53KO cells could potentially confirm our findings in another, non-epithelial cell model.

Microtubule dynamics are minorly altered in CLASP-depleted cells

MAPs thoroughly regulate microtubule dynamic instability. In CLASP-depleted cells, where microtubules are incredibly scarce, the ratio of MAPs to microtubules might be dramatically altered. It has previously been shown that specific MAPs can compete for binding to the microtubule lattice, regulating the recruitment of motor proteins (Monroy *et al.,* 2018). Therefore, we wondered whether, in CLASP-depleted cells, where microtubules are low in number, MAPs would vastly compete with each other for binding the remaining microtubules. In turn, this could lead to altered microtubule dynamics in these cells. Moreover, as CLASPs have been implicated as vital microtubule-stabilizing factors (Yu *et al.,* 2016; Aher *et al.,* 2018), their removal would be expected to lead to altered microtubule dynamics. To evaluate these microtubule dynamics, we sought to employ live-cell imaging. Unfortunately, we could not transfect fluorescent fusion constructs in RPE1 C2KO and RPE1 C2p53KO cells after sequential CLASP-depletion. Therefore we could not image the microtubules directly and had to resort to other methods. With the help of Boris Shneyer (Akhmanova lab, Cell Biology department, Utrecht University), we generated lentivirally induced RPE1 C2KO cell lines, stably expressing EB3-GFP. In these cells, we were able to visualize the growing ends of the microtubules through EB3-GFP decoration and study their dynamics (**Fig. 7**). CLASP-depletion in these cells strongly reduced the microtubule number

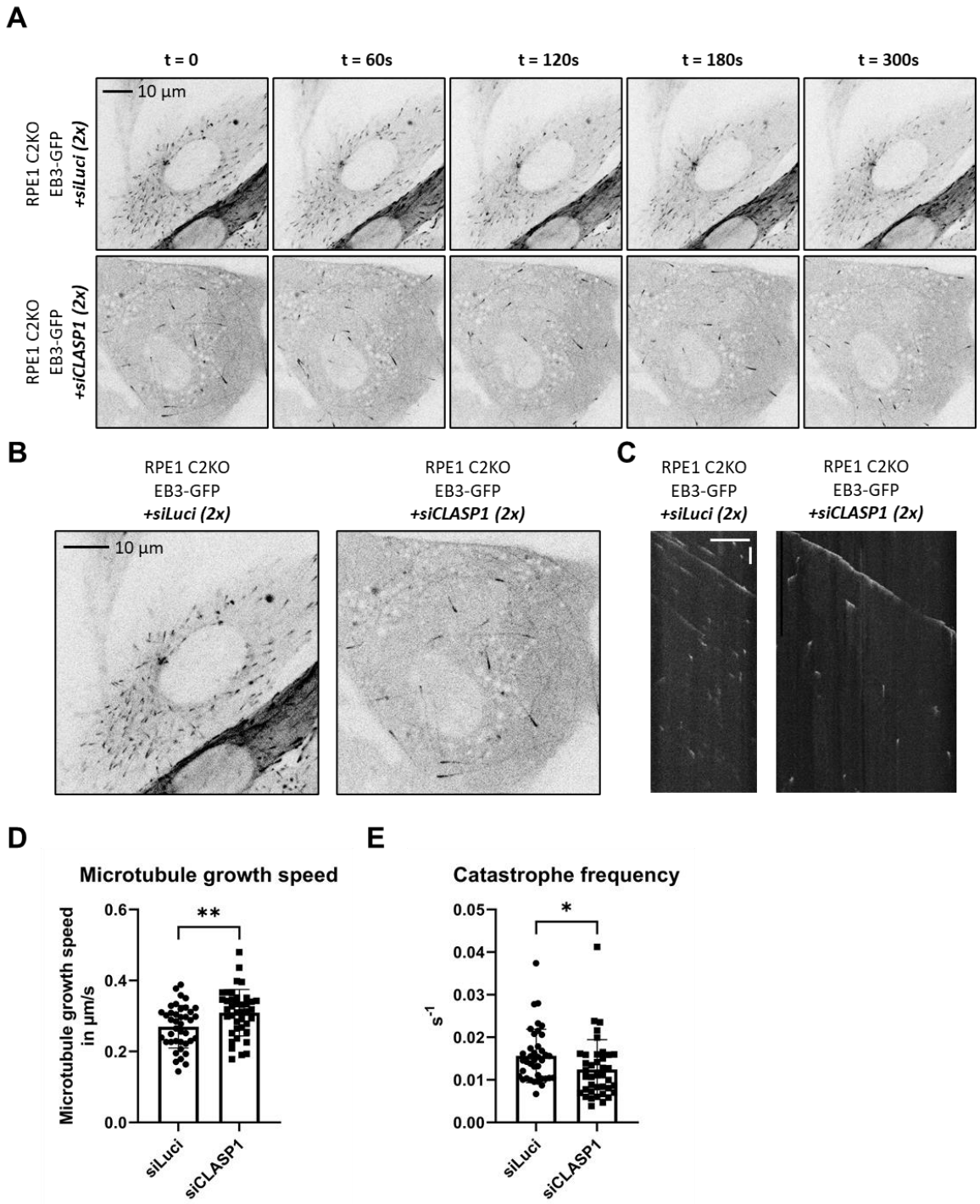

Figure 7. Microtubule dynamics are slightly affected upon CLASP-depletion. (A). *Single timeframes of RPE1 CLASP2 KO cells stably expressing EB3-GFP depleted with either siCLASP1 (bottom panels) or siLuciferase as a control (top panels).* ***(B).*** *Enlarged images of timeframe 0 images shown in panel A.* ***(C).*** *Kymographs were generated from microtubules in the cells, as mentioned before. Scale bars, 10 µm (horizontal) and 20 seconds (vertical).* ***(D).*** *Quantitative comparison of microtubule growth speed in cells as mentioned before. Using an unpaired t-test gave a significance value of p = 0.006, **. The standard deviation is displayed through the error bars.* ***(E)****. Quantitative comparison of the catastrophe rate given in events/second in cells as mentioned before. Using an unpaired t-test gave a significance value of p = 0.0363, *. The standard deviation is displayed through the error bars. Panel* ***D*** *and* ***E*** *are plotted with n = 40 microtubules per condition, taken from 8 separate cells, imaged from only one experiment.*

as expected (**Fig. 7A, B**). We found that microtubules in CLASP-depleted (0.31 ± 0.06 µm/s) cells grew 1.15-fold faster than control cells (0.27 ± 0.06 µm/s) (**Fig. 7D**). Mammalian CLASPs have previously been shown *in vitro* to slow down the microtubule growth (Moriwaki & Goshima, 2016; Yu *et al.,* 2016; Aher *et al.,* 2018); therefore, their removal might increase the microtubule growth rate *in vivo*. Moreover, the soluble tubulin pool available in these CLASP-depleted cells will be higher than the control, and it could lead to a faster growth rate. Additionally, we found the catastrophe frequency per second to be minorly decreased upon CLASP-depletion (0.012 ± 0.007 catastrophes/s) when compared to control (0.016 ± 0.006 catastrophes/s) (**Fig. 7E**). These results are surprising, as CLASPs are well-known to reduce the catastrophe rate of microtubules, suggesting that their removal would increase the catastrophe rate. This reduction likely originates from the prolonged lifetime of the remaining stable population of microtubules in CLASP-depleted cells (**Fig. 7B**), causing the catastrophe frequency to decrease. Moreover, it could be that the remaining microtubules in these CLASP-depleted cells are stabilized by various factors, owing to their prolonged lifetime, but also their increased overall polymer length (**Fig. 7A, B, C**).

MAP7 family proteins do not stabilize distinct microtubule subsets

To understand whether specific MAPs highly stabilize the remaining microtubules in CLASP-depleted cells, we started looking for potential factors that could facilitate this. Robin Hoogenbeen (2021, unpublished) reported MAP7 family proteins to hyper-decorate remaining microtubule stretches. MAP7 decorated almost all remaining microtubules in CLASP-depleted cells, decorating less than half of the microtubules in control cells. Furthermore, MAP7D1 localized to very curly microtubule stretches reminiscent of acetylated-tubulin stretches upon CLASP-depletion, whereas MAP7D3 decoration was almost completely lost, remaining only at the centrosome. As MAP7 and MAP7D1 hyper-decorated these distinct subpopulations of microtubules, we wondered whether their removal would result in loss or destabilization of said populations. Henceforth, we attempted to co-deplete CLASPs together with the MAP7 family proteins (**Fig. S2**). Co-depletion of CLASPs and MAP7D1 did not result in loss of the acetylated-tubulin population (**Fig. S2A**), showing that it does not stabilize this remaining population rather decorates them. Moreover, the microtubule density is not reduced further when MAP7D1 is co-depleted together with CLASPs (**Fig. S2D**). Co-depletion of MAP7 and CLASPs proved to be lethal for cells (data not shown). However, MAP7 depletion on its own already proved to be lethal to cells, indicating a potential unwanted target or response of siRNA transfection, as the knock-out of MAP7 was completely viable (Hooikaas *et al.,* 2019). Interestingly MAP7D3 has previously been implicated in enhancing nucleation efficiency of microtubules *in vivo* (Sun *et al.,* 2011). Furthermore, mass-spectrometry analysis highlighted a potential interaction of MAP7D3 with PCNT and CDK5RAP2 (Hooikaas *et al.,* 2019), two proteins implicated in increasing microtubule nucleation from the centrosome by tethering or activating γ-TuRC. Co-depleting MAP7D3 with CLASPs, however, did not further reduce the microtubule density (**Fig. S2B, C**). Additionally, the remaining microtubule population seemed to be still organized at the centrosome. The depletion of MAP7D3 on its own reduced the microtubule density significantly (**Fig. S2B, C**). Therefore, MAP7D3 is involved in the nucleation of microtubules yet acts in a pathway downstream of CLASPs, as no further reduction was observed upon their co-depletion.

Microtubule depolymerizing agents do not increase microtubule density upon their removal

With the loss of such an indispensable stabilizing agent, we wondered whether microtubules would be more susceptible to depolymerizing agents. Among which are the mammalian kinesin-

13 family, that among others contains KIF2A and MCAK. KIF2A uses its ATPase activity to induce destabilizing conformations of the tubulin subunits, directly depolymerizing microtubules at the plus- and minus-end (Walczak, Gayek & Ohi, 2013). MCAK possesses end-stimulated ATPase activity, processively removing tubulin heterodimers, leading to microtubule depolymerization (Hunter *et al.,* 2003). As kinesin-13 family proteins are known to destabilize microtubules, we wondered whether their removal might increase the microtubule density in these cells and could partly restore the microtubule network in CLASP-depleted cells. Consequently, this would imply that CLASP removal might lead to an offset between microtubule depolymerizing agents and microtubule-stabilizing agents. To investigate this, we first depleted KIF2A alone in RPE1 C2KO cells and found no significant alterations in microtubule density when compared to control (**Fig. S3**). Furthermore, co-depletion of CLASPs with KIF2A was lethal to cells (data not shown), likely originating from the high stress induced on the cells.

CLASP-depletion strongly affects microtubule nucleation

CLASPs have been thoroughly identified as a microtubule-stabilizing +TIP, promoting rescue and inhibiting catastrophe (Yu *et al.,* 2016; Aher *et al.,* 2018). Additionally, CLASPs are significant for microtubule nucleation and organization at the Golgi-apparatus, with their removal leading to perturbation of noncentrosomal microtubules (Efimov *et al.,* 2007). Efimov *et al.* (2007) already observed this phenotype in cells depleted ~75% of both CLASP homologs. Therefore we investigated whether our rigorously CLASP-depleted cells would show even stronger phenotypes. First, we depolymerized microtubules from cells using the drug nocodazole, which sequesters soluble tubulin, sequentially inducing depolymerization of microtubules. After removing nocodazole, cells were allowed to re-polymerize their microtubule networks for 30 seconds at 37°C. We performed these nocodazole washout based microtubule nucleation assays on our strongly depleted RPE1 C2p53KO cells and counted the microtubules nucleated from the Golgi, centrosome, or cytosol (**Fig. 8A**).

Quantification of microtubule nucleation events originating at the Golgi, centrosome, and cytosol revealed a reduction in microtubules nucleated from all three MTOCs. Consistent with results found by Efimov *et al.* (2007), thorough CLASP-depletion resulted in an approximate 10.4-fold reduction in Golgi-based microtubule nucleation (50.7 ± 18.4 Golgi-based microtubule nucleations in control cells and 4.8 ± 3.0 Golgi-based nucleations in CLASP-depleted cells) (**Fig. 8B**, left panel). Furthermore, we observed a 2.68-fold reduction in microtubule nucleation in the cytosol (9.44 ± 5.33 cytosolic nucleations in control and 3.53 ± 3.22 cytosolic nucleations in CLASP-depleted cells) (**Fig. 8B**, right panel). CLASPs are implicated in lowering the critical threshold of soluble tubulin required for microtubule outgrowth *in vitro* (Aher *et al.,* 2018). Therefore, CLASPs might directly promote microtubule nucleation *in vivo*, explaining the loss in cytosolic-based microtubule nucleation upon their removal.

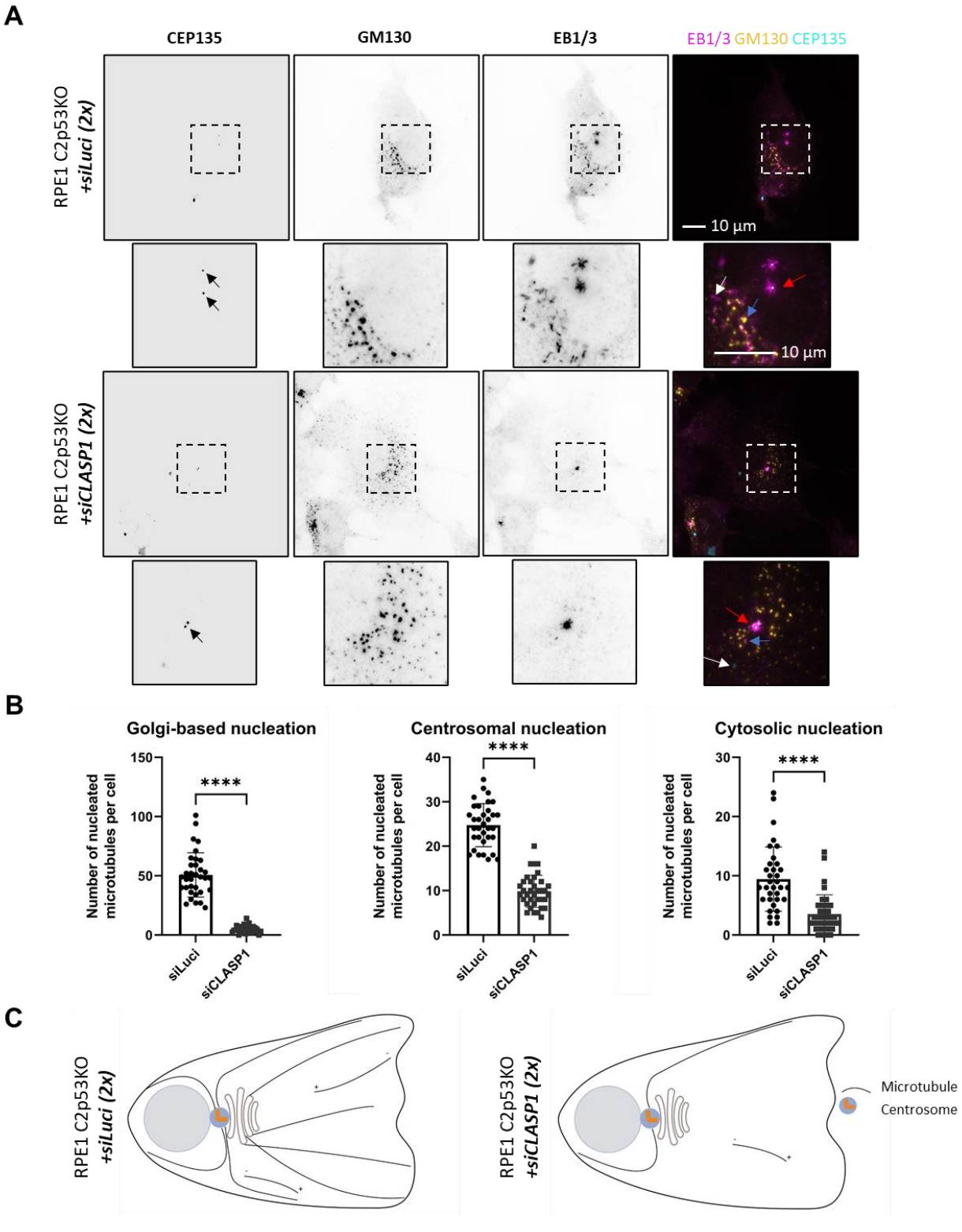
A
CEP135
GM130
EB1/3
EB1/3 GM130 CEP135
RPE1 C2p53KO
+siLuci (2x)
10 µm
10 µm
RPE1 C2p53KO
+siCLASP1 (2x)
B
Golgi-based nucleation
Centrosomal nucleation
Cytosolic nucleation
Number of nucleated microtubules per cell
****
siLuci
siCLASP1
C
RPE1 C2p53KO
+siLuci (2x)
RPE1 C2p53KO
+siCLASP1 (2x)
Microtubule
Centrosome

Figure 8. CLASP-depletion leads to a reduction in microtubule nucleation from the Golgi, centrosome, and cytosol. (A). *Immunofluorescence staining of RPE1 C2p53KO cells depleted with siCLASP1 (bottom-panels) or siLuciferase (top-panels) as a control, which were subjected to a nocodazole washout and allowed to recover for 30 seconds at 37°C before fixation. Cells were stained for the Golgi (GM130, yellow), centrioles (CEP135, cyan), and microtubules (EB1/3, magenta). Arrows point at centrosomal-based (red), Golgi-based (blue), and cytosolic-based (white) microtubule nucleation* ***(B).*** *Quantification of the number of nucleated microtubules that are Golgi-based (left panel), centrosomal-based (middle panel), or cytosolic-based (right panel) in the cells as mentioned above Per condition, 30 cells were used that were imaged from three independent experimental repetitions. Using an unpaired t-test gave a significance value of $p < 0.0001$, ****. The standard deviation is displayed through the error bars.* ***(C).*** *A schematic overview of the effect of CLASP-depletion on microtubule nucleation from the centrosome, Golgi, and cytosol.*

Interestingly, rigorous depletion of CLASPs revealed a 2.51-fold reduction in microtubules nucleated from the centrosome (24.74 ± 4.78 centrosomal nucleations in control cells and 9.83 ± 3.61 centrosomal nucleations in CLASP-depleted cells) (**Fig. 8B**, middle panel). This result has not been reported previously. Robin Hoogenbeen (2021, unpublished) deemed 72 hours of CLASP1 depletion insufficient to remove the CLASP1 signal from the centrosome, whereas two sequential 72-hour depletions were sufficient. Consequently, CLASPs became less abundant at the centrosome, reducing centrosomal-based microtubule nucleation, thus implicating a role of CLASPs in efficient nucleation from the centrosome. As previous studies did not deplete CLASPs to the same extent as reported here, they might have been unable to report a similar finding.

In summary, CLASP-depletion almost entirely perturbs nucleation from the Golgi-apparatus while lowering microtubule nucleation from the cytosol and centrosome (**Fig. 8C**).

The γ-tubulin signal at the centrosome is vastly reduced upon CLASP-depletion

Several core components required for centrosomal microtubule nucleation are also involved in Golgi-based microtubule nucleation (Sanders & Kaverina, 2015). Thus, it would not be unexpected for CLASPs to facilitate microtubule nucleation at both of these major MTOCs. Consistently, centrosomal nucleation is reduced upon CLASP-depletion (**Fig. 8B**), indicating a possible role here. Intriguingly, mass-spectrometry studies have revealed a potential interaction between CLASPs and the centriolar proteins CPAP and Ninein (Maffini *et al*., 2009). As CLASPs are thought to lower the kinetic barrier required for microtubule outgrowth from γ-TuRC at the Golgi (Sanders & Kaverina, 2015), they might be involved similarly at the centrosome. In an endeavor to investigate this, we immunofluorescently stained γ-tubulin in our CLASP-depleted cells. Strikingly, CLASP-depletion lowers the γ-tubulin signal at the centrosome by 4.9-fold (mean intensity of 16800.0 ± 4968.8 a.u. for control cells and mean intensity of 3421.0 ± 1573.3 a.u. for CLASP-depleted cells) (**Fig. 9A, B**). Due to the vital importance of γ-TuRC in the organization and nucleation of microtubules, we wondered whether the substantial reduction in microtubule density upon CLASP-depletion was γ-tubulin dependent. For this, we first depleted RPE1 wild-type cells with two γ-tubulin siRNAs targeting two different sequences, theoretically increasing the knockdown efficiency, and then compared the microtubule density in these cells with our CLASP-depleted cells (**Fig. 9C**). However, the efficiency of our γ-tubulin-depletion was low, with few cells reaching γ-tubulin intensities comparable to our CLASP-depleted cells. Therefore, we only compared cells with similar signals of γ-tubulin at the centrosome that are either depleted of γ-tubulin or CLASPs (**Fig. 9D**, top panel). Upon γ-tubulin-depletion, the microtubule density is not reduced to the same extent as upon CLASP-depletion (25.0 ± 4.5 microtubules/ 10 µm in γ-tubulin-depleted cells, 5.9 ± 0.7 microtubules/ 10 µm in CLASP-depleted cells, and 28.4 ± 3.7 microtubules/ 10 µm for control cells with an unaffected γ-tubulin localization to the centrosome)

(**Fig. 9D**, bottom panel), indicating that the reduction in the microtubule density is at least not fully γ-tubulin dependent.

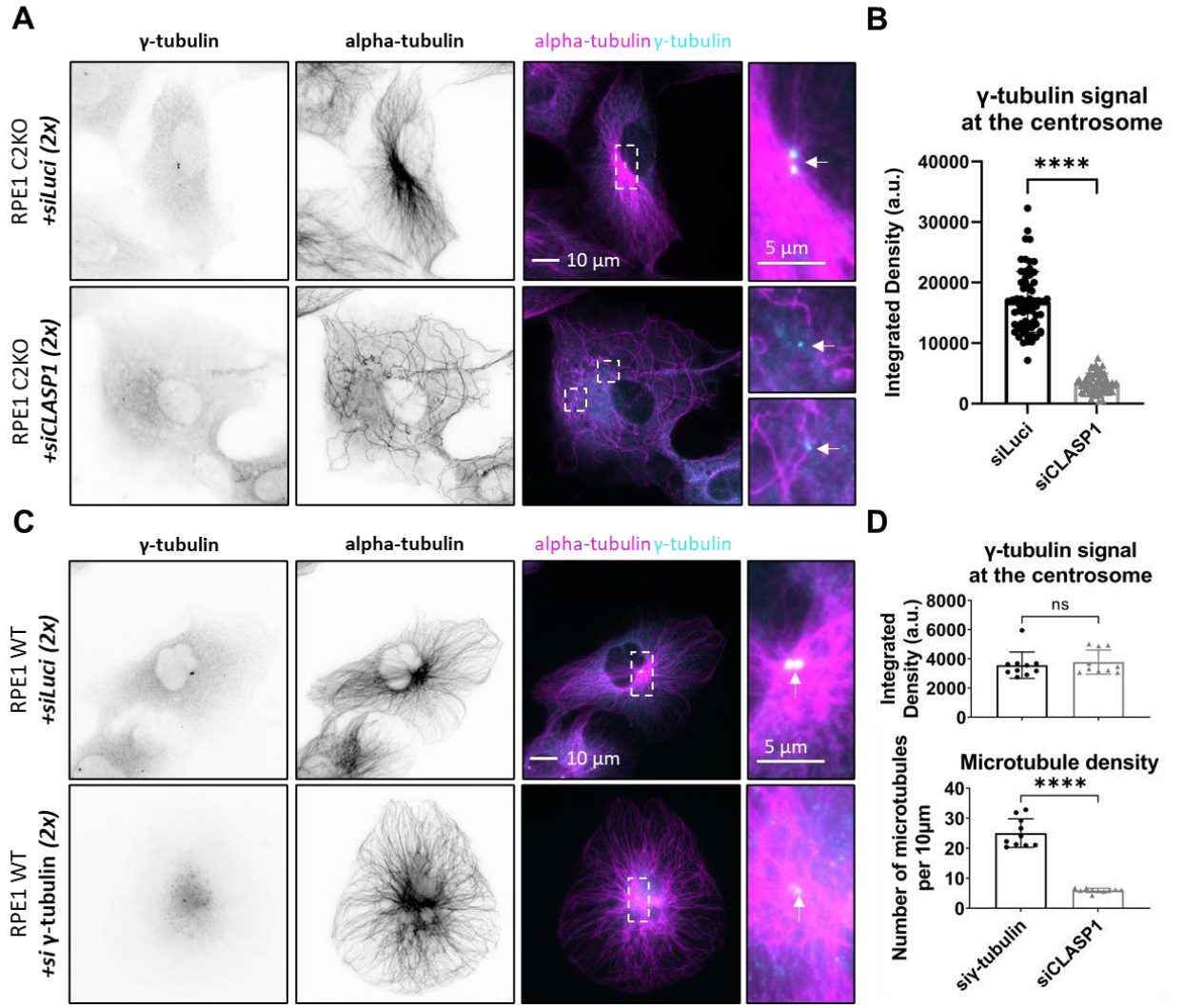

Figure 9. The γ-tubulin signal at the centrosome is vastly reduced upon CLASP-depletion. (A). *Immunofluorescence staining showing γ-tubulin signal in RPE1 C2KO cells depleted with siCLASP1 (bottom-panels) or siLuciferase (top-panels) as a control. The arrows in the insets point at the γ-tubulin at the centrosome.* ***(B).*** *Quantification of the γ-tubulin signal at the mother centrosome in the cells as mentioned above, represented in integrated density (a.u.). Using an unpaired t-test gave a p < 0.0001, ****. The standard deviation is displayed through the error bars.* ***(C).*** *Immunofluorescence staining of γ-tubulin in RPE1 wild-type cells depleted with siγ-tubulin (bottom panels) or siLuciferase (top-panels) as a control. The arrows in the insets point at the γ-tubulin at the centrosome.* ***(D).*** *Quantitative comparison of the microtubule density in RPE1 wild-type cells depleted with siγ-tubulin and RPE1 C2KO cells depleted with siCLASP1 (bottom-panel). For this, cells were compared with a similar integrated density of γ-tubulin at the centrosome (top-panel). For each condition, 10 cells were used that were imaged from three independent experimental repetitions. Using an unpaired t-test gave significance values of p < 0.0001, ****; and p = 0.5868, ns. The standard deviation is displayed through the error bars.*

Consistently, studies in *C. elegans* (Srayko *et al.,* 2005; Hannak *et al.,* 2002; Bobinnec *et al.,* 2000; Strome *et al.,* 2001;), *Drosophila* cells (Bouissou *et al.,* 2009), and human cells (Vinopal *et al.,* 2012; Tsuchiya & Goshima, 2021, preprint) have all shown a significant reduction in microtubule density upon γ-tubulin depletion, but not a complete loss of microtubules. Even removing the main microtubule nucleation template does not yield the same microtubule density

reduction as removing CLASPs, highlighting their crucial role in regulating the microtubule density. Interestingly, Tsuchiya *et al.* (2021, preprint) show that TPX2, CAMSAPs, chTOG, and CLASP1 are necessary for γ-tubulin-independent microtubule assembly in interphase. Herein, they report that removing γ-tubulin in combination with TPX2 or CLASP1, but not chTOG or CAMSAPs, led to a specific delay of microtubule growth. This delay implies a possible role of CLASP1 and TPX2 in the first stages of microtubule polymerization, possibly even nucleation.

PCM proteins, such as PCNT, NEDD1, CEP192, and CDK5RAP2 highly regulate γ-TuRC recruitment and tethering to the centrosome (Haren *et al.,* 2006; Choi *et al.,* 2010; Fong *et al.,* 2008; Zhu *et al.,* 2008; O'Rourke *et al.,* 2014; Lin *et al.,* 2014). Thus, we wondered whether their signal at the centrosome would also be reduced upon CLASP-depletion, subsequently leading to the observed reduction in γ-tubulin signal. Immunofluorescent stainings show a reduction in Ninein (**Fig. 10A, B**) and NEDD1 signal (**Fig. 10C, D**), a minor increase in PCNT signal (**Fig. 10E, F**), and no alteration in CEP152 (**Fig. S4A, B),** CDK5RAP2 (**Fig. S4C, D)** or CEP192 signal (**Fig. S4E, F)** at the centrosome, upon CLASP-depletion. As NEDD1 is known to bind γ-TuRC directly (Haren *et al.,* 2006; Wieckzorik *et al.,* 2020), its loss could also contribute to loss of the γ-TuRC population, thereby decreasing the γ-tubulin signal. However, no evidence suggests any direct interaction between CLASPs and NEDD1. Furthermore, the PCNT signal is minorly increased, which could be explained by its significant organization role in the PCM, where it may try to compensate for the loss of NEDD1 through its increase. Moreover, the CDK5RAP2 signal remains unaffected at the centrosome. CDK5RAP2 is recruited to the centrosome by binding to PCNT or AKAP450 through its centrosomin motif 2 (CM2) domain. As the PCNT signal is not reduced, rather minorly increased, CDK5RAP2 recruitment to the centrosome is not perturbed. Subsequently, we also investigated whether the integrity of the PCM would be retained upon CLASP-depletion. CEP152 also organizes and constitutes the PCM fibrils, yet it regulates the centrosome duplication and PCM size through interacting with Plk1 and CPAP (Cizmecioglu *et al.,* 2010; Mennela *et al.,* 2014). Therefore, reduction of CEP152 would implicate a smaller PCM, explaining the possible decrease in γ-TuRC signal upon CLASP-depletion. However, immunostaining shows that the CEP152 signal at the centrosome is not reduced upon CLASP-depletion (**Fig. S4A, B**).

Mass-spectrometry studies have shown a potential interaction between CLASPs and Ninein (Maffini *et al*., 2009). This coiled-coil rich protein localizes to the subdistal appendages of the mother centriole (Delgehyr *et al.,* 2005). Here, Ninein tethers γ-TuRC directly or tethers microtubules that lose their transient anchoring by γ-TuRC (Delgehyr *et al.,* 2005). CLASP-depletion substantially reduces the Ninein signal at the centrosome (**Fig. 10A, B**). Previously, it was found by Ariana Sandron (2019, unpublished) that knocking out Ninein from cells led to a significant separation of their two centrosomes. Consistently, we find that CLASP-depletion strongly increases the separation of the two centrosomes, together with the loss in the Ninein population (**Fig. S5)**. However, they also report that either the knock-out or depletion of Ninein from cells does not lower the γ-tubulin signal at the centrosome. Consequently, this implies that the reduction in Ninein signal at the centrosome does not correlate to the reduced γ-tubulin signal at the centrosome in our CLASP-depleted cells. Potentially, the loss of Ninein upon CLASPs depletion might reduce the anchoring of microtubules at the centrosome, consequently being partly responsible for the lack of microtubule organization that we observe. Furthermore, in light of our data, we cannot rule out any direct role of CLASPs in regulating the recruitment of γ-TuRC to the centrosome. However, further work needs to be done to dissect any direct interaction of CLASPs with γ-TuRC or NEDD1.

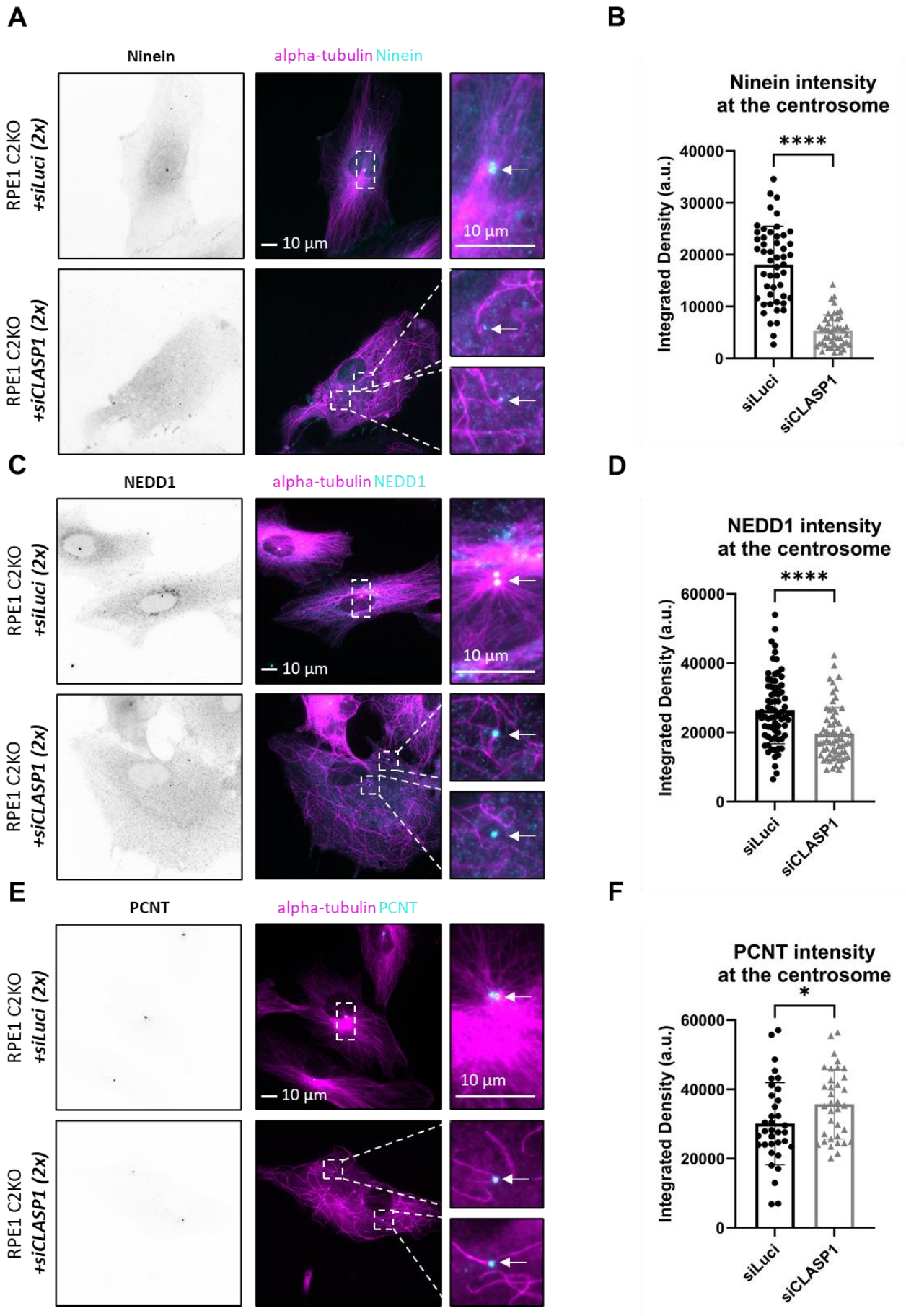
A
Ninein
alpha-tubulin Ninein
RPE1 C2KO +siLuci (2x)
RPE1 C2KO +siCLASP1 (2x)
10 µm
10 µm
B
Ninein intensity at the centrosome
****
Integrated Density (a.u.)
40000
30000
20000
10000
0
siLuci
siCLASP1
C
NEDD1
alpha-tubulin NEDD1
RPE1 C2KO +siLuci (2x)
RPE1 C2KO +siCLASP1 (2x)
10 µm
10 µm
D
NEDD1 intensity at the centrosome
****
Integrated Density (a.u.)
60000
40000
20000
0
siLuci
siCLASP1
E
PCNT
alpha-tubulin PCNT
RPE1 C2KO +siLuci (2x)
RPE1 C2KO +siCLASP1 (2x)
10 µm
10 µm
F
PCNT intensity at the centrosome
*
Integrated Density (a.u.)
60000
40000
20000
0
siLuci
siCLASP1

Figure 10. Centrosomal proteins Ninein, NEDD1, and PCNT show an altered signal at the centrosome upon CLASP-depletion. (A, C, E). *Immunofluorescent staining of* ***(A.)*** *Ninein,* ***(C.)*** *NEDD1, and* ***(E).*** *PCNT (cyan) in RPE1 C2KO cells depleted with siCLASP1 (bottom panels) or siLuciferase (top panels) control. The arrows in the insets point at the centrosomes.* ***(B, D, F)*** *Quantitative comparison of* ***(B).*** *Ninein,* ***(D).*** *NEDD1, and* ***(F).*** *PCNT signals at the centrosome in RPE1 C2KO cells depleted with either siCLASP1 or siLuciferase as a control. The following number of cells was used per condition: 46 cells for Ninein, 70 for NEDD1, and 35 for PCNT, which were imaged from at least three independent experimental repetitions. Using an unpaired t-test gave significance values of p < 0.0001, ****; and p = 0.036, *. The standard deviation is displayed through the error bars.*

Centrinone-B treatment robustly enhances the reduction in microtubule density upon CLASP-depletion

In our thoroughly CLASP-depleted cells, microtubules are mainly nucleated and organized from the centrosome (**Fig. 8A, B**). Thus, we postulated about the consequence of removing the centrosome in these microtubule scarce cells. In an endeavor to explore this, we used the well-established drug, Centrinone-B, which chemically inhibits Plk4, a serine-threonine protein kinase that initiates centriole-duplication (Wong *et al.,* 2015; Denu *et al.,* 2018). We combined

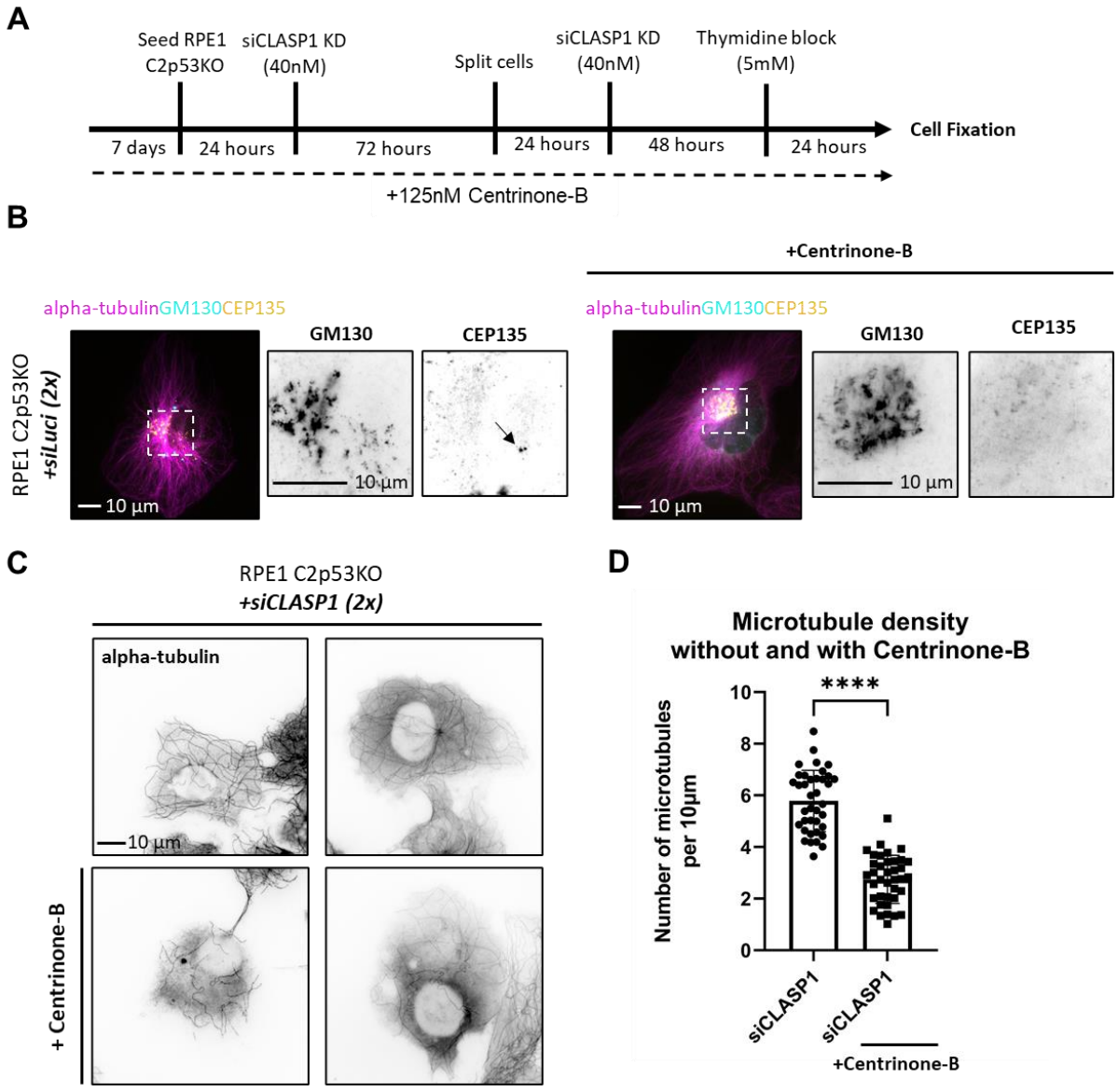

Figure 11. Treatment with Centrinone-B enhances the reduction in microtubule density upon CLASP-depletion. ***(A).*** *Schematic overview of the established double CLASP-depletion (Robin Hoogebeen, 2021, unpublished) combined with the Centrinone-B treatment.* ***(B).*** *Immunofluorescent staining of RPE1 C2p53KO cells depleted with siLuciferase that are either treated without (left panels) or with Centrinone-B (right panels). The black arrow in the inset points to the centrioles.* ***(C).*** *Immunofluorescent staining of RPE1 C2p53KO cells depleted with siCLASP1 treated without (top-panels) or with Centrinone-B (bottom-panels).* ***(D).*** *Quantitative comparison of the microtubule density in siCLASP1 depleted RPE1 C2p53KO cells that are either treated with or without Centrinone-B. For each condition, 30 cells were used that were imaged from three independent experimental repetitions. Using an unpaired t-test gave a significance value of $p < 0.0001$, ****. The standard deviation is displayed through the error bars.*

Centrinone-B treatment with our established CLASP-depletion protocol (**Fig. 11A**). Consequently, centrioles were depleted even in control cells, as no signal for CEP135 was observed (**Fig. 11B**), a known centriole biogenesis factor (Carvalho-Santos *et al.,* 2010). Centrinone-B treatment in RPE1 C2KO cells depleted of CLASPs did not yield a significant phenotype in microtubule density (data not shown), likely due to mitotic arrest induced by both the Centrinone-B treatment (Denu *et al.,* 2018) and CLASP-depletion (Mimori-Kiyosue *et al.,* 2006), consequentially inducing apoptosis through a p53-mediated pathway (Orth *et al.,* 2012). Interestingly, Centrinone-B treatment in CLASP-depleted RPE1 C2p53KO cells led to an even more significant reduction in microtubule density (**Fig. 11C, D**), highlighting the increase in viability upon p53 knock-out.

The combination of CLASP-depletion with Centrinone-B treatment abrupted any noticeable and significant MTOCs in cells, resulting in a vigorously reduced microtubule density (**Fig. 11D**). As the few remaining microtubules in these cells did not originate from any clear MTOCs, we set out to identify their nucleation sites. Thus, we depolymerized the microtubules with nocodazole in RPE1 C2p53KO cells depleted of CLASPs, treated with Centrinone-B, and let the microtubules re-nucleate for 30 seconds at 37°C **(Fig. 12A**). Treatment of Centrinone-B in control cells significantly increased the microtubule nucleation events from the Golgi by 1.65-fold compared to cells not treated with Centrinone-B (50.7 ± 18.4 nucleation events in control cells without Centrinone-B, and 83.7 ± 27.4 nucleation events in cells treated with Centrinone-B) (**Fig. 12B**, left panel). Logically, all the PCM components that cannot form a compact structure at the centrosome could localize to the Golgi instead, increasing the microtubule organization and nucleation here (Wu *et al.,* 2016). Strikingly, CLASP-depletion in these Centrinone-treated cells still almost wholly abrupted the Golgi-based microtubule nucleation **(Fig. 12B**, left panel). Due to treatment with Centrinone-B, no centrosomes were present. Thus, no centrosomal-based nucleation events were observed (**Fig 12B**, middle panel). However, the Centrinone-B treatment increased the number of microtubules nucleated in the cytoplasm by 2.0-fold compared to cells not treated with Centrinone-B (9.4 ± 5.3 cytosolic-based nucleation events in cells treated without Centrinone-B and 19.4 ± 10.0 cytosolic-nucleation events in cells treated with Centrinone-B) (**Fig. 12B**, right panel). Again, this is likely caused by the PCM components that cannot form their compact structure at the centrosome and instead form small clusters capable of microtubule nucleation in the cytosol. In cells, the centrosome is one of the major MTOCs, and removing the centrosome in these cells firmly shifts the MTOC to the Golgi and cytosol (**Fig. 12B, C**). Depleting CLASPs in these cells strongly perturbs the Golgi-based and cytosolic microtubule nucleation, leaving only a few nucleation events that mainly originate in the cytosol (**Fig. 12B, C**). Altogether, Centrinone-B treatment in combination with CLASP-depletion and p53 knock-out is a robust method to severely deplete the microtubule network and any MTOC in cells.

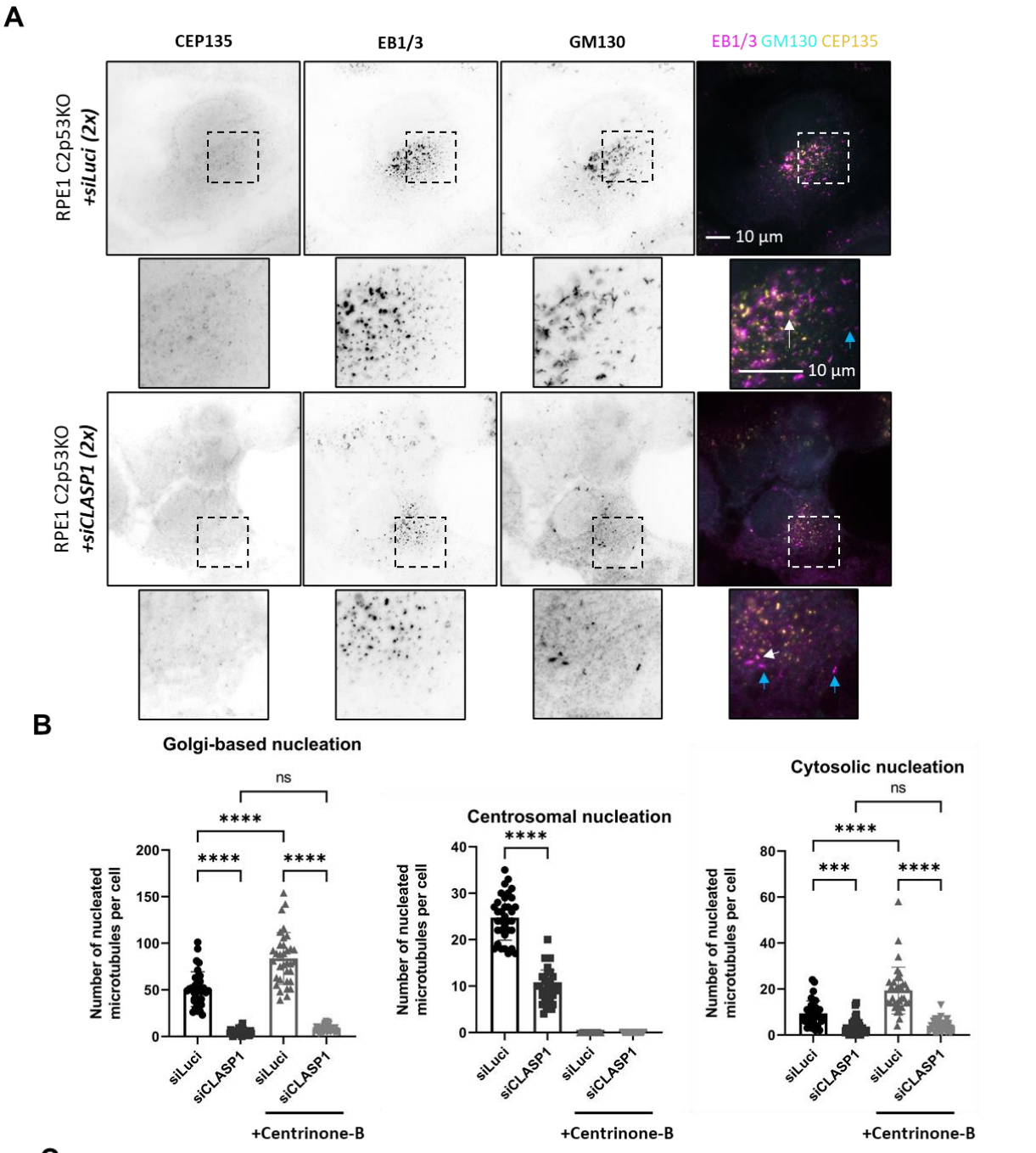
A
CEP135
EB1/3
GM130
EB1/3 GM130 CEP135
RPE1 C2p53KO
+siLuci (2x)
10 µm
10 µm
RPE1 C2p53KO
+siCLASP1 (2x)
B
Golgi-based nucleation
Centrosomal nucleation
Cytosolic nucleation
Number of nucleated microtubules per cell
ns
****
***
siLuci
siCLASP1
+Centrinone-B
C
+Centrinone-B
RPE1 C2p53KO
+siLuci (2x)
RPE1 C2p53KO
+siCLASP1 (2x)
Microtubule

Figure 12. CLASP-depletion in combination with Centrinone-B treatment results in few nucleated microtubules that mainly originate from the cytosol. (A). *Immunofluorescent staining of RPE1 C2p53KO cells treated with Centrinone-B and depleted with either siCLASP1 (bottom-panels) or siLuciferase (top-panels) as a control, which were subjected to a nocodazole washout and allowed to recover for 30 seconds at 37°C before fixation. Cells were stained for the Golgi (GM130, yellow), centrioles (CEP135, cyan), and microtubules (EB1/3, magenta). Arrows point at Golgi-based (white) and cytosolic-based (blue) microtubule nucleation.* ***(B).*** *Quantification of the number of nucleated microtubules that are Golgi-based (left panel), centrosomal-based (middle panel), or cytosolic-based (right panel) in the cells as mentioned above. For each condition, 30 cells were used that were imaged from three independent experimental repetitions. Using a One-Way Anova gave significance values of $p < 0.0001$, ****; and $p = 0.0004$, ***. The standard deviation is displayed through the error bars.* ***(C).*** *A schematic overview of the effect of CLASP-depletion combined with Centrinone-B treatment on microtubule nucleation from the centrosome, Golgi, and cytosol.*

CLASP-depletion in combination with Centrinone-B treatment perturbs the organization of the Golgi-apparatus and endoplasmic reticulum

It is well-known that the microtubule network plays a significant role in regulating membrane dynamics. Hence, we wondered how the intracellular organization of membranous organelles, such as the Golgi or endoplasmic reticulum (ER), would be affected in cells scarce of microtubules. The interaction between the Golgi-apparatus dynamics and the microtubule network has been extensively studied (Minin, 1997; Ho *et al.,* 1989; Thyberg & Moskalewski, 1999; Zhu & Kaverina, 2013). Apart from its role in the nucleation of microtubules, the Golgi-apparatus structural assembly is tightly regulated by microtubules (Minin, 1997; Ho *et al*., 1989; Chabin-Brion *et al.,* 2001). The dispersal of the Golgi membranes occurs upon depolymerization of microtubules (Minin, 1997), whereas newly polymerized microtubules and microtubule-associated motor transport drive its assembly (Ho *et al.,* 1989; Zhu & Kaverina, 2013). Consistent with the findings of Robin Hoogenbeen (2021, unpublished), the Golgi stacks are associated with a more compact barrel-like structure in CLASP-depleted cells, as opposed to its classic ribbon structure in control cells (**Fig. 13A,** left panels). It is well-known that microtubule-depolymerizing drugs are responsible for the dispersion of Golgi membranes (Zhu & Kaverina, 2013). Consistently, in cells depleted of CLASPs and treated with Centrinone-B, where the number of microtubules is extremely low, we observed a substantial dispersion of the Golgi-ministacks (**Fig. 13A,** right panels).

Furthermore, a strong interplay between the ER and the microtubule network is well-established (Klopfenstein *et al.,* 1998; Park & Blackstone, 2010; Gurel *et al.,* 2014). The ER is a large organelle extending throughout the entire cell and consists of interconnecting sheets and tubules. The ER has a crucial role in the synthesis, modification, quality control, and transport of proteins (Gurel *et al.,* 2014). The microtubule network regulates the ER distribution and its sheet/tubule ratio in mammalian cells (Therasaki *et al.,* 1986; Lee & Chen, 1988; Waterman-Storer & Salmon, 1998; Gurel *et al.,* 2014). Henceforth, we wondered how a severe reduction in microtubule density would affect this highly structured organelle. With the kind help of Milena Pasoli (Akhmanova lab, Department of Cell Biology, University of Utrecht), we stained for the ER chaperone, calnexin, in CLASP-depleted cells. Upon CLASP-depletion, we found that the ER assumes a more sheet-like structure with fewer visible tubules (**Fig. 13B**, left panels). However, in cells depleted of CLASPs and treated with Centrinone-B, where microtubules are even fewer, the tubular structures of the ER were lost completely (**Fig. 13B**, right panels). Consistently, depolymerization of the microtubule network with nocodazole causes the ER to retract from the periphery and lose its peripheral tubular structures for more extended sheet-like conformations (Lu *et al.,* 2009).

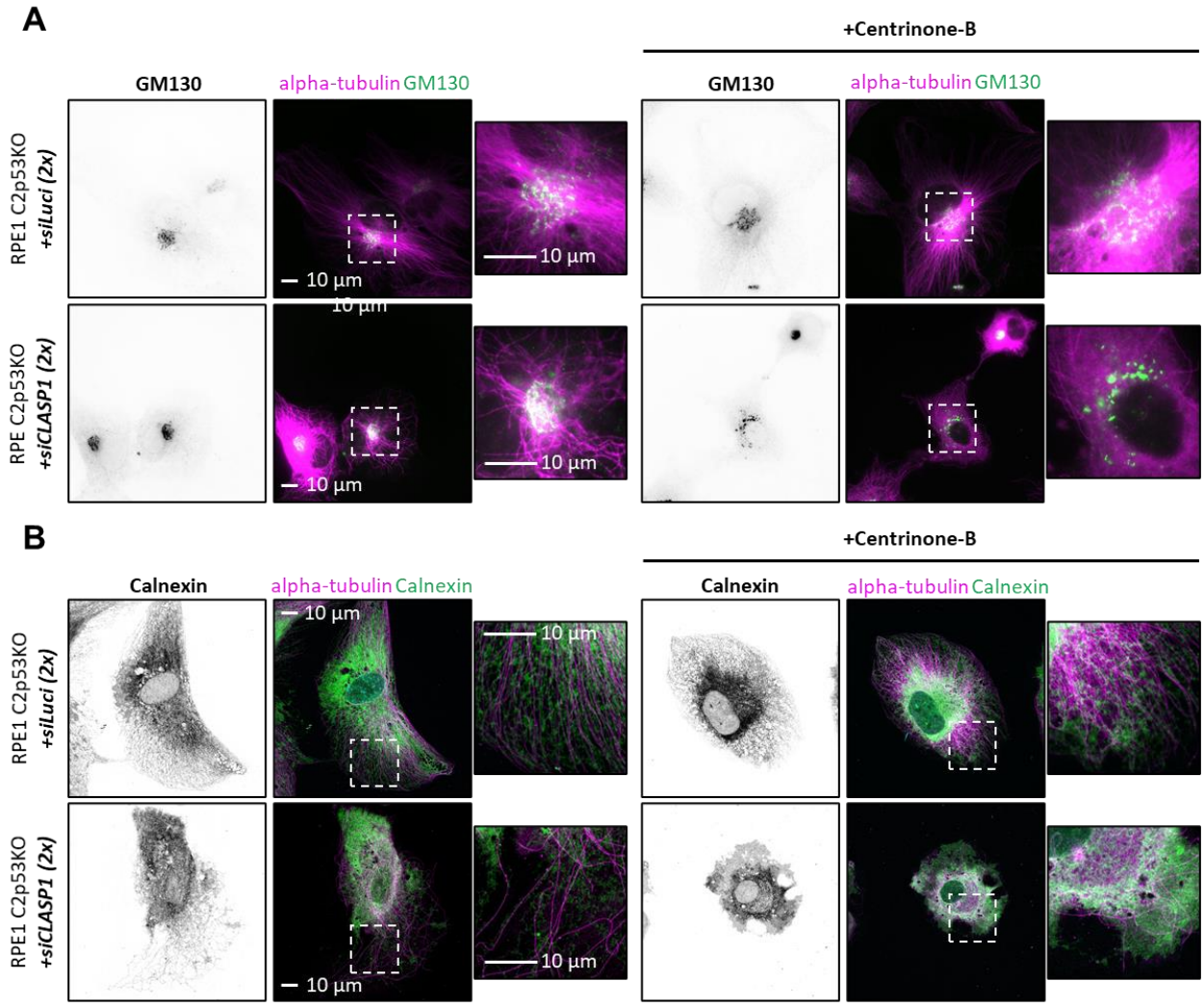

Figure 13. CLASP-depletion in combination with Centrinone-B treatment perturbs the organization of the Golgi-apparatus and endoplasmic reticulum. (A). *Immunofluorescence staining showing the structure of Golgi-apparatus in RPE1 C2p53KO cells treated with or without Centrinone-B depleted with siCLASP1 or siLuciferase as control. Cells were stained for GM130 (green) and alpha-tubulin (magenta)* ***(B).*** *Immunofluorescence staining showing the effect on the endoplasmic-reticulum structure in the cells as mentioned above. Cells were stained for Calnexin (green) and alpha-tubulin (magenta), which was performed together with Milena Pasoli (Akhmanova Lab, Department of Cell Biology, Utrecht University).*

A potential critical microtubule number is required for the proper distribution of organelles

In addition to the structure of organelles, we decided to look at the transport and distribution of organelles in our thoroughly microtubule-depleted cells. In cells, microtubules provide a framework for two classes of molecular motor-proteins, namely kinesins and dyneins, to move on (Barlan & Gelfand, 2017). As the intracellular distribution of organelles is highly dependent on microtubule-based transport by these motor proteins, we wondered how organelles were distributed in cells with a severely reduced microtubule density. We used immunofluorescence stainings to evaluate the distribution of mitochondria and Rab6 associated-vesicles.

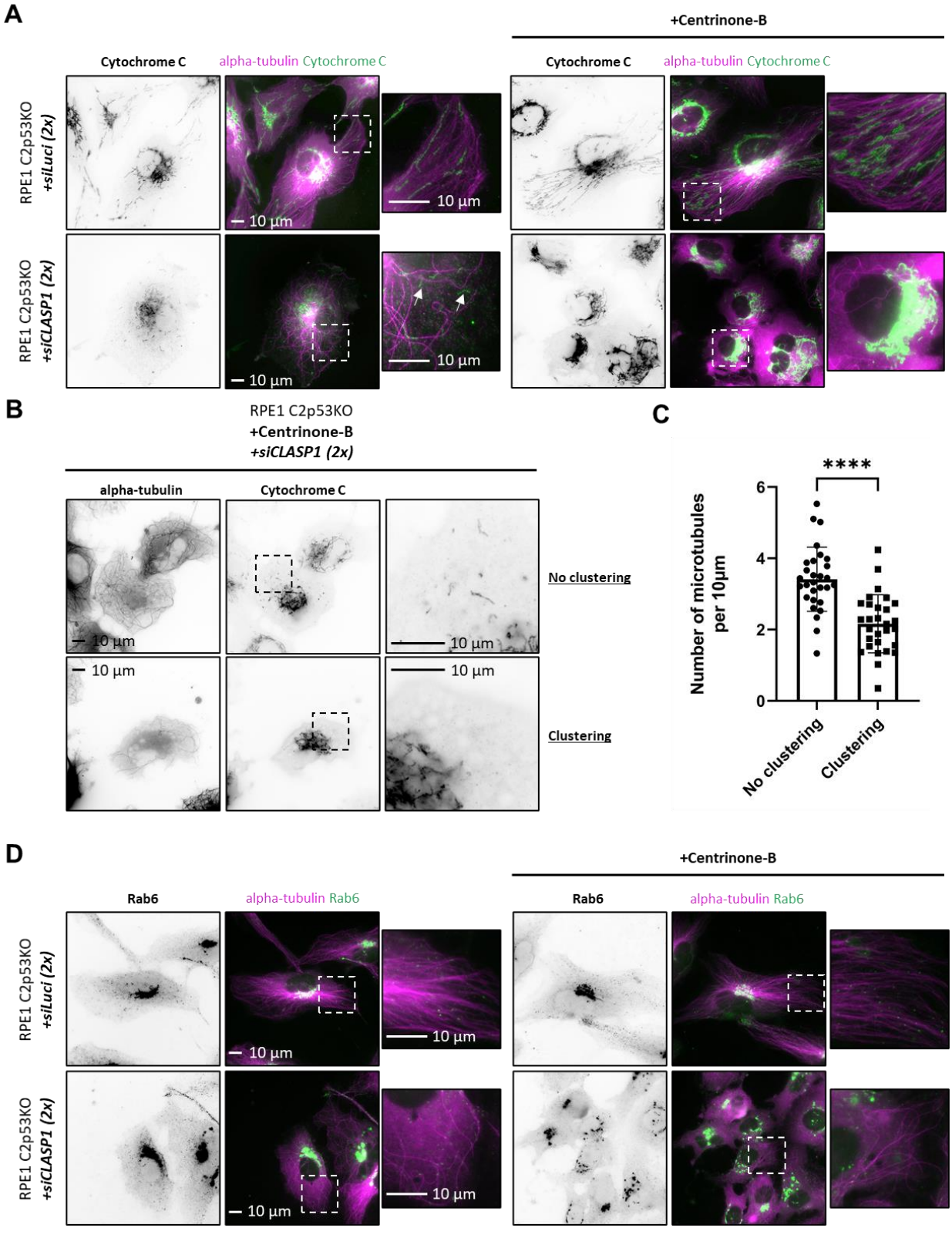
A
+Centrinone-B
Cytochrome C
alpha-tubulin Cytochrome C
Cytochrome C
alpha-tubulin Cytochrome C
RPE1 C2p53KO
+siLuci (2x)
RPE1 C2p53KO
+siCLASP1 (2x)
10 µm
10 µm
10 µm
10 µm
B
RPE1 C2p53KO
+Centrinone-B
+siCLASP1 (2x)
alpha-tubulin
Cytochrome C
No clustering
Clustering
10 µm
10 µm
10 µm
10 µm
C
****
Number of microtubules per 10µm
6
4
2
0
No clustering
Clustering
D
+Centrinone-B
Rab6
alpha-tubulin Rab6
Rab6
alpha-tubulin Rab6
RPE1 C2p53KO
+siLuci (2x)
RPE1 C2p53KO
+siCLASP1 (2x)
10 µm
10 µm
10 µm
10 µm

Figure 14. CLASP-depletion in combination with Centrinone-B treatment perturbs the distribution of mitochondria and Rab6$^+$-vesicles in RPE1 C2p53KO cells. (A). *Immunofluorescent staining showing RPE1 C2p53KO cells treated with or without Centrinone-B that are depleted with siCLASP1 or siLuciferase as a control, and how these treatments affect mitochondrial distribution. White arrows point at mitochondria in areas devoid of microtubules.* ***(B).*** *Immunofluorescent staining of cells treated with Centrinone-B and depleted with siCLASP1 that show either no clustering of mitochondria (top panels) or clustering of mitochondria around the nucleus (bottom panels).* ***(C).*** *Quantitative comparison of the microtubule density in the cells as mentioned above that show either no clustering or clustering. For each condition, 30 cells were used that were imaged from three independent experimental repetitions. Using an unpaired t-test gave a $p < 0.0001$, ****. The standard deviation is displayed through the error bars.* ***(D).*** *Immunofluorescent staining showing the effect of treatments as mentioned above on Rab6$^+$-vesicle distribution.*

Consistent with Robin Hoogenbeen (2021, unpublished), the distribution of mitochondria remained unaltered in CLASP-depleted cells, as they were still distributed towards the periphery (**Fig. 14A**). Concomitantly, in our CLASP-depleted cells, we observed mitochondria distributed in the cytoplasm in places devoid of microtubules, which we do not observe in control cells (**Fig. 14A, white arrows**). Possibly, these mitochondria are left behind when their microtubule track depolymerizes, or they are attached to the actin cortex. Interestingly, cells depleted of CLASPs and treated with Centrinone-B, with even fewer microtubules, show robust mitochondrial clustering around the nucleus (**Fig. 14A**). A similar phenotype has previously been reported by Hooikaas *et al.* (2019), where they perturbed the recruitment of kinesin-1, the motor protein responsible for mitochondrial transport, by removing its MAP7-family adapter proteins. These results made us hypothesize about a potential critical threshold of microtubule number required for the proper distribution of mitochondria or organelles in general. To investigate this, we looked at cells depleted of CLASPs and treated with Centrinone-B that showed either no clustering or clustering of mitochondria around the nucleus, and looked at their microtubule density (**Fig. 14B**). Upon comparing the two conditions, we found an approximate 1.6-fold reduction in microtubule density in cells that showed mitochondrial clustering compared to no clustering (3.4 ± 0.9 microtubules per 10 µm for no clustering and 2.2 ± 0.8 microtubules per 10 µm for cells with clustering) (**Fig. 14C**). These results indicate a potential critical threshold in the microtubule number required for the proper distribution of mitochondria around the cell. Furthermore, we looked at the distribution of another organelle, namely the Rab6-associated vesicles. Again, consistent with the results observed by Robin Hoogenbeen (2021, unpublished), Rab6-associated vesicle distribution was not affected upon CLASP-depletion when compared to control in Centrinone-B untreated cells. Strikingly, lowering the microtubule density further through treating CLASP-depleted cells with Centrinone-B resulted in less distribution towards the periphery of the cell when compared to control (**Fig. 14D**). Interestingly, we observed this phenomenon occur even in compartments of cells where several microtubules were present, strengthening our hypothesis of a potential critical number of microtubules required for the proper distribution of organelles. The vesicles that still reached the cell's periphery could have been distributed there by diffusion (Grigoriev *et al.,* 2007).

Discussion

Here, we report a severe reduction in microtubule density upon thorough removal of both CLASP homologs, which, to our knowledge, has not been reported before at this extent. Comparison of the density in the microtubule network upon CLASP-depletion with, for example, the quadruple knock-out cell line of Wu *et al.* (2016) further emphasizes the essential role of CLASPs in regulating the microtubule density. This cell line is a knock-out of CAMSAP2, AKAP450, Myomegalin, and CDK5RAP2, all implicated in microtubule organization from the Golgi-

apparatus. The removal of all these essential proteins still does not result in a similar reduction in microtubule density as removal of both mammalian CLASP homologs. Furthermore, co-depleting NEDD1 and PCNT in these cells, both involved in the recruitment and tethering of γ-TuRC at the centrosome, leads to a less organized and dense microtubule network (Chen *et al.,* 2021, preprint). Yet, efficient depletion of both mammalian CLASP homologs still yields a more substantial reduction in microtubule density and organization. Accordingly, this highlights the indispensable role of mammalian CLASPs in regulating the microtubule density during interphase.

The depletion of CLASPs has previously been shown to abrupt Golgi-based organization almost entirely (Efimov *et al.,* 2007). Yet, centrosomal-based microtubule organization did not seem to be affected in these experiments. Robin Hoogenbeen (2021, unpublished) reports that the conventional 72-hour depletion of CLASP1 in RPE1 C2KO cells is insufficient to remove the CLASP1 signal from the centrosome, whereas it is removed from the Golgi. Therefore, they developed a sequential 2-times depletion protocol of CLASP1 in these RPE1 C2KO cells, removing the CLASP1 signal from the centrosome as well. As previously mentioned, a cell line incapable of microtubule organization from the Golgi still had a higher microtubule density than cells depleted of CLASPs, indicating an additional role of CLASP in regulating the microtubule density. We found that efficient depletion of CLASPs results in a lower number of microtubules nucleated from the centrosome. A few proteins involved in Golgi-based nucleation are also implicated in efficient centrosomal nucleation (Kaverina & Sanders, 2015), where CLASP could also regulate efficient microtubule nucleation from γ-TuRC. Consequently, we found CLASP-depletion to greatly diminish the γ-tubulin signal at the centrosome, implying that its localization or recruitment is compromised. In CLASP-depleted cells, we investigated this reduction further by visualizing the localization of various centrosomal γ-TuRC tethering and recruiting proteins. Here, we found several proteins to be altered in their signal; namely, the NEDD1 and Ninein signal was reduced, whereas the PCNT signal was slightly increased, while CEP192, CEP152, and CDK5RAP2 remain unaltered.

The loss of NEDD1 is interesting, as NEDD1 is one of the main γ-TuRC recruitment factors at the PCM (Haren *et al.,* 2006; Lüders *et al.,* 2006). Consequentially, its depletion results in perturbation of γ-TuRC recruitment to the centrosome (Haren *et al.,* 2006). Moreover, Wieczorek *et al.* (2020) suggest that NEDD1 might be associated with GCP6 inside the γ-TuRC complex, where Plk1 could subsequentially phosphorylate it to drive centrosomal recruitment (Haren *et al.,* 2006; Johmura *et al.,* 2011). Therefore, the loss of NEDD1 upon CLASP-depletion might indicate loss of NEDD1 associated γ-TuRC and can thus lead to reduced γ-tubulin signal through inefficient γ-TuRC recruitment at the centrosome.

CLASPs are known to interact with Ninein (Maffini *et al.,* 2009; Arianna Sandron, 2019, unpublished), and depletion of either protein lowers the centrosomal signal of the other (Logarinho *et al.,* 2012; Fangrui Chen, unpublished). Ninein anchors microtubules at the subdistal appendages of the centrosome, where its C-terminus binds to the centriole, and its N-terminus interacts with γ-TuRC (Delgehyr *et al.,* 2005). However, efficient depletion or the knock-out of Ninein does not alter γ-tubulin levels at the centrosome (Arianna Sandron, 2019, unpublished). Interestingly, microtubule seeds nucleated distant from the subdistal appendages are temporarily anchored by γ-TuRC and steadily released from the centrosome (Keating & Borisy, 1999; Abal *et al.,* 2002). Therefore, Ninein might promote microtubule organization by docking γ-TuRC, followed by anchoring the microtubule (Delgehyr *et al.,* 2005). Thus, the loss of Ninein at the subdistal appendages might reduce microtubule organization at the centrosome. Consequently, Ninein

might be responsible for a part of the reduction in microtubule organization we observe upon removal of CLASPs.

Moreover, CLASP-depletion led to a slight increase in PCNT signal at the centrosome. PCNT is a significant structural component of the PCM responsible for recruiting CDK5RAP2, CEP192, and its binding partner NEDD1 and dispositioning them inside the concentric layers of the PCM (Menella *et al.,* 2014; Woodruff *et al.,* 2014). No links between CLASPs and PCNT are known from literature, including mass-spectrometry studies. Thus, CLASPs are unlikely to be directly involved in PCNT localization to the centrosome. However, as a significant structural component of the PCM, PCNT might try to compensate structurally for the loss of other proteins inside the concentric layers of the PCM, subsequently preventing loss of PCM size. Interestingly, the CEP152 and CEP192 signals at the centrosome remain unaltered upon CLASP-depletion. These proteins cooperate in recruiting Plk4, which subsequently initiates the centriole duplication pathway (Sonnen *et al.,* 2013). Thus, any perturbation in their localization to the centrosome would fail to induce centriole duplication. Moreover, CEP192 synergizes with PCNT and CDK5RAP2 to accumulate PCM components during mitosis (Gomez-Ferreria *et al.,* 2007; Zhu *et al.,* 2008), meaning its loss might have imposed perturbation on centrosome maturation. Additionally, CEP192 is responsible for recruiting NEDD1 to the centrosome, which acts as the significant centrosomal γ-TuRC recruiting factor (Haren *et al.,* 2006; Lüders *et al.,* 2006). However, as both CEP152 and CEP192 signal is not altered upon depletion of CLASPs, their implicated pathways of centriole duplication would still function; and therefore, loss of NEDD1 and γ-TuRC could be a direct effect of CLASP-depletion.

Furthermore, the CDK5RAP2 signal at the centrosome was not altered upon CLASP-depletion. Interestingly, the PCNT signal, which recruits CDK5RAP2 to the centrosome in interphase (Woodruff *et al.,* 2014), slightly increased upon CLASP-depletion. The CM1 domain of CDK5RAP2 has been shown to not only tether γ-TuRC but also increase its microtubule nucleation activity (Choi *et al.,* 2010). Therefore, if this protein would be reduced due to CLASP-depletion, it might have explained the reduced centrosomal-based microtubule nucleation we observed. Moreover, the depletion of CDK5RAP2 demonstrated to reduce γ-tubulin signals at the centrosome during mitosis and led to mitotic defects (Fong *et al.,* 2008). However, as its signal is not reduced, it is not responsible for the reduction in the γ-tubulin signal we observe upon CLASP-depletion. Altogether, our data suggests that CLASPs might not only act at the early stages of microtubule assembly, as suggested previously, but they can also act downstream in PCNT and CEP192 pathways and might be directly involved in the recruitment of NEDD1 or γ-TuRC. Besides, the functional role of its interaction with Ninein and CPAP still needs to be investigated further.

Additionally, we observed that efficient depletion of CLASPs reduces the number of microtubules nucleated from the cytosol. *In vitro* experiments performed by Wieczorek *et al.* (2015) show that microtubule depolymerizing and catastrophe factors, such as MCAK, slow down templated microtubule nucleation and increase the soluble tubulin concentration required for outgrowth. Moreover, they show that anti-catastrophe factors and microtubule polymerases promote templated microtubule outgrowth, reducing the soluble tubulin concentration required for outgrowth. Consistently, Aher *et al.* (2018) show that CLASPs promote templated microtubule outgrowth *in vitro* by lowering the critical concentration of free soluble tubulin. Moreover, in mammalian cells, removal of γ-tubulin does not result in a complete loss of microtubule nucleation (Srayko *et al.,* 2005; Bobinnec *et al.,* 2000; Strome *et al.,* 2001; Hannak *et al.,* 2002*;* Bouissou *et*

al., 2009*;* Vinopal *et al.,* 2012). Supportive of this, a recent preprint (Tsuchiya & Goshima, 2021 preprint) implicates different MAPs, including chTOG and CLASP1, to be involved in microtubule generation in the absence of γ-tubulin during interphase. Here, they showed that co-depleting CLASP1 with γ-tubulin, but not co-depleting chTOG with γ-tubulin, delays the first appearance of microtubules. This delay indicates that CLASP1 is involved in the initial phases of microtubule assembly, possibly even in nucleation, in cells lacking γ-tubulin during interphase. As both *in vitro* and *in vivo* data indicate a potential role of CLASPs in promoting microtubule nucleation, the loss in cytosolic-based nucleation we observed in this study could be regulated by CLASPs directly.

Microtubules can assemble and show regular dynamics *in vitro* in the absence of CLASPs. However, based on our results, CLASPs are critical regulators of microtubule density in cells. Therefore, we investigated a potential offset in the balance between the microtubule-stabilizing role of CLASPs and the microtubule destabilizing factors in cells, such as kinesin-13 family proteins (Walczak, Gayek & Ohi, 2013) or stathmin (Belmont & Mitchison, 1996). Here, CLASP removal would leave microtubules less protected against the destabilization and eventual depolymerization induced by said factors. We found that depletion of KIF2A, a member of the kinesin-13 family, does not change the microtubule density in cells, indicating that removing one such destabilizing factor is not sufficient to alter the balance between microtubule-stabilizing and destabilizing factors, if active at all; and therefore in regulating the microtubule density. However, co-depletion of KIF2A with CLASPs was highly lethal to cells, possibly due to high-stress levels induced by the removal of two essential mitotic proteins. Furthermore, it could also be that multiple depolymerizing agents act together upon the removal of CLASPs.

The depletion of CLASPs does not solely lead to a potential offset in forces; it also results in a robust reduction in microtubule density. Therefore we wondered how structures highly dependent on microtubules, like the Golgi, would react in these cells, where microtubules are intrinsically low. It is known that the assembly of a single Golgi-apparatus structure depends on both centrosomal and Golgi-derived microtubules (Wu & Akhmanova, 2017). As such, the Golgi disperses upon depolymerization of microtubules and restructures through newly polymerized microtubules and interactions with motor-proteins (Minin, 1997*;* Ho *et al.,* 1989; Zhu & Kaverina, 2013). Interestingly, cells knocked out of AKAP450, which is essential for Golgi-based microtubule organization, and depleted of centrioles through Centrinone-B, were still able to form a single compact Golgi structure, densely populated by transport vesicles upon the regrowth of their microtubule network (Wu *et al.,* 2016). Importantly, these cells were still abundant in non-centrosomal microtubules. This data indicates that the restructuring of the Golgi is driven by microtubule-based transport instead of microtubule anchoring from the Golgi. Upon CLASP-depletion, we observed a phenotype consistent with previous observations by Wu *et al.* (2016) found in RPE1 AKAP450 knock-out cells. The reduction in microtubule density altered the Golgi morphology to a more dense barrel-like structure compared to its classical ribbon-like structure. Interestingly, CLASP-depletion does not change the perinuclear localization of the Golgi. During mitosis, the then dispersed Golgi mini-stacks are restructured and relocated to surround the nucleus by dynein-based transport on centrosomal-derived microtubules (Miller *et al.,* 2009; Zhu & Kaverina, 2013). Consistently, we found that chemically removing the centrosome, and thus centrosomal-based microtubule nucleation, in CLASP-depleted cells almost entirely dispersed the Golgi, likely owing to the lack of centrosomal-derived microtubules, which allow dynein to structure the Golgi. These data highlight the importance of the microtubule network in the organization of the Golgi-apparatus.

Centriole depletion using Centrinone-B treatment in our CLASP-depleted cells led to an even more severe reduction in microtubule density. In these cells, we found that the distribution of Rab6-positive vesicles and mitochondria was strikingly perturbed. As Golgi-based microtubules are polarized, they can drive asymmetric vesicle transport throughout the cell (Vinogradova *et al.,* 2009; Hurtado *et al.,* 2011). We found the reduction in microtubule density upon removal of CLASPs insufficient for perturbation of Rab6-positive vesicle distribution, likely due to the centrosomal-based microtubules being sufficient for their distribution. Interestingly, removing the centrosome in CLASP-depleted cells, and thus the centrosome-derived microtubules, resulted in fewer Rab6-positive vesicles distributed towards the cell's periphery. Consistently, cells depleted of CLASPs and their centrosome showed a robust clustering of mitochondria around the nucleus, while this phenotype was not apparent by just depleting CLASPs. Hence we hypothesize about a potential critical threshold in microtubule number required for proper distribution of organelles. The same mitochondrial clustering phenotype was observed by Hooikaas *et al.* (2019), where they perturbed kinesin-1 recruitment to the microtubules by depleting its adapter proteins, MAP7, MAP7D1, and MAP7D3. In neurons, MAP7 competes with tau to direct motor transport (Monroy *et al.,* 2018). As MAPs can compete for binding to microtubules, and overexpression of MAPs usually leads to complete microtubule lattice binding, the presence of few microtubules in our CLASP-depleted, centrosome-lacking cells could induce a vast competition for the binding of different MAPs. Consequentially, this could imply that MAPs with an intrinsically higher affinity for the microtubules could outcompete others for binding places. This competition could lead to drastically altered microtubule dynamics and loss of, for example, the MAP7 population required for kinesin-1 recruitment, sequentially required for mitochondrial transport.

We found the microtubule dynamics to be minorly altered upon removal of CLASPs. Here, the microtubule growth rate was significantly increased upon their removal, likely owing to the role of CLASPs in slowing down microtubule growth *in vitro* and an increase in the available soluble tubulin pool (Moriwaki & Goshima, 2016; Yu *et al.,* 2016; Aher *et al.,* 2018). Counterintuitively, CLASP-depletion minorly decreased the catastrophe frequency of microtubules. This is surprising due to the well-established role of CLASPs in reducing the catastrophe frequency (Yu *et al.,* 2016; Aher *et al.,* 2018). However, we should note that the remaining microtubules in CLASP-depleted cells are very long and curly and often loop and spread around the entire cell, indicating that they could be a highly stable population of the microtubules. Moreover, we observe microtubules growing for prolonged periods, steadily increasing their total microtubule polymer mass. As these microtubules grow for more extended periods, they would be expected to become more unstable through the intrinsic 'ageing' property of microtubules (Gardner *et al.,* 2011; Coombes *et al.,* 2013), unless certain factors highly stabilize them. However, in this study, we were unable to identify such potential stabilizing factors acting on the remaining microtubules.

To date, we have been unable to extend the scope of our research to another mammalian cell line. Previously, we attempted to reduce the microtubule density through CLASP-depletion in U2OS C2KO cells (Tonja Pavlovič, 2018, unpublished). Yet, these cells were sensitive to our rigorous CLASP-depletion, and thus their viability was low. Due to our success in increasing cell viability upon knocking out p53, we also knocked out p53 in U2OS C2KO cells. Although the viability was still low, we could strongly reduce the microtubule density in these U2OS C2p53KO cells, albeit only in ~1-2% of the cells. Optimizing CLASP-depletion in this cell line will allow us to confirm our findings in an additional, non-epithelial, cancerous cell model.

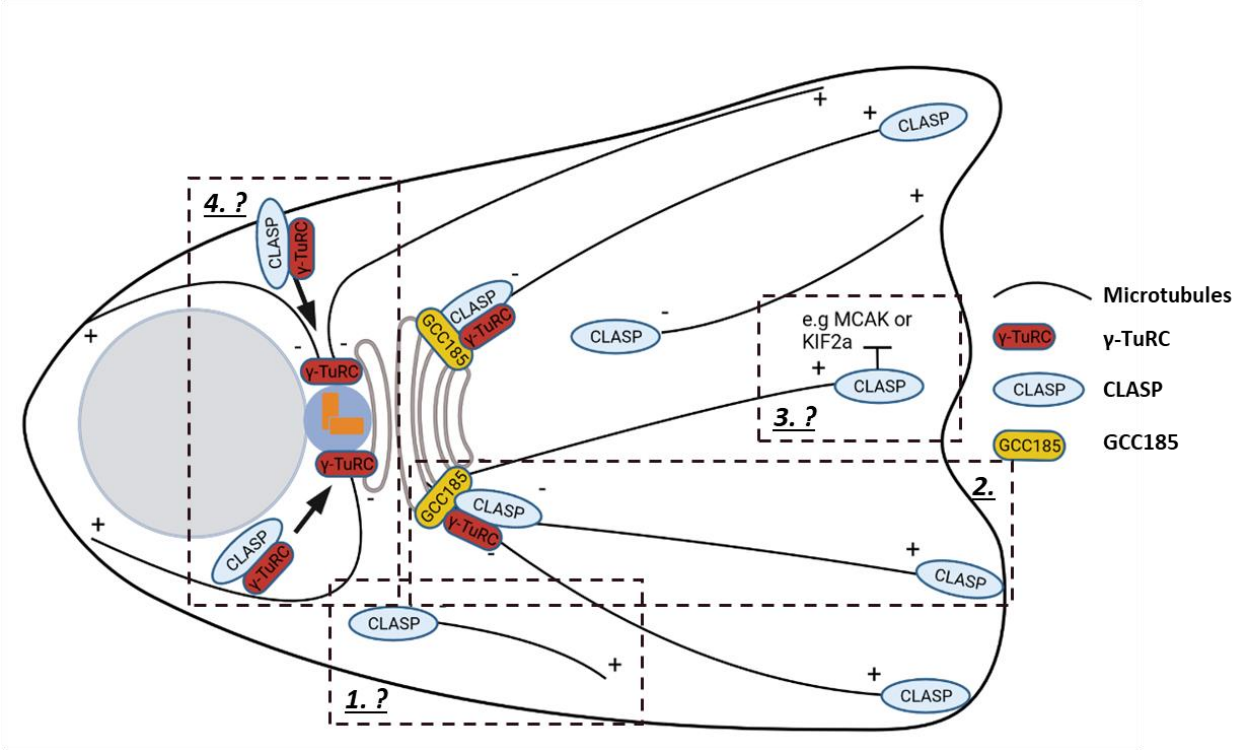

Figure 15. Model showing the possible roles of CLASP in regulating the microtubule density during interphase. ***1.*** *CLASP-depleted cells show a reduction in microtubule nucleation events in the cytosol, indicating that CLASP has either a direct or partnered role in the nucleation of microtubules in the cytosol.* ***2.*** *Moreover, consistent with previous findings, this study reports a substantial reduction in microtubule nucleation from the Golgi upon depletion of CLASP, highlighting the previously published, critical role of CLASP in Golgi-based nucleation* ***3.*** *Furthermore, CLASP is a strong microtubule-stabilizing protein. Therefore, its removal might offset the balance of stabilizing and depolymerizing agents (e.g., MCAK, KIF2A, Stathmin), which could depolymerize more microtubules, resulting in a loss of density.* ***4.*** *Finally, this study reports a reduction in γ-tubulin signal at the centrosome upon CLASP-depletion. We could not find any clear explanation for this loss by looking at known γ-tubulin interactors, although we cannot rule out NEDD1 completely. Even though no direct interaction of CLASP and γ-tubulin/γ-TuRC is known, we cannot rule out any direct role of CLASP in the recruitment of γ-TuRC at the centrosome.*

Summarizing, we list the potential and known functions of CLASPs in regulating the microtubule density based on the phenotypes we observed on their removal and known literature (**Fig. 15**). Firstly, CLASPs have been shown to lower the tubulin concentration required for microtubule outgrowth *in vitro* (Aher *et al.,* 2018) and are possibly implicated in nucleating microtubules independent of γ-tubulin (Tsuchiya & Goshima, 2021 preprint). Furthermore, thorough CLASP-depletion perturbs nucleation from the cytoplasm. Taken together, these data indicate that CLASPs could be regulating microtubule nucleation and organization in the cytoplasm directly (**Fig. 15, panel 1**). Next, CLASPs have multiple well-established roles in microtubule organization at the Golgi. Here, CLASPs are thought to lower the kinetic barrier required for microtubule outgrowth from γ-TuRC (Sanders & Kaverina, 2015). Additionally, they are necessary for stabilizing the microtubule stretches decorated by CAMSAP2 (Wu *et al.,* 2016). Moreover, CLASPs can tether microtubules through binding to the *trans*-Golgi protein GCC185 (Efimov *et al.,* 2007). Consequentially, rigorous depletion of CLASPs results in an almost total loss of Golgi-derived microtubules (**Fig. 15, panel 2**). Additionally, CLASPs have a role in stabilizing the plus-end of microtubules by preventing catastrophe and increasing rescue frequency (Aher *et al.,* 2018). Here it might reside in a balance with microtubule destabilizing agents, such as MCAK, KIF2A, or stathmin, that induce microtubule destabilization and sequentially depolymerization.

However, as we were unable to find data supporting this hypothesis, it will require more thorough investigation (**Fig. 15, panel 3**). Finally, we report a reduction in centrosomal-based nucleation upon rigorous CLASP-depletion, likely owing to the significant decrease in the centrosomal γ-tubulin signal that we observed. As we were unable to find a reduction in centrosomal localization of γ-TuRC interacting proteins that could explain our results, apart from a slight decrease in NEDD1, we cannot exclude any direct involvement of CLASPs in γ-TuRC recruitment to the centrosome (**Fig. 15, panel 4**).

In conclusion, we highlight the extreme significance of CLASPs in regulating the microtubule density in RPE1 cells, possibly extended to other cell lines as well, owing to their varied roles in microtubule nucleation and stabilization. Moreover, removing the centrosome in CLASP-depleted cells unveiled a reduction in microtubule density, that to our knowledge, has not been observed before, revealing a critical threshold requirement for regulating the efficient distribution of organelles.

Materials & Methods

Cell culture, knockdowns, and drug treatment.

RPE1 wild-type, RPE1 C2KO, RPE1 C2p53KO, and U2OS C2p53KO cells were cultured in a medium containing 90% Dulbecco's Modified Eagle Medium (DMEM, Lonza) and 10% Fetal Calf Serum (FBS, GE Healthcare) supplemented with 1% streptomycin and penicillin (Sigma-Aldrich). Cells were cultured in incubators set at 37°C and 5% CO_2. Knockdowns were achieved by transfecting siRNAs incubated for 12 minutes at room temperature with lipofectamine RNAiMAX (Thermofisher Scientific) in a 3:1 volume ratio (RNAiMAX:siRNA). The following siRNA concentrations were used: 40 nM CLASP1 siRNA; 20 nM γ-tubulin siRNA; 25 nM MAP7D1 siRNA; 25 nM MAP7D3 siRNA; 20 nM KIF2A siRNA; or 20 nM chTOG siRNA. 40 nM Luciferase siRNA was used as a control. Sequences of siRNA's are listed in the key reagent table below. For a two-round, sequential knockdown, cells at 30% confluency were incubated with the desired siRNA for 72 hours. Next, the already depleted cells were seeded again to 40-50% confluency and were subsequentially allowed to recover for 24 hours. Cells were then transfected with the desired siRNA again, refreshing the medium after 24 hours. Finally, cells were treated for 24 hours with medium supplemented with 5 mM thymidine to block cell proliferation, followed by fixation or lysate preparation.

Removal of centrioles was achieved by treating RPE1 C2p53KO cells with a complete medium supplemented with 125 nM Centrinone-B for seven days before additional treatments. The Centrinone-B containing medium was refreshed daily. Moreover, during the Centrinone-B treatment, cell confluency was maintained below 70-90% confluency.

For the microtubule nucleation assay, RPE1 C2p53KO cells treated with siRNA and Centrinone-B were treated with a complete medium supplemented with 10 µM nocodazole for 1 hour at 37°C, 5% CO_2, followed by an additional hour on ice to accomplish complete microtubule disassembly. Cells were then washed at least six times with an ice-cold 1x PBS before being moved to a 37°C water bath where a pre-warmed medium was added to the cells to allow microtubule regrowth. After 30 seconds of regrowth, cells were subsequentially fixed with methanol.

Generation of U2OS C2p53KO knock-out cell lines

Cells were knocked out of their p53-encoding gene through the previously established CRISPR/Cas9 method (Ran *et al.,* 2013). In brief, U2OS C2KO cells (Tonja Pavlovič, 2018,

unpublished) were transfected with the pSpCas9-2A-Puro (PX459) vector in a 1:3 v/v ratio with FuGENE 6 (Promega). The guide sequences targeting p53 were previously cloned into a PX459 vector and kindly provided to us by Fangrui Chen (see key reagent table below, Akhmanova lab, department of Cell Biology at Utrecht University). After 24 hours, the medium was replaced by a medium supplemented with 20 µg/mL of Puromycin. Cells were selected for 4 days, after which the cells were recovered for 10 days in regular culture medium. After recovery, ~100 cells were seeded into a 15 cm cell culture dish to grow colonies. After seven days, colonies were trypsinized and transferred to a 24-well. Isolated clones were characterized by western blotting and Sanger sequencing (performed by Lilian Sluimer).

Generation of transgenic stable cell lines

RPE1 C2KO, RPE1 wild-type, RPE1 C2p53KO, U2OS C2KO, and U2OS wild-type cells at 5% confluency were infected with 2 µL 100x concentrated (titer unknown) lentivirus packaged with the pLVIP-EB3-GFP-Lenti-Hygro lentiviral cassette (kindly provided by Ben Bouchet, Akhmanova Lab, Department of Cell Biology, University of Utrecht; Bouchet *et al.,* 2016). After 48 hours, the medium was replaced by medium supplemented with 1 mg/mL Hygromycin, and the media was replaced every two days for new Hygromycin-containing media. The abovementioned infection steps were kindly performed by Boris Shneyer (Anna Akhmanova lab, Department of Cell Biology, Utrecht University). Cells were selected for three weeks, after which the efficiency of transgenic integration was determined by immunofluorescence staining. Next, 100 cells were seeded into a 15 cm cell culture dish and allowed to form colonies for seven days. Next, depending on the determined stable expression efficiency of the cell line, 24-72 colonies were picked per cell line and isolated in 24-well plates. Finally, desired clones were selected through immunofluorescence staining based on their EB3-GFP expression level and localization pattern.

Immunofluorescence staining and Western Blotting

The antibodies utilized for immunofluorescence staining during this project are itemized in the main reagent table below. Immunofluorescence stainings were performed on fixed cells. For fixation, cultured cells were incubated for 10 minutes with pre-chilled methanol at -20°C for 10 minutes. An additional pre-fixation step was performed for Rab6 and Cytochrome C stainings by incubating cells in 0.1% Glutaraldehyde in PBS for 1 minute at room temperature. Subsequentially pre-fixed cells were fixed in pre-warmed 4% PFA in PBS for 10 minutes at 37°C. Following glutaraldehyde/PFA fixation, cells were permeabilized with 0.15% Triton-X in 1x PBS for 5 minutes at RT and subsequentially quenched three times, 5 minutes each, with 100mM $NaBH_4$. Fixation was followed by three washing steps with 0.05% Tween-20 in PBS. Next, epitopes were blocked with 2% BSA in 0.05% Tween-20/PBS for 1 hour. Subsequently, cells were labeled with primary antibodies diluted in blocking buffer for 1 hour at RT. Following primary incubation, cells were washed three times and incubated for 1 hour at RT with secondary antibodies in blocking buffer. Subsequentially, cells were washed three times, 5 minutes each, and incubated with secondary antibodies in blocking buffer for 1 hour at RT. Finally, cells were washed three times with 0.05% Tween-20 in PBS, washed once with 70% ethanol, and immediately rinsed once with 96% ethanol. Next, the coverslips were air-dried, placed on glass microscope slides using Vectashield mounting medium (Vector Laboratories), and painted shut with nail polish. As secondary antibodies, Alexa Fluor 405-, 488-, and 594-conjugated goat antibodies against mouse, rat, or rabbit were used.

For Western Blotting, cells grown in 6-well plates at 90% confluency were harvested and lysed in RIPA lysis buffer containing 50 mM Tris-HCL pH 8.0, 150 mM NaCl, 0.5% sodium deoxycholate,

0.1% SDS, 1 mM EDTA, 1% Triton-X supplemented with complete protease inhibitor cocktail (Roche). Cell lysates were run on 8% polyacrylamide gels, then transferred onto a nitrocellulose membrane (Sigma-Aldrich). Epitope blocking was achieved by incubating the membrane in 2% BSA in 0.05% Tween-20/PBS for one hour at RT. Following epitope blocking, primary antibodies, diluted in blocking buffer, were added to the membrane and left to incubate overnight at 4°C. After antibody incubation, the membrane was washed three times with 0.05% Tween-20/PBS. Next, the membrane was incubated with secondary antibodies for two hours at RT before being washed three more times. For this, we used the IRDye-800CW goat anti-rat and anti-mouse as secondary antibodies (Li-Cor Biosciences, Lincoln, LE). The Odessey CLx infrared imaging system was used to image the membranes.

Fixed cell imaging and analysis

Fixed cells were imaged on a Nikon Eclipse Ni-U upright microscope with a Nikon DS-Qi2 Mono Digital Microscope Camera controlled by the Nikon NS Br software. Moreover, a Plan Apo Lambda 100x (N.A. 1.45) oil objective with a pixel-size of 0.072 µm was used to image. Furthermore, an Intensilight C-HGFI epi-fluorescence illuminator (Nikon), and Chroma ET-GFP2 (49002), -mCherry (49008), -BFP (49021) filters were used on the microscope to image fixed cells.

The ImageJ plug-in, Fiji (Schindelin *et al.,* 2012), was used to process taken images by adjusting the contrast and brightness linearly. To analyze the microtubule density in cells depleted of CLASPs, γ-tubulin, MAP7D3, luciferase, chTOG, or KIF2A, three equidistant lines, ~10 µm long lines were drawn perpendicular to the microtubule polarization from the MTOC to the cell's periphery. Next, the number of microtubules crossing these three lines was counted and averaged, giving an approximation of microtubules per 10 µm in these cells. In cells with two distinct microtubule densities, this quantification was repeated in the other direction and averaged globally.

Cells depleted of CLASPs and luciferase were blocked in the G1/S phase through thymidine block and imaged with the same acquisition settings to quantify the immunofluorescent intensity of centrosomal localized proteins. Here, ImageJ/Fiji was used to draw tight circles around the mother centrosome in cells, after which the integrated density was measured. Furthermore, background subtraction was performed by drawing five circles of similar size as the centrosomal ROI, averaging their integrated density, and subtracting it from the centrosomal ROI's integrated density.

Imaging and analysis of live cells

Movies of live cell dynamics were taken on an inverted Nikon EclipseTi spinning disc microscope, equipped with a Perfect Focus system (Nikon), a Nikon Plan Apo VC 60x (N.A. 1.40) oil objective with a pixel-size of 0.10989 µm, a Photometrics Evolve 512 EMCCD camera (Photometrics), an ASI motorized stage with the MS-2000-XYZ (AS) piezo top-plate, a Chroma ET-GFP (49002) filter, and a Vortan Stradus 488 nm, 150 mW laser, was used as a light source. The microscope was controlled with the Metamorph 7.7 software. To keep cells at 37°C and 5% CO_2, we used a Tokai Hit (INUBG2E-ZILCS) stage top incubator. Cells were seeded on 25mm coverslips mounted and in an AttoFluor Cell Chamber (Thermo fisher). Images were acquired with 100ms exposure time, two frames per second, and a 950 EM gain.

The ImageJ plug-in KymographBuilder was used to generate kymographs out of manually traced microtubule tracks. The growth speed of microtubules was analyzed by calculating the slope of

every microtubule growth event and averaging them per microtubule. The catastrophe frequency was determined from the same kymographs and by looking at the movie to confirm every event. Lastly, the rescue frequency was determined by analyzing the kymographs and movies carefully. For automatic tracking of EB3-GFP comets in live cells, the plug-in previously described in Serra-Marques *et al.* (2020) was used. In brief, they combined the 'SOS detector 3D module' (developed by Yao *et al.,* 2017) for particle detection and the 'SOS linker (NGMA) module' for particle tracking (MTrackJ, Rueden *et al.,* 2015). This 'Simple Track Segment' module was used on the resulting tracks from taken movies, giving directional runs' speed, length, and distance. Tracks were only considered if they lasted 20 or more frames. Moreover, tracks were split if two sequential displacements of one pixel or more occurred and the cosine angle between two velocities exceeded 10°.

Statistical analysis

All the statistical analysis in this study was performed using GraphPad Prism 9. The statistical details, such as p-values, are listed in the corresponding figure legends.

Key reagents

Type of reagent	Name/Target	Source or reference	Identifiers	Additional information
Antibody	PCNT Host: Rabbit	Abcam	ab4448	1 on 300 for IF
Antibody	CDK5RAP2 Host: Rabbit	Bethyl Laboratories	A300-554A	1 on 300 for IF
Antibody	γ-tubulin Host: Mouse	Sigma-Aldrich	T6557	1 on 100 for IF
Antibody	NEDD1 Host: Mouse	Abnova	H00121441-M05	1 on 300 for IF
Antibody	Ninein Host: Rabbit	Bethyl Laboratories	A301-504A	1 on 300 for IF
Antibody	CEP192 Host: Rabbit	Bethyl Laboratories	A302-324A	1 on 300 for IF
Antibody	CEP152 Host: Rabbit	Abcam	ab183911	1 on 300 for IF
Antibody	CEP135 Host: Rabbit	Sigma-Aldrich	SAB4503685	1 on 300 for IF
Antibody	GM130 Host: Mouse	BD Biosciences	610823	1 on 200 for IF
Antibody	α-tubulin YL1/2 Host: Rat	Pierce	MA1-80017	1 on 800 for IF
Antibody	acetylated-tubulin Host: Mouse	Sigma-Aldrich	T7451	1 on 200 for IF
Antibody	Ku80 Host: Mouse	BD Biosciences	611360	1 on 2000 for WB
Antibody	Cytochrome C Host: Mouse	BD Biosciences	556432	1 on 100 for IF

Antibody	Calnexin Host: Rabbit	Abcam	Ab22595	1 on 300 for IF
Antibody	chTOG Host: Rabbit	Charrasse *et al.,* 1998		1 on 100 for IF
Antibody	KIF2A Host: Rabbit	(Ganem and Compton, 2004)		1 on 200 for IF
Antibody	MAP7D1 Host: Rabbit	Sigma/Atlas	HPA028075	1 on 100 for IF
Antibody	MAP7D3 Host: Rabbit	Sigma/Atlas	HPA035598	1 on 100 for IF
Antibody	p53 Host: Mouse	Bethyl Laboratories	628082	1 on 1000 for WB
Antibody	Rab6 Host: Mouse	Gift of A. Barkenow – University of Muenster, Germany		1 on 100 for IF
Antibody	EB1/3 Host: Rat	Absea; Van der Vaart *et al.,* 2012	Clone #15H11	1 on 5 for IF
siRNA	CLASP1 siRNA	Mimori-Kiyosue *et al.,* 2005	5'GCCATTATGCCAACTATCT 3'	40 nM working concentration
siRNA	γ-tubulin #1	Luders *et al.,* 2006	5'GGAGGACAUGUUCAAGGAA 3'	20 nM working concentration
siRNA	γ-tubulin #2	Luders *et al.,* 2006	5′ CGCAUCUCUUUCUCAUAU 3'	20 nM working concentration
siRNA	Luciferase	Lansbergen *et al.,* 2004	5' CGTACGCGGAATACTTCGA' 3	40 nM working concentration
siRNA	KIF2A	Ganem *et al.,* 2005; Tanenbaum *et al.,* 2009	5' GGCAAAGAGAUUGACCUGG '3	20 nM working concentration
siRNA	MAP7D1	Hooikaas *et al.,* 2019	5′-TCATGAAGAGGACTCGGAA-3′	25 nM working concentration
siRNA	MAP7D3	Hooikaas *et al.,* 2019	5′-AACCTACATTCGTCTACT GAT-3′	25 nM working concentration
siRNA	chTOG	Cassimeris and Morabito, 2004	5′ GAGCCCAGAGUGGUCCAAA '3	20 nM working concentration

Oligo	sgRNA target p53 exon2	Fangrui Chen, Akhmanova Lab, Cell Biology department, Utrecht University Chen *et al.,* 2021, preprint	5' gCCATTGTTCAATATCGTCCG 3'	
Oligo	sgRNA target p53 exon 4	Fangrui Chen, Akhmanova Lab, Cell Biology department, Utrecht University Chen *et al.,* 2021, preprint	5' gTCCATTGCTTGGGACGGCAA ’3	
Viral vector	pLVIP-EB3-GFP-Lenti-Hygro	Bouchet *et al.,* 2016.	Kindly provided by Ben Bouchet, Akhmanova lab, Department of Cell Biology, Utrecht University	
Chemical	Centrinone B	Tocris Bioscience	#5690	125 nM working concentration
Chemical	Nocodazole	Sigma-Aldrich	M1404-10MG	10 µM working concentration
Chemical	Thymidine	Sigma-Aldrich	T9250-25G	5 mM working concentration

Supplementary Figures

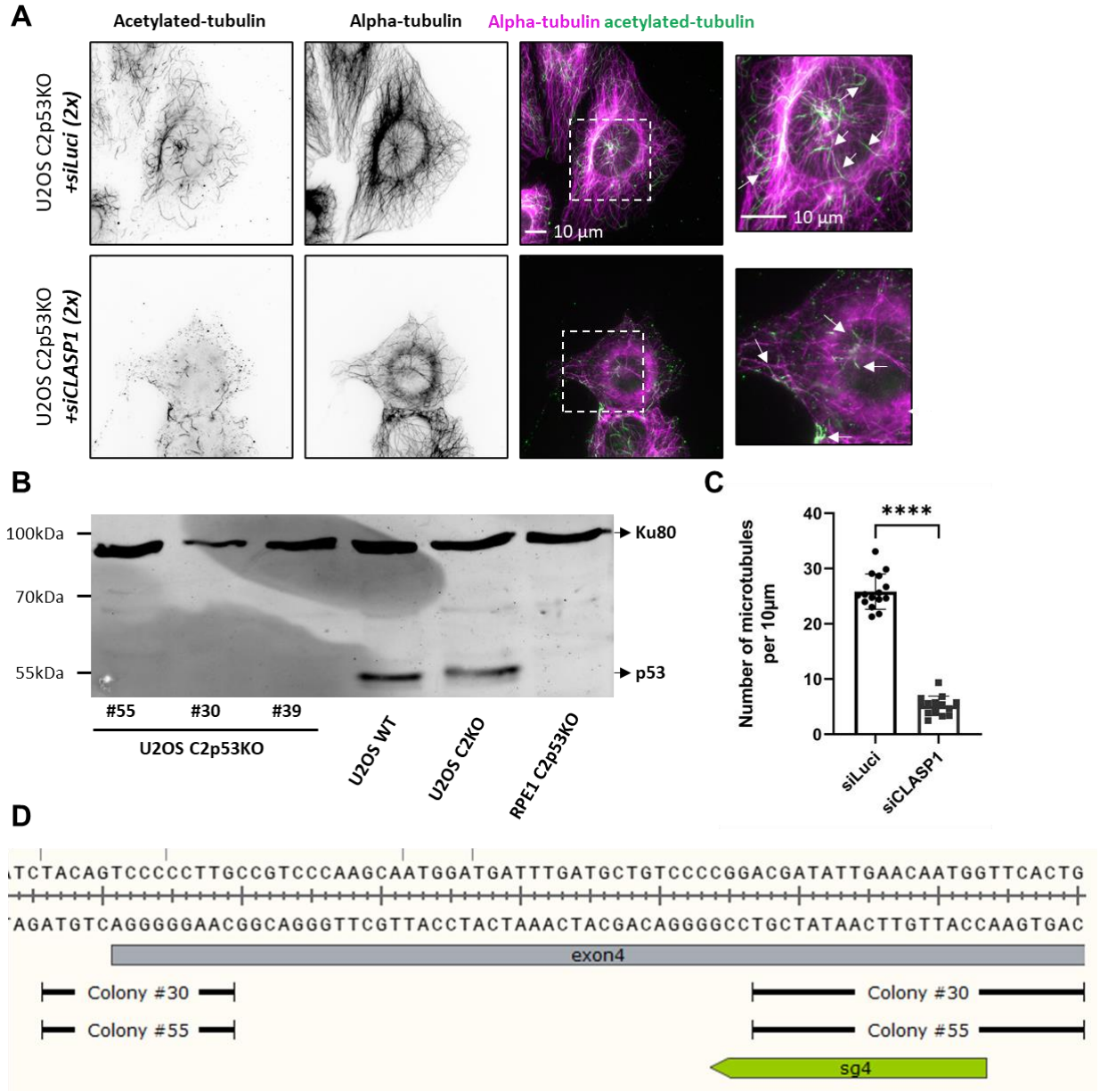

Figure S1. CLASP-depletion severely reduces the microtubule density also in U2OS C2p53KO cells. (A). *Immunofluorescence staining of U2OS C2p53KO cells depleted with either siCLASP1 (bottom panels) or siLuciferase (top panels) as a control. Cells were stained for acetylated-tubulin (green) and alpha-tubulin (magenta). Arrows in the insets point to acetylated-tubulin stretches.* ***(B).*** *Western blot confirms the knock-out of p53 and, therefore, the generation of C2p53KO cells in clones #30, #39, and #55. U2OS wild-type and U2OS C2KO cells were used as negative controls, whereas RPE1 C2p53KO cells were used as a positive control.* ***(C).*** *Quantitative comparison of the microtubule density in U2OS C2p53KO cells depleted with either siCLASP1 or siLuciferase. For each condition, 15 cells were used that were imaged from one experiment. Using an unpaired t-test gave a significance value of p < 0.0001, ****. The standard deviation is displayed through the error bars.* ***(D).*** *Sanger sequencing revealed a 37 base pair deletion in exon 4 of p53 for clones #30 and #55 (performed by Lilian Sluimer).*

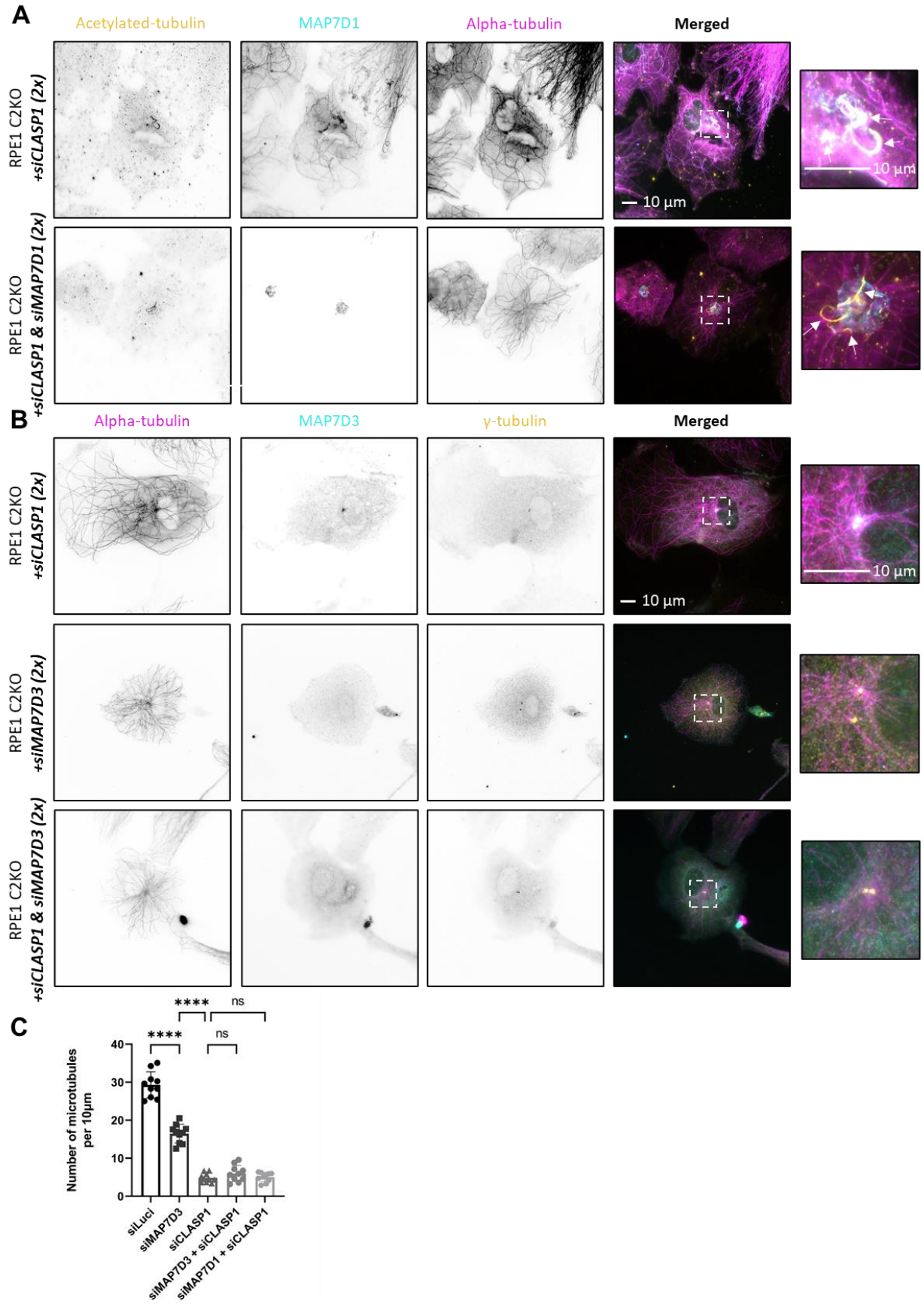
A
Acetylated-tubulin
MAP7D1
Alpha-tubulin
Merged
RPE1 C2KO +siCLASP1 (2x)
RPE1 C2KO +siCLASP1 & siMAP7D1 (2x)
10 µm
B
Alpha-tubulin
MAP7D3
γ-tubulin
Merged
RPE1 C2KO +siCLASP1 (2x)
RPE1 C2KO +siMAP7D3 (2x)
RPE1 C2KO +siCLASP1 & siMAP7D3 (2x)
C
****
ns
Number of microtubules per 10µm
siLuci
siMAP7D3
siCLASP1
siMAP7D3 + siCLASP1
siMAP7D1 + siCLASP1

Figure S2. The depletion of MAP7 isoforms in combination with CLASP does not result in further loss of microtubule populations. (A). *Immunofluorescence staining of RPE1 C2KO cells depleted with siCLASP1 (top panels) or siCLASP1 & siMAP7D1 (bottom panels). Cells were stained for acetylated-tubulin (green), MAP7D1 (cyan), and alpha-tubulin (magenta). Arrows in the insets point at the acetylated microtubules.* ***(B).*** *Immunofluorescence staining of RPE1 C2KO cells depleted with siCLASP1 (top panels), siMAP7D3 (middle panels), or siCLASP1 & siMAP7D3 (bottom panels). Cells were stained for alpha-tubulin (magenta), MAP7D3 (cyan), and γ-tubulin (yellow).* ***(C).*** *Quantitative comparison of the microtubule density in RPE1 C2KO cells depleted with either siCLASP1, siMAP7D3, siCLASP1 & siMAP7D3, siCLASP1 & MAP7D1, or siLuciferase as a control. For each condition, 10 cells were used that were imaged from one experiment. Using an unpaired t-test gave significance values of p < 0.0001, ****; and p =0.8003, ns . The standard deviation is displayed through the error bars.*

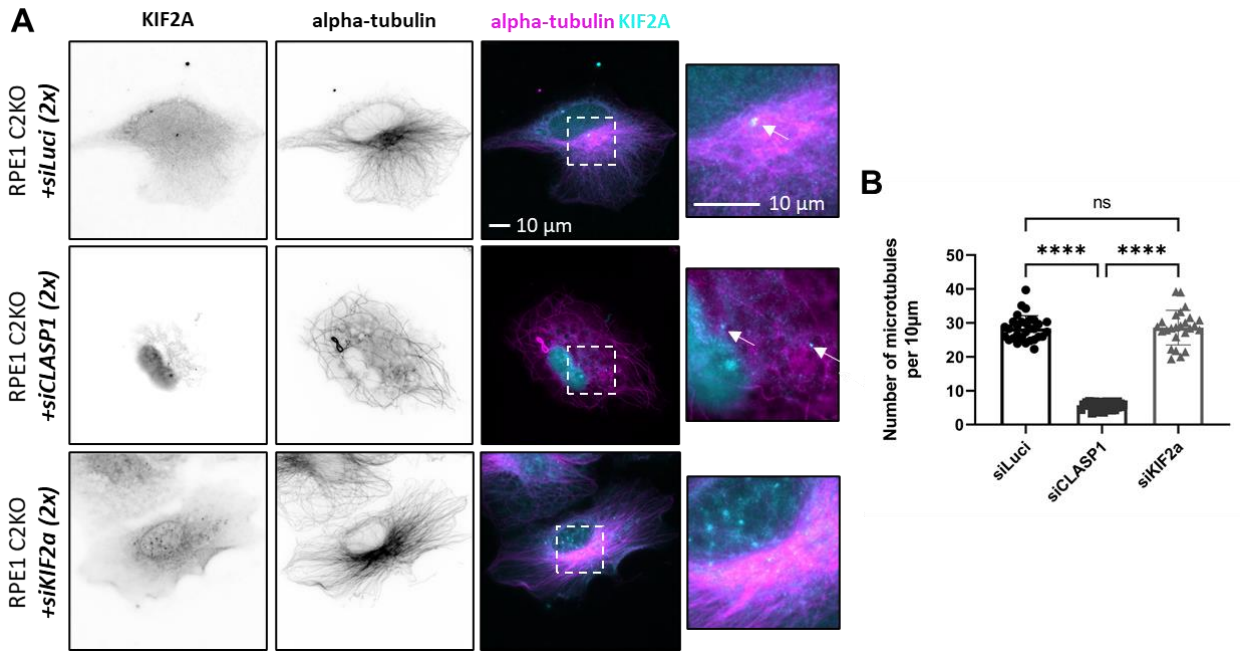

Figure S3. Depletion of KIF2A does not affect the microtubule density (A). *Immunofluorescence staining of RPE1 C2KO cells depleted with siCLASP1 (middle panels), siKIF2A (bottom panels), or siLuciferase (top panels) as a control. Arrows in the insets point at the centrosomal KIF2A signal. Cells were stained for KIF2A (cyan) and alpha-tubulin (magenta)* ***(B).*** *Quantitative comparison of the microtubule density in the cells as mentioned above. For each condition, at least 25 cells were used that were imaged from two independent experiment repetitions. Using a One-Way Anova gave a significance value of p < 0.0001, ****. The standard deviation is displayed through the error bars.*

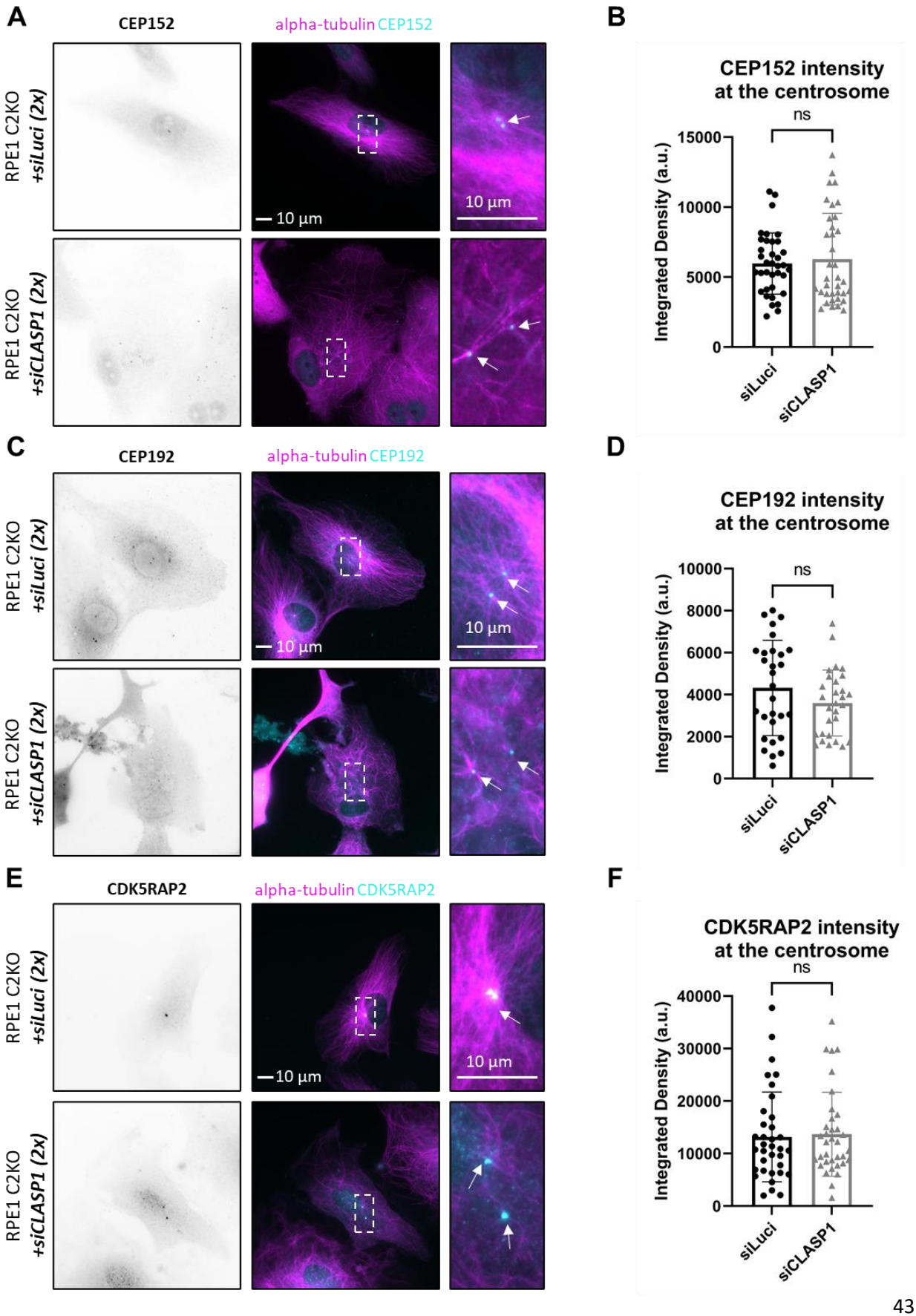
A
CEP152
alpha-tubulin CEP152
RPE1 C2KO +siLuci (2x)
RPE1 C2KO +siCLASP1 (2x)
10 µm
10 µm
B
CEP152 intensity at the centrosome
ns
Integrated Density (a.u.)
15000
10000
5000
0
siLuci
siCLASP1
C
CEP192
alpha-tubulin CEP192
RPE1 C2KO +siLuci (2x)
RPE1 C2KO +siCLASP1 (2x)
10 µm
10 µm
D
CEP192 intensity at the centrosome
ns
Integrated Density (a.u.)
10000
8000
6000
4000
2000
0
siLuci
siCLASP1
E
CDK5RAP2
alpha-tubulin CDK5RAP2
RPE1 C2KO +siLuci (2x)
RPE1 C2KO +siCLASP1 (2x)
10 µm
10 µm
F
CDK5RAP2 intensity at the centrosome
ns
Integrated Density (a.u.)
40000
30000
20000
10000
0
siLuci
siCLASP1

Figure S4. Centrosomal proteins CEP152, CEP192, and CDK5RAP2 signals remain unaltered upon CLASP-depletion. (A, C, E). *Immunofluorescence staining of* ***(A).*** *CEP152,* ***(C).*** *CEP192, and* ***(E).*** *CDK5RAP2 (cyan) in RPE1 C2KO cells depleted with siCLASP1 (bottom panels) or siLuciferase (top panels) control. Arrows in the insets show protein signals at the centrosomes.* ***(B, D, F)*** *Quantitative comparison of* ***(B).*** *CEP152,* ***(D).*** *CEP192, and* ***(F).*** *CDK5RAP2 signals at the centrosome in RPE1 C2KO cells depleted with either siCLASP1 or siLuciferase as a control. Data is represented in integrated density (a.u). The following number of cells was used per condition: 36 cells for CEP152, 29 for CEP192, and 35 were imaged from at least three independent experiment repetitions. Using an unpaired t-test gave significance values of CEP152, n.s, p = 0.6270; CEP192, n.s, p = 0.1667; CDK5RAP2, n.s, p = 0.7920. The standard deviation is displayed through the error bars.*

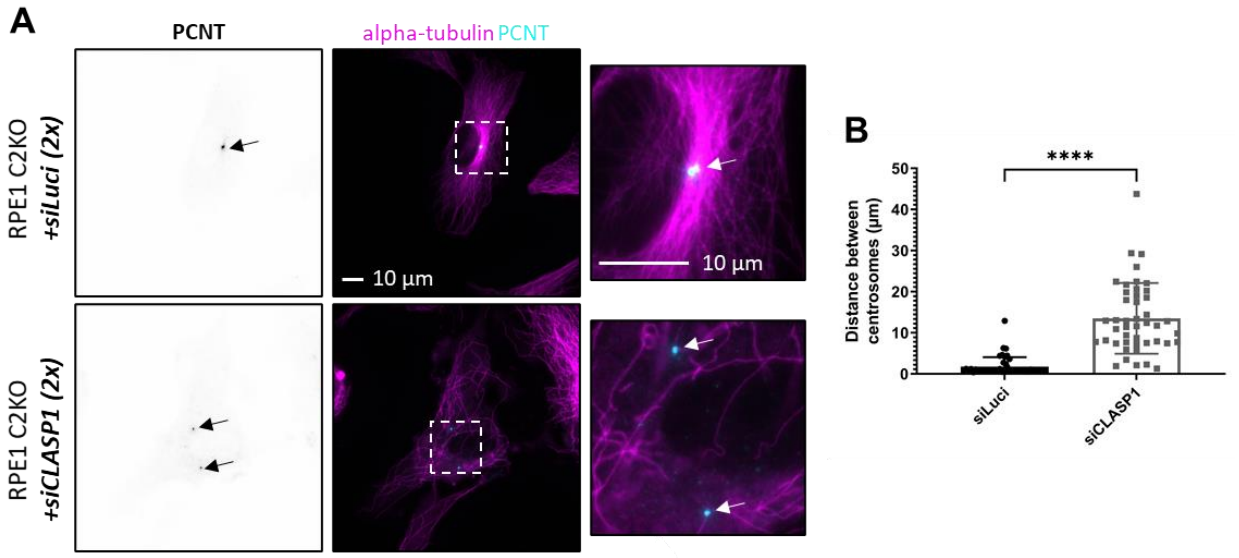

Figure S5. CLASP-depletion leads to strong separation of the two centrosomes. (A). *Immunofluorescence staining of RPE1 C2KO cells depleted with siCLASP1 (bottom panels) or siLuciferase (top panels) as a control. Arrows point at the centrosomes. Cells were stained for PCNT (cyan) and alpha-tubulin (magenta).* ***(B).*** *Quantitative comparison of the distance between the centrosomes in cells as mentioned before. For each condition, 30 cells were used that were imaged from three independent experiment repetitions. Using an unpaired t-test gave a significance value of p < 0.0001, ****. The standard deviation is displayed through the error bars.*

References

Abal, M., Piel, M., Bouckson-Castaing, V., Mogensen, M., Sibarita, J., & Bornens, M. (2002). Microtubule release from the centrosome in migrating cells. *The Journal of Cell Biology, 159*(5), 731-737. doi:10.1083/jcb.200207076

Aher, A., & Akhmanova, A. (2018). Tipping microtubule dynamics, one protofilament at a time. *Current Opinion in Cell Biology, 50*, 86-93. doi:10.1016/j.ceb.2018.02.015

Aher, A., Kok, M., Sharma, A., Rai, A., Olieric, N., Rodriguez-Garcia, R., . . . Akhmanova, A. (2018). CLASP suppresses microtubule catastrophes through a single TOG domain. *Developmental Cell, 46*(1), 40-58.e8. doi:10.1016/j.devcel.2018.05.032

Aher, A., Rai, D., Schaedel, L., Gaillard, J., John, K., Liu, Q., . . . Akhmanova, A. (2020). CLASP mediates microtubule repair by restricting lattice damage and regulating tubulin incorporation. *Current Biology, 30*(11), 2175-2183.e6. doi:10.1016/j.cub.2020.03.070

Akhmanova, A., Hoogenraad, C. C., Drabek, K., Stepanova, T., Dortland, B., Verkerk, T., . . . Galjart, N. (2001). CLASPs are CLIP-115 and -170 associating proteins involved in the regional regulation of microtubule dynamics in motile fibroblasts. *Cell, 104*(6), 923-935. doi:10.1016/S0092-8674(01)00288-4

Akhmanova, A., & Steinmetz, M. O. (2010). Microtubule +TIPs at a glance. *Journal of Cell Science, 123*(Pt 20), 3415-3419. doi:10.1242/jcs.062414

Asenjo, A., Chatterjee, C., Tan, D., DePaoli, V., Rice, W., Diaz-Avalos, R., . . . Sosa, H. (2013). Structural model for tubulin recognition and deformation by kinesin-13 microtubule depolymerases. *Cell Reports, 3*(3), 759-768. doi:10.1016/j.celrep.2013.01.030

Avidor-Reiss, T., & Gopalakrishnan, J. (2013). Building a centriole. *Current Opinion in Cell Biology, 25*(1), 72-77. doi:10.1016/j.ceb.2012.10.016

Azimzadeh, J., & Marshall, W. F. (2010). Building the centriole. *Current Biology: CB, 20*(18), 816. doi:10.1016/j.cub.2010.08.010

Barbier, P., Zejneli, O., Martinho, M., Lasorsa, A., Belle, V., Smet-Nocca, C., . . . Landrieu, I. (2019). Role of tau as a microtubule-associated protein: Structural and functional aspects. *Frontiers in Aging Neuroscience, 0* doi:10.3389/fnagi.2019.00204

Barlan, K., & Gelfand, V. I. (2017). Microtubule-based transport and the distribution, tethering, and organization of organelles. *Cold Spring Harbor Perspectives in Biology, 9*(5) doi:10.1101/cshperspect.a025817

Belmont, L. D., & Mitchison, T. J. (1996). Identification of a protein that interacts with tubulin dimers and increases the catastrophe rate of microtubules. *Cell, 84*(4), 623-631. doi:10.1016/s0092-8674(00)81037-5

Bieling, P., Kandels-Lewis, S., Telley, I. A., van Dijk, J., Janke, C., Surrey, T. (2008). CLIP-170 tracks growing microtubule ends by dynamically recognizing composite EB1/tubulin-binding sites. *Journal of Cell Biology, 183*(7), 1223-1233. doi:10.1083/jcb.200809190 46

Bobinnec, Y., Fukuda, M., & Nishida, E. (2000). Identification and characterization of caenorhabditis elegans gamma-tubulin in dividing cells and differentiated tissues. *Journal of Cell Science, 113 Pt 21*, 3747-3759. doi: 10.1242/jcs.113.21.3747

Bouchet, B. P., Noordstra, I., van Amersfoort, M., Katrukha, E. A., Ammon, Y., Ter Hoeve, N. D., . . . Akhmanova, A. (2016). Mesenchymal cell invasion requires cooperative regulation of persistent microtubule growth by SLAIN2 and CLASP1. *Developmental Cell, 39*(6), 708-723. doi:10.1016/j.devcel.2016.11.009

Bouissou, A., Vérollet, C., Sousa, A., Sampaio, P., Wright, M., Sunkel, C. E., . . . Raynaud-Messina, B. (2009). Γ-tubulin ring complexes regulate microtubule plus end dynamics. *The Journal of Cell Biology, 187*(3), 327-334. doi:10.1083/jcb.200905060

Brouhard, G. J., Stear, J. H., Noetzel, T. L., Al-Bassam, J., Kinoshita, K., Harrison, S. C., . . . Hyman, A. A. (2008). XMAP215 is a processive microtubule polymerase. *Cell, 132*(1), 79-88. doi:10.1016/j.cell.2007.11.043

Carvalho-Santos, Z., Machado, P., Branco, P., Tavares-Cadete, F., Rodrigues-Martins, A., Pereira-Leal, J. B., & Bettencourt-Dias, M. (2010). Stepwise evolution of the centriole-assembly pathway. *Journal of Cell Science, 123*(Pt 9), 1414-1426. doi:10.1242/jcs.064931

Cassimeris, L. (2002). The oncoprotein 18/stathmin family of microtubule destabilizers. *Current Opinion in Cell Biology, 14*(1), 18-24. doi:10.1016/s0955-0674(01)00289-7

Cassimeris, L., & Morabito, J. (2004). TOGp, the human homolog of XMAP215/Dis1, is required for centrosome integrity, spindle pole organization, and bipolar spindle assembly. *Molecular Biology of the Cell, 15*(4), 1580-1590. doi:10.1091/mbc.E03-07-0544

Chabin-Brion, K., Marceiller, J., Perez, F., Settegrana, C., Drechou, A., Durand, G., & Poüs, C. (2001). The golgi complex is a microtubule-organizing organelle. *Molecular Biology of the Cell, 12*(7), 2047-2060. doi:10.1091/mbc.12.7.2047

Charrasse, S., Schroeder, M., Gauthier-Rouviere, C., Ango, F., Cassimeris, L., Gard, D. L., & Larroque, C. (1998). The TOGp protein is a new human microtubule-associated protein homologous to the xenopus XMAP215. *Journal of Cell Science, 111 (Pt 10)*, 1371-1383. doi: 10.1242/jcs.111.10.1371

Chaudhary, A. R., Lu, H., Krementsova, E. B., Bookwalter, C. S., Trybus, K. M., & Hendricks, A. G. (2019). MAP7 regulates organelle transport by recruiting kinesin-1 to microtubules. *The Journal of Biological Chemistry, 294*(26), 10160-10171. doi:10.1074/jbc.RA119.008052

Chen, C., Hehnly, H., Yu, Q., Farkas, D., Zheng, G., Redick, S. D., . . . Doxsey, S. (2014). A unique set of centrosome proteins requires pericentrin for spindle-pole localization and spindle orientation. *Current Biology : CB, 24*(19), 2327-2334. doi:10.1016/j.cub.2014.08.029

Chen, F., Wu, J., Iwanski, M. K., Jurriens, D., Sandron, A., Pasolli, M., . . . Akhmanova, A. (2021). Centriole-independent centrosome assembly in interphase mammalian cells. *BioRxiv,* doi:10.1101/2021.08.22.457259v1 47

Choi, Y., Liu, P., Sze, S. K., Dai, C., & Qi, R. Z. (2010). CDK5RAP2 stimulates microtubule nucleation by the gamma-tubulin ring complex. *The Journal of Cell Biology, 191*(6), 1089-1095. doi:10.1083/jcb.201007030

Cizmecioglu, O., Arnold, M., Bahtz, R., Settele, F., Ehret, L., Haselmann-Weiss, U., . . . Hoffmann, I. (2010). Cep152 acts as a scaffold for recruitment of Plk4 and CPAP to the centrosome. *The Journal of Cell Biology, 191*(4), 731-739. doi:10.1083/jcb.201007107

Consolati, T., Locke, J., Roostalu, J., Chen, Z. A., Gannon, J., Asthana, J., . . . Surrey, T. (2020). Microtubule nucleation properties of single human γTuRCs explained by their cryo-EM structure. *Developmental Cell, 53*(5), 603-617.e8. doi:10.1016/j.devcel.2020.04.019

Coombes, C. E., Yamamoto, A., Kenzie, M. R., Odde, D. J., & Gardner, M. K. (2013). Evolving tip structures can explain age-dependent microtubule catastrophe. *Current Biology: CB, 23*(14), 1342-1348. doi:10.1016/j.cub.2013.05.059

Delaval, B., & Doxsey, S. J. (2010). Pericentrin in cellular function and disease. *The Journal of Cell Biology, 188*(2), 181-190. doi:10.1083/jcb.200908114

Delgehyr, N., Sillibourne, J., & Bornens, M. (2005). Microtubule nucleation and anchoring at the centrosome are independent processes linked by ninein function. *Journal of Cell Science, 118*(Pt 8), 1565-1575. doi:10.1242/jcs.02302

Denu, R. A., Shabbir, M., Nihal, M., Singh, C. K., Longley, B. J., Burkard, M. E., & Ahmad, N. (2018). Centriole overduplication is the predominant mechanism leading to centrosome amplification in melanoma. *Molecular Cancer Research: MCR, 16*(3), 517-527. doi:10.1158/1541-7786.MCR-17-0197

Desai, A., & Mitchison, T. J. (1997). Microtubule polymerization dynamics. *Annual Review of Cell and Developmental Biology, 13*, 83-117. doi:10.1146/annurev.cellbio.13.1.83

Efimov, A., Kharitonov, A., Efimova, N., Loncarek, J., Miller, P. M., Andreyeva, N., . . . Kaverina, I. (2007). Asymmetric CLASP-dependent nucleation of noncentrosomal microtubules at the trans-golgi network. *Developmental Cell, 12*(6), 917-930. doi:10.1016/j.devcel.2007.04.002

Fletcher, D. A., & Mullins, R. D. (2010). Cell mechanics and the cytoskeleton. *Nature, 463*(7280), 485-492. doi:10.1038/nature08908

Fong, K., Choi, Y., Rattner, J. B., & Qi, R. Z. (2008). CDK5RAP2 is a pericentriolar protein that functions in centrosomal attachment of the γ-tubulin ring complex. *Molecular Biology of the Cell, 19*(1), 115-125. doi:10.1091/mbc.e07-04-0371

Ganem, N. J., Upton, K., & Compton, D. A. (2005). Efficient mitosis in human cells lacking poleward microtubule flux. *Current Biology: CB, 15*(20), 1827-1832. doi:10.1016/j.cub.2005.08.065

Gardner, M., Zanic, M., Gell, C., Bormuth, V., & Howard, J. (2011). Depolymerizing kinesins Kip3 and MCAK shape cellular microtubule architecture by differential control of catastrophe. *Cell, 147*(5), 1092-1103. doi:10.1016/j.cell.2011.10.037 48

Gillingham, A. K., & Munro, S. (2000). The PACT domain, a conserved centrosomal targeting motif in the coiled-coil proteins AKAP450 and pericentrin. *EMBO Reports, 1*(6), 524-529. doi:10.1093/embo-reports/kvd105

Gomez-Ferreria, M. A., Rath, U., Buster, D. W., Chanda, S. K., Caldwell, J. S., Rines, D. R., & Sharp, D. J. (2007). Human Cep192 is required for mitotic centrosome and spindle assembly. *Current Biology: CB, 17*(22), 1960-1966. doi:10.1016/j.cub.2007.10.019

Goodson, H. V., & Jonasson, E. M. (2018). Microtubules and microtubule-associated proteins. *Cold Spring Harbor Perspectives in Biology, 10*(6) doi:10.1101/cshperspect.a022608

Grigoriev, I., Splinter, D., Keijzer, N., Wulf, P. S., Demmers, J., Ohtsuka, T., . . . Akhmanova, A. (2007). Rab6 regulates transport and targeting of exocytotic carriers. *Developmental Cell, 13*(2), 305-314. doi:10.1016/j.devcel.2007.06.010

Grimaldi, A. D., Maki, T., Fitton, B. P., Roth, D., Yampolsky, D., Davidson, M. W., . . . Kaverina, I. (2014). CLASPs are required for proper microtubule localization of end-binding proteins. *Developmental Cell, 30*(3), 343-352. doi:10.1016/j.devcel.2014.06.026

Guillet, V., Knibiehler, M., Gregory-Pauron, L., Remy, M., Chemin, C., Raynaud-Messina, B., . . . Mourey, L. (2011). Crystal structure of γ-tubulin complex protein GCP4 provides insight into microtubule nucleation. *Nature Structural & Molecular Biology, 18*(8), 915-919. doi:10.1038/nsmb.2083

Gundersen, G. G., & Worman, H. J. (2013). Nuclear positioning. *Cell, 152*(6), 1376-1389. doi:10.1016/j.cell.2013.02.031

Gurel, P., Hatch, A., & Higgs, H. (2014). Connecting the cytoskeleton to the endoplasmic reticulum and golgi. *Current Biology, 24*(14), R660-R672. doi:10.1016/j.cub.2014.05.033

Hain, K. O., Colin, D. J., Rastogi, S., Allan, L. A., & Clarke, P. R. (2016). Prolonged mitotic arrest induces a caspase-dependent DNA damage response at telomeres that determines cell survival. *Scientific Reports, 6*(1), 26766. doi:10.1038/srep26766

Hammond, J. W., Cai, D., & Verhey, K. J. (2008). Tubulin modifications and their cellular functions. *Current Opinion in Cell Biology, 20*(1), 71-76. doi:10.1016/j.ceb.2007.11.010.

Hannak, E., & Heald, R. (2006). Investigating mitotic spindle assembly and function in vitro using xenopus laevis egg extracts. *Nature Protocols, 1*(5), 2305-2314. doi:10.1038/nprot.2006.396

Hannak, E., Oegema, K., Kirkham, M., Gönczy, P., Habermann, B., & Hyman, A. A. (2002). The kinetically dominant assembly pathway for centrosomal asters in caenorhabditis elegans is gamma-tubulin dependent. *The Journal of Cell Biology, 157*(4), 591-602. doi:10.1083/jcb.200202047

Haren, L., Remy, M., Bazin, I., Callebaut, I., Wright, M., & Merdes, A. (2006). NEDD1-dependent recruitment of the γ-tubulin ring complex to the centrosome is necessary for centriole duplication and spindle assembly. *Journal of Cell Biology, 172*(4), 505-515. doi:10.1083/jcb.200510028

Hayashi, I., & Ikura, M. (2003). Crystal structure of the amino-terminal microtubule-binding domain of end-binding protein 1 (EB1). *The Journal of Biological Chemistry, 278*(38), 36430-36434. doi:10.1074/jbc.M305773200

Hendershott, M. C., & Vale, R. D. (2014). Regulation of microtubule minus-end dynamics by CAMSAPs and patronin. *Proceedings of the National Academy of Sciences of the United States of America, 111*(16), 5860-5865. doi:10.1073/pnas.1404133111

Ho, W. C., Allan, V. J., van Meer, G., Berger, E. G., & Kreis, T. E. (1989). Reclustering of scattered golgi elements occurs along microtubules. *European Journal of Cell Biology, 48*(2), 250-263. PMID: 2743999

Honnappa, S., Okhrimenko, O., Jaussi, R., Jawhari, H., Jelesarov, I., Winkler, F. K., & Steinmetz, M. O. (2006). Key interaction modes of dynamic +TIP networks. *Molecular Cell, 23*(5), 663-671. doi:10.1016/j.molcel.2006.07.013

Hooikaas, P. J., Martin, M., Mühlethaler, T., Kuijntjes, G., Peeters, C. A. E., Katrukha, E. A., . . . Akhmanova, A. (2019). MAP7 family proteins regulate kinesin-1 recruitment and activation. *The Journal of Cell Biology, 218*(4), 1298-1318. doi:10.1083/jcb.201808065

Howes, S. C., Alushin, G. M., Shida, T., Nachury, M. V., Nogales, E. (2014). Effects of tubulin acetylation and tubulin acetyltransferase binding on microtubule structure. *Molecular Biology of the Cell, 25*(2), 257-266. doi:10.1091/mbc.E13-07-0387

Hunter, A. W., Caplow, M., Coy, D. L., Hancock, W. O., Diez, S., Wordeman, L., & Howard, J. (2003). The kinesin-related protein MCAK is a microtubule depolymerase that forms an ATP-hydrolyzing complex at microtubule ends. *Molecular Cell, 11*(2), 445-457. doi:10.1016/S1097-2765(03)00049-2

Hurtado, L., Caballero, C., Gavilan, M. P., Cardenas, J., Bornens, M., & Rios, R. M. (2011). Disconnecting the golgi ribbon from the centrosome prevents directional cell migration and ciliogenesis. *The Journal of Cell Biology, 193*(5), 917-933. doi:10.1083/jcb.201011014

Inoue, Y. H., do Carmo Avides, M., Shiraki, M., Deak, P., Yamaguchi, M., Nishimoto, Y., . . . Glover, D. M. (2000). Orbit, a novel microtubule-associated protein essential for mitosis in drosophila melanogaster. *The Journal of Cell Biology, 149*(1), 153-166. doi:10.1083/jcb.149.1.153

Janson, M. E., de Dood, M. E., & Dogterom, M. (2003). Dynamic instability of microtubules is regulated by force. *Journal of Cell Biology, 161*(6), 1029-1034. doi:10.1083/jcb.200301147

Jiang, K., Hua, S., Mohan, R., Grigoriev, I., Yau, K. W., Liu, Q., . . . Akhmanova, A. (2014). Microtubule minus-end stabilization by polymerization-driven CAMSAP deposition. *Developmental Cell, 28*(3), 295-309. doi:10.1016/j.devcel.2014.01.001

Johmura, Y., Soung, N., Park, J., Yu, L., Zhou, M., Bang, J. K., . . . Lee, K. S. (2011). Regulation of microtubule-based microtubule nucleation by mammalian polo-like kinase 1. *Proceedings of the National Academy of Sciences of the United States of America, 108*(28), 11446-11451. doi:10.1073/pnas.1106223108 50

Keating, T. J., & Borisy, G. G. (1999). Centrosomal and non-centrosomal microtubules. *Biology of the Cell, 91*(4), 321-329. doi:10.1016/S0248-4900(99)80093-8

Kinoshita, K., Habermann, B., & Hyman, A. A. (2002). XMAP215: A key component of the dynamic microtubule cytoskeleton. *Trends in Cell Biology, 12*(6), 267-273. doi:10.1016/s0962-8924(02)02295-x

Klopfenstein, D. R. C., Kappeler, F., & Hauri, H. (1998). A novel direct interaction of endoplasmic reticulum with microtubules. *The EMBO Journal, 17*(21), 6168-6177. doi:10.1093/emboj/17.21.6168

Kollman, J. M., Merdes, A., Mourey, L., & Agard, D. A. (2011). Microtubule nucleation by γ-tubulin complexes. *Nature Reviews. Molecular Cell Biology, 12*(11), 709-721. doi:10.1038/nrm3209

Koning, R. I. (2010). Cryo-electron tomography of cellular microtubules. *Methods in Cell Biology, 97*, 455-473. doi:10.1016/S0091-679X(10)97024-6

Lansbergen, G., Grigoriev, I., Mimori-Kiyosue, Y., Ohtsuka, T., Higa, S., Kitajima, I., . . . Akhmanova, A. (2006). CLASPs attach microtubule plus ends to the cell cortex through a complex with LL5β. *Developmental Cell, 11*(1), 21-32. doi:10.1016/j.devcel.2006.05.012

Lansbergen, G., Komarova, Y., Modesti, M., Wyman, C., Hoogenraad, C. C., Goodson, H. V., . . . Akhmanova, A. (2004). Conformational changes in CLIP-170 regulate its binding to microtubules and dynactin localization. *The Journal of Cell Biology, 166*(7), 1003-1014. doi:10.1083/jcb.200402082

Lawo, S., Hasegan, M., Gupta, G. D., & Pelletier, L. (2012). Subdiffraction imaging of centrosomes reveals higher-order organizational features of pericentriolar material. *Nature Cell Biology, 14*(11), 1148-1158. doi:10.1038/ncb2591

Lawrence, E. J., & Zanic, M. (2019). Rescuing microtubules from the brink of catastrophe: CLASPs lead the way. *Current Opinion in Cell Biology, 56*, 94-101. doi:10.1016/j.ceb.2018.10.011

Lawrence, E. J., Arpag, G., Norris, S. R., & Zanic, M. (2018). Human CLASP2 specifically regulates microtubule catastrophe and rescue. *Molecular Biology of the Cell, 29*(10), 1168-1177. doi:10.1091/mbc.E18-01-0016

LeDizet, M., & Piperno, G. (1987). Indefication of an acetylation site of Chlamydomonas alpha-tubulin. *Proceedings of the National Academy of Sciences of the United States of America, 84*(16), 5720-5724. doi:10.1073/pnas.84.16.5720

Lee, C., & Chen, L. B. (1988). Dynamic behavior of endoplasmic reticulum in living cells. *Cell, 54*(1), 37-46. doi:10.1016/0092-8674(88)90177-8

LeGuennec, M., Klena, N., Aeschlimann, G., Hamel, V., & Guichard, P. (2021). Overview of the centriole architecture. *Current Opinion in Structural Biology, 66*, 58-65. doi:10.1016/j.sbi.2020.09.015 51

Lemos, C. L., Sampaio, P., Maiato, H., Costa, M., Omel'yanchuk, L. V., Liberal, V., & Sunkel, C. E. (2000). Mast, a conserved microtubule-associated protein required for bipolar mitotic spindle organization. *The EMBO Journal, 19*(14), 3668-3682. doi:10.1093/emboj/19.14.3668

Lin, T., Neuner, A., Flemming, D., Liu, P., Chinen, T., Jäkle, U., . . . Schiebel, E. (2016). MOZART1 and γ-tubulin complex receptors are both required to turn γ-TuSC into an active microtubule nucleation template. *The Journal of Cell Biology, 215*(6), 823-840. doi:10.1083/jcb.201606092

Lin, T., Neuner, A., Schlosser, Y. T., Scharf, A. N. D., Weber, L., & Schiebel, E. (2014). Cell-cycle dependent phosphorylation of yeast pericentrin regulates γ-TuSC-mediated microtubule nucleation. *eLife, 3*, e02208. doi:10.7554/eLife.02208

Liu, P., Zupa, E., Neuner, A., Böhler, A., Loerke, J., Flemming, D., . . . Schiebel, E. (2020). Insights into the assembly and activation of the microtubule nucleator γ-TuRC. *Nature, 578*(7795), 467-471. doi:10.1038/s41586-019-1896-6

Logan, C. M., & Menko, A. S. (2019). Microtubules: Evolving roles and critical cellular interactions. *Experimental Biology and Medicine (Maywood, N.J.), 244*(15), 1240-1254. doi:10.1177/1535370219867296

Logarinho, E., Maffini, S., Barisic, M., Marques, A., Toso, A., Meraldi, P., & Maiato, H. (2012). CLASPs prevent irreversible multipolarity by ensuring spindle-pole resistance to traction forces during chromosome alignment. *Nature Cell Biology, 14*(3), 295-303. doi:10.1038/ncb2423

Lomakin, A. J., Semenova, I., Zaliapin, I., Kraikivski, P., Nadezhdina, E., Slepchenko, B. M., . . . Rodionov, V. (2009). CLIP-170-dependent capture of membrane organelles by microtubules initiates minus-end directed transport. *Developmental Cell, 17*(3), 323-333. doi:10.1016/j.devcel.2009.07.010

Lu, L., Ladinsky, M. S., & Kirchhausen, T. (2009). Cisternal organization of the endoplasmic reticulum during mitosis. *Molecular Biology of the Cell, 20*(15), 3471-3480. doi:10.1091/mbc.e09-04-0327

Lüders, J., Patel, U. K., & Stearns, T. (2006). GCP-WD is a gamma-tubulin targeting factor required for centrosomal and chromatin-mediated microtubule nucleation. *Nature Cell Biology, 8*(2), 137-147. doi:10.1038/ncb1349

Ly. N., Elkhatib, N., Bresteau, E., Piétrement, O., Khaled, M., Magiera, M. M., Janke, C., Le Cam, E., Rutenberg, A. D., Montagnac, G. (2016). αTAT1 controls longtidunal spreading of acetylation marks from open microtubules extremities. *Scientific Reports, 6,* 35624. doi:10.1038/srep35624

Maffini, S., Maia, A. R. R., Manning, A. L., Maliga, Z., Pereira, A. L., Junqueira, M., . . . Maiato, H. (2009). Motor-independent targeting of CLASPs to kinetochores by CENP-E promotes microtubule turnover and poleward flux. *Current Biology: CB, 19*(18), 1566-1572. doi:10.1016/j.cub.2009.07.059

Maiato, H., Fairley, E. A. L., Rieder, C. L., Swedlow, J. R., Sunkel, C. E., & Earnshaw, W. C. (2003). Human CLASP1 is an outer kinetochore component that regulates spindle microtubule dynamics. *Cell, 113*(7), 891-904. doi:10.1016/S0092-8674(03)00465-3

Maiato, H., Hergert, P. J., Moutinho-Pereira, S., Dong, Y., Vandenbeldt, K. J., Rieder, C. L., & McEwen, B. F. (2006). The ultrastructure of the kinetochore and kinetochore fiber in drosophila somatic cells. *Chromosoma, 115*(6), 469-480. doi:10.1007/s00412-006-0076-2

Maki, T., Grimaldi, A. D., Fuchigami, S., Kaverina, I., Hayashi, I. (2016). CLASP2 has two distinct TOG domains that contribute differently to microtubule dynamics. *Journal of Molecular Biology, 427*(14), 2379-2395. doi:10.1016/j.jmb.2015.05.012

Mennella, V., Agard, D. A., Bo, H., & Pelletier, L. (2014). Amorphous no more: Subdiffraction view of the pericentriolar material architecture. *Trends in Cell Biology, 24*(3), 188-197. doi:10.1016/j.tcb.2013.10.001

Miller, P. M., Folkmann, A. W., Maia, A. R. R., Efimova, N., Efimov, A., & Kaverina, I. (2009). Golgi-derived CLASP-dependent microtubules control golgi organization and polarized trafficking in motile cells. *Nature Cell Biology, 11*(9), 1069-1080. doi:10.1038/ncb1920

Mimori-Kiyosue, Y., Grigoriev, I., Lansbergen, G., Sasaki, H., Matsui, C., Severin, F., . . . Akhmanova, A. (2005). CLASP1 and CLASP2 bind to EB1 and regulate microtubule plus-end dynamics at the cell cortex. *The Journal of Cell Biology, 168*(1), 141-153. doi:10.1083/jcb.200405094

Mimori-Kiyosue, Y., Grigoriev, I., Sasaki, H., Matsui, C., Akhmanova, A., Tsukita, S., & Vorobjev, I. (2006). Mammalian CLASPs are required for mitotic spindle organization and kinetochore alignment. *Genes to Cells, 11*(8), 845-857. doi:10.1111/j.1365-2443.2006.00990.x

Minin, A. A. (1997). Dispersal of golgi apparatus in nocodazole-treated fibroblasts is a kinesin-driven process. *Journal of Cell Science, 110 (Pt 19)*, 2495-2505.doi: 10.1242/jcs.110.19.2495

Monroy, B. Y., Sawyer, D. L., Ackermann, B. E., Borden, M. M., Tan, T. C., & Ori-McKenney, K. M. (2018). Competition between microtubule-associated proteins directs motor transport. *Nature Communications, 9*(1), 1-12. doi:10.1038/s41467-018-03909-2

Monroy, B. Y., Tan, T. C., Oclaman, J. M., Han, J. S., Simó, S., Niwa, S., . . . Ori-McKenney, K. M. (2020). A combinatorial MAP code dictates polarized microtubule transport. *Developmental Cell, 53*(1), 60-72.e4. doi:10.1016/j.devcel.2020.01.029

Moriwaki, T., & Goshima, G. (2016). Five factors can reconstitute all three phases of microtubule polymerization dynamics. *The Journal of Cell Biology, 215*(3), 357-368. doi:10.1083/jcb.201604118

Muroyama, A., Seldin, L., & Lechler, T. (2016). Divergent regulation of functionally distinct γ-tubulin complexes during differentiation. *The Journal of Cell Biology, 213*(6), 679-692. doi:10.1083/jcb.201601099

Nirschl, J. J., Magiera, M. M., Lazarus, J. E., Janke, C., & Holzbaur, E. L. F. (2016). A-tubulin tyrosination and CLIP-170 phosphorylation regulate the initiation of dynein-driven transport in neurons. *Cell Reports, 14*(11), 2637-2652. doi:10.1016/j.celrep.2016.02.046

Nogales, E., Wolf, S. G., & Downing, K. H. (1998). Structure of the alpha beta tubulin dimer by electron crystallography. *Nature, 391*(6663), 199-203. doi:10.1038/34465 53

O'Rourke, B. P., Gomez-Ferreria, M. A., Berk, R. H., Hackl, A. M. U., Nicholas, M. P., O'Rourke, S. C., . . . Sharp, D. J. (2014). Cep192 controls the balance of centrosome and non-centrosomal microtubules during interphase. *Plos One, 9*(6), e101001. doi:10.1371/journal.pone.0101001

Orth, J. D., Loewer, A., Lahav, G., & Mitchison, T. J. (2012). Prolonged mitotic arrest triggers partial activation of apoptosis, resulting in DNA damage and p53 induction. *Molecular Biology of the Cell, 23*(4), 567-576. doi:10.1091/mbc.E11-09-0781

Park, S. H., & Blackstone, C. (2010). Further assembly required: Construction and dynamics of the endoplasmic reticulum network. *EMBO Reports, 11*(7), 515-521. doi:10.1038/embor.2010.92

Pasqualone, D., & Huffaker, T. C. (1994). STU1, a suppressor of a beta-tubulin mutation, encodes a novel and essential component of the yeast mitotic spindle. *The Journal of Cell Biology, 127*(6 Pt 2), 1973-1984. doi:10.1083/jcb.127.6.1973

Pegoraro, A. F., Janmey, P., & Weitz, D. A. (2017). Mechanical properties of the cytoskeleton and cells. *Cold Spring Harbor Perspectives in Biology, 9*(11) doi:10.1101/cshperspect.a022038

Pereira, A. L., Pereira, A. J., Maia, A. R. R., Drabek, K., Sayas, C. L., Hergert, P. J., . . . Maiato, H. (2006). Mammalian CLASP1 and CLASP2 cooperate to ensure mitotic fidelity by regulating spindle and kinetochore function. *Molecular Biology of the Cell, 17*(10), 4526-4542. doi:10.1091/mbc.e06-07-0579

Pierre, P., Scheel, J., Rickard, J. E., & Kreis, T. E. (1992). CLIP-170 links endocytic vesicles to microtubules. *Cell, 70*(6), 887-900. doi:10.1016/0092-8674(92)90240-d

Piperno, G., & Fuller, M. T. (1985). Monoclonal antibodies specific for an acetylated form of alpha-tubulin recognize the antigen in cilia and flagella from a variety of organisms. *Journal of Cell Biology, 101*(6), 2085-2094. doi:10.1083/jcb.101.6.2085

Ran, F. A., Hsu, P. D., Wright, J., Agarwala, V., Scott, D. A., & Zhang, F. (2013). Genome engineering using the CRISPR-Cas9 system. *Nature Protocols, 8*(11), 2281-2308. doi:10.1038/nprot.2013.143

Rice, L. M., Montabana, E. A., & Agard, D. A. (2008). The lattice as allosteric effector: Structural studies of alphabeta- and gamma-tubulin clarify the role of GTP in microtubule assembly. *Proceedings of the National Academy of Sciences of the United States of America, 105*(14), 5378-5383. doi:10.1073/pnas.0801155105

Roll-Mecak, A., & McNally, F. J. (2010). Microtubule-severing enzymes. *Current Opinion in Cell Biology, 22*(1), 96-103. doi:10.1016/j.ceb.2009.11.001

Roostalu, J., & Surrey, T. (2017). Microtubule nucleation: Beyond the template. *Nature Reviews. Molecular Cell Biology, 18*(11), 702-710. doi:10.1038/nrm.2017.75

Sanders, Anna A. W. M., & Kaverina, I. (2015). Nucleation and dynamics of golgi-derived microtubules. *Frontiers in Neuroscience, 9*, 431. doi:10.3389/fnins.2015.00431

Schindelin, J., Arganda-Carreras, I., Frise, E., Kaynig, V., Longair, M., Pietzsch, T., . . . Cardona, A. (2012). Fiji: An open-source platform for biological-image analysis. *Nature Methods, 9*(7), 676-682. doi:10.1038/nmeth.2019 54

Sirajuddin, M., Rice, L. M., & Vale, R. D. (2014). Regulation of microtubule motors by tubulin isotypes and post-translational modifications. *Nature Cell Biology, 16*(4), 335-344. doi:10.1038/ncb2920

Slep, K. C., & Vale, R. D. (2007). Structural basis of microtubule plus end tracking by XMAP215, CLIP-170 and EB1. *Molecular Cell, 27*(6), 976-991. doi:10.1016/j.molcel.2007.07.023

Sonnen, K. F., Gabryjonczyk, A., Anselm, E., Stierhof, Y., & Nigg, E. A. (2013). Human Cep192 and Cep152 cooperate in Plk4 recruitment and centriole duplication. *Journal of Cell Science, 126*(Pt 14), 3223-3233. doi:10.1242/jcs.129502

Srayko, M., Kaya, A., Stamford, J., & Hyman, A. A. (2005). Identification and characterization of factors required for microtubule growth and nucleation in the early C. elegans embryo. *Developmental Cell, 9*(2), 223-236. doi:10.1016/j.devcel.2005.07.003

Strome, S., Powers, J., Dunn, M., Reese, K., Malone, C. J., White, J., . . . Saxton, W. (2001). Spindle dynamics and the role of gamma-tubulin in early caenorhabditis elegans embryos. *Molecular Biology of the Cell, 12*(6), 1751-1764. doi:10.1091/mbc.12.6.1751

Sun, X., Shi, X., Liu, M., Li, D., Zhang, L., Liu, X., & Zhou, J. (2011). Mdp3 is a novel microtubule-binding protein that regulates microtubule assembly and stability. *Cell Cycle (Georgetown, Tex.), 10*(22), 3929-3937. doi:10.4161/cc.10.22.18106

Szyk, A., Deaconescu, A. M., Spector, J., Goodman, B., Valenstein, M. L., Ziolkowska, N. E., Kormendi, V., Grigorieff, N., Roll-Mecal, A. (2014). Molecular basis for age-dependent microtubule acetylation by tubulin acetyltransferase. *Cell, 157*(6), 1405-1415. doi: 10.1016/j.cell.2014.03.061

Sweeney, H. L., & Holzbaur, E. L. F. (2018). Motor proteins. *Cold Spring Harbor Perspectives in Biology, 10*(5) doi:10.1101/cshperspect.a021931

Tanenbaum, M. E., Macůrek, L., Janssen, A., Geers, E. F., Alvarez-Fernández, M., & Medema, R. H. (2009). Kif15 cooperates with Eg5 to promote bipolar spindle assembly. *Current Biology, 19*(20), 1703-1711. doi:10.1016/j.cub.2009.08.027

Tas, R. P., Chazeau, A., Cloin, B. M. C., Lambers, M. L. A., Hoogenraad, C. C., Kapitein, L. C. (2017). Differentiation between oppositely oriented microtubules controls polarized neuronal transport. *Neuron, 96*(6), 1264-1271. doi:10.1016/j.neuron.2017.11.018

Terasaki, M., Chen, L. B., & Fujiwara, K. (1986). Microtubules and the endoplasmic reticulum are highly interdependent structures. *Journal of Cell Biology, 103*(4), 1557-1568. doi:10.1083/jcb.103.4.1557

Thawani, A., Kadzik, R. S., & Petry, S. (2018). XMAP215 is a microtubule nucleation factor that functions synergistically with the γ-tubulin ring complex. *Nature Cell Biology, 20*(5), 575-585. doi:10.1038/s41556-018-0091-6

Thyberg, J., & Moskalewski, S. (1999). Role of microtubules in the organization of the golgi complex. *Experimental Cell Research, 246*(2), 263-279. doi:10.1006/excr.1998.4326 55

Tilney, L. G., Bryan, J., Bush, D. J., Fujiwara, K., Mooseker, M. S., Murphy, D. B., & Snyder, D. H. (1973). Microtubules: Evidence for 13 protofilaments. *The Journal of Cell Biology, 59*(2 Pt 1), 267-275. doi:10.1083/jcb.59.2.267

Tovey, C. A., & Conduit, P. T. (2018). Microtubule nucleation by γ-tubulin complexes and beyond. *Essays in Biochemistry, 62*(6), 765-780. doi:10.1042/EBC20180028

Triclin, S., Inoue, D., Gaillard, J., Htet, Z. M., DeSantis, M. E., Portran, D., . . . Théry, M. (2021). Self-repair protects microtubules from destruction by molecular motors. *Nature Materials, 20*(6), 883-891. doi:10.1038/s41563-020-00905-0

Tsuchiya, K., & Goshima, G. (2021). Microtubule-associated proteins promote microtubule generation in the absence of γ-tubulin in human colon cancer cells. *BioRxiv,* doi:10.1101/2021.08.13.456214v1

Tymanskyj, S. R., Yang, B. H., Verhey, K. J., & Ma, L. (2018). MAP7 regulates axon morphogenesis by recruiting kinesin-1 to microtubules and modulating organelle transport. *eLife, 7*, e36374. doi:10.7554/eLife.36374

van der Vaart, B., Manatschal, C., Grigoriev, I., Olieric, V., Gouveia, S. M., Bjelic, S., . . . Akhmanova, A. (2011). SLAIN2 links microtubule plus end-tracking proteins and controls microtubule growth in interphase. *The Journal of Cell Biology, 193*(6), 1083-1099. doi:10.1083/jcb.201012179

Vaughan, K. T. (2005). TIP maker and TIP marker; EB1 as a master controller of microtubule plus ends. *The Journal of Cell Biology, 171*(2), 197-200. doi:10.1083/jcb.200509150

Vinogradova, T., Miller, P. M., & Kaverina, I. (2009). Microtubule network asymmetry in motile cells: Role of golgi-derived array. *Cell Cycle, 8*(14), 2168-2174. doi:10.4161/cc.8.14.9074

Vinopal, S., Cernohorská, M., Sulimenko, V., Sulimenko, T., Vosecká, V., Flemr, M., . . . Dráber, P. (2012). Γ-tubulin 2 nucleates microtubules and is downregulated in mouse early embryogenesis. *PloS One, 7*(1), e29919. doi:10.1371/journal.pone.0029919

Vukušić, K., & Tolić, I. M. (2021). Anaphase B: Long-standing models meet new concepts. *Seminars in Cell & Developmental Biology, 117*, 127-139. doi:10.1016/j.semcdb.2021.03.023

Wade, R. H. (2009). On and around microtubules: An overview. *Molecular Biotechnology, 43*(2), 177-191. doi:10.1007/s12033-009-9193-5

Walczak, C. E., Gayek, S., & Ohi, R. (2013). Microtubule-depolymerizing kinesins. *Annual Review of Cell and Developmental Biology, 29*, 417-441. doi:10.1146/annurev-cellbio-101512-122345

Wang, Z., Wu, T., Shi, L., Zhang, L., Zheng, W., Qu, J. Y., . . . Qi, R. Z. (2010). Conserved motif of CDK5RAP2 mediates its localization to centrosomes and the golgi complex. *The Journal of Biological Chemistry, 285*(29), 22658-22665. doi:10.1074/jbc.M110.105965

Wang, Z., Zhang, C., & Qi, R. Z. (2014). A newly identified myomegalin isoform functions in golgi microtubule organization and ER–Golgi transport. *Journal of Cell Science, 127*(22), 4904-4917. doi:10.1242/jcs.155408

Waterman-Storer, C. M., & Salmon, E. D. (1998). Endoplasmic reticulum membrane tubules are distributed by microtubules in living cells using three distinct mechanisms. *Current Biology: CB, 8*(14), 798-806. doi:10.1016/s0960-9822(98)70321-5

Weisbrich, A., Honnappa, S., Jaussi, R., Okhrimenko, O., Frey, D., Jelesarov, I., . . . Steinmetz, M. O. (2007). Structure-function relationship of CAP-gly domains. *Nature Structural & Molecular Biology, 14*(10), 959-967. doi:10.1038/nsmb1291

Widlund, P. O., Stear, J. H., Pozniakovsky, A., Zanic, M., Reber, S., Brouhard, G. J., . . . Howard, J. (2011). XMAP215 polymerase activity is built by combining multiple tubulin-binding TOG domains and a basic lattice-binding region. *Proceedings of the National Academy of Sciences of the United States of America, 108*(7), 2741-2746. doi:10.1073/pnas.1016498108

Wieczorek, M., Bechstedt, S., Chaaban, S., & Brouhard, G. J. (2015). Microtubule-associated proteins control the kinetics of microtubule nucleation. *Nature Cell Biology, 17*(7), 907-916. doi:10.1038/ncb3188

Wieczorek, M., Urnavicius, L., Ti, S., Molloy, K. R., Chait, B. T., & Kapoor, T. M. (2020). Asymmetric molecular architecture of the human γ-tubulin ring complex. *Cell, 180*(1), 165-175.e16. doi:10.1016/j.cell.2019.12.007

Wiese, C., & Zheng, Y. (2000). A new function for the gamma-tubulin ring complex as a microtubule minus-end cap. *Nature Cell Biology, 2*(6), 358-364. doi:10.1038/35014051

Wloga, D., Joachimiak, E., & Fabczak, H. (2017). Tubulin post-translational modifications and microtubule dynamics. *International Journal of Molecular Sciences, 18*(10), 2207. doi:10.3390/ijms18102207

Wong, Y. L., Anzola, J. V., Davis, R. L., Yoon, M., Motamedi, A., Kroll, A., . . . Oegema, K. (2015). Cell biology. reversible centriole depletion with an inhibitor of polo-like kinase 4. *Science (New York, N.Y.), 348*(6239), 1155-1160. doi:10.1126/science.aaa5111

Woodruff, J. B., Wueseke, O., & Hyman, A. A. (2014). Pericentriolar material structure and dynamics. *Philosophical Transactions of the Royal Society B: Biological Sciences, 369*(1650), 20130459. doi:10.1098/rstb.2013.0459

Woodruff, J. B., Wueseke, O., Viscardi, V., Mahamid, J., Ochoa, S. D., Bunkenborg, J., . . . Hyman, A. A. (2015). Regulated assembly of a supramolecular centrosome scaffold in vitro. *Science (New York, N.Y.), 348*(6236), 808-812. doi:10.1126/science.aaa3923

Wu, J., & Akhmanova, A. (2017). Microtubule-organizing centers. *Annual Review of Cell and Developmental Biology, 33*, 51-75. doi:10.1146/annurev-cellbio-100616-060615

Wu, J., de Heus, C., Liu, Q., Bouchet, B. P., Noordstra, I., Jiang, K., . . . Akhmanova, A. (2016). Molecular pathway of microtubule organization at the golgi apparatus. *Developmental Cell, 39*(1), 44-60. doi:10.1016/j.devcel.2016.08.009

Xia, P., Liu, X., Wu, B., Zhang, S., Song, X., Yao, P. Y., . . . Yao, X. (2014). Superresolution imaging reveals structural features of EB1 in microtubule plus-end tracking. *Molecular Biology of the Cell, 25*(25), 4166-4173. doi:10.1091/mbc.E14-06-1133 57

Yu, N., Signorile, L., Basu, S., Ottema, S., Lebbink, J. H. G., Leslie, K., . . . Galjart, N. (2016). Isolation of functional tubulin dimers and of tubulin-associated proteins from mammalian cells. *Current Biology: CB, 26*(13), 1728-1736. doi:10.1016/j.cub.2016.04.069

Zhu, F., Lawo, S., Bird, A., Pinchev, D., Ralph, A., Richter, C., . . . Pelletier, L. (2008). The mammalian SPD-2 ortholog Cep192 Regulates Centrosome biogenesis. *Current Biology, 18*(2), 136-141. doi:10.1016/j.cub.2007.12.055

Zhu, X., & Kaverina, I. (2013). Golgi as an MTOC: Making microtubules for its own good. *Histochemistry and Cell Biology, 140*(3), 361-367. doi:10.1007/s00418-013-1119-4

Zupa, E., Liu, P., Würtz, M., Schiebel, E., & Pfeffer, S. (2021). The structure of the γ-TuRC: A 25-years-old molecular puzzle. *Current Opinion in Structural Biology, 66*, 15-21. doi:10.1016/j.sbi.2020.08.008

Layman's Summary

Microtubules are highly dynamic structures that function as the highways of the cell, allowing motor proteins to use them as tracks to distribute their cargo. Microtubules are hollow, tube-like structures formed through the lateral association of building blocks, called 'tubulin dimers.' These microtubules are inherently unstable, constantly switching between phases of growth and shrinkage caused by the addition and loss of their building blocks. Together, many microtubules form a dense and organized structure to apply their function throughout the cell. These microtubules can assemble spontaneously in cells; however, this spontaneous assembly is energetically unfavorable. Therefore, cells have developed specialized locations that promote microtubule nucleation, called microtubule-organizing centers (MTOCs), including the Golgi-apparatus and centrosome. Cells have evolved a specialized 'microtubule template' called γ-TuRC to promote microtubule nucleation at these MTOCs. Following their nucleation, a broad array of regulatory proteins bind to microtubules and shape the microtubule network as the cell requires. This is of great importance during, for example, the preparation of cell division, where the microtubule network is shaped into a 'mitotic spindle,' essential for the proper segregation of chromosomes. These factors that associate with the microtubules are collectively called microtubule-associated proteins, or MAPs. This research focuses on one particular MAP, namely CLASP, that prevents microtubules from shrinking and, therefore, stabilizes them. Previous studies have shown how CLASP is implicated in many aspects of regulating the microtubule network, such as promoting microtubule nucleation at MTOCs, tethering, and stabilizing the free ends of microtubules at the Golgi-apparatus, and stabilizing microtubules at their growing ends. Moreover, CLASP is involved in repairing damaged microtubules by incorporating new tubulin dimers at the damaged sites.

In this study, we used cells thoroughly depleted of CLASP, where CLASP is almost entirely removed. In these cells, the microtubule network is way below proper density and organized mainly from the centrosome. Therefore, we set out to find the mechanistic link between the lack of CLASP and the reduction in microtubule density. We found that removing CLASP results in lower microtubule nucleation from the Golgi, cytosol, and centrosome. Interestingly, we show a significant reduction in the microtubule nucleation template, γ-TuRC, at the centrosome. However, our results highlight how the removal of γ-TuRC does not yield the same reduction in microtubule density that we observe in the absence of CLASP. Moreover, we show that removing the centrosome in cells lacking CLASP results in an even more substantial reduction in microtubule density and organization, that to our knowledge, has not been observed before. This further reduction perturbed the proper distribution and organization of different organelles throughout the cell, revealing a potential critical microtubule number required for correct organelle distribution. In summary, we show the essential role of CLASP in regulating the microtubule density, owing to its varied roles in microtubule stabilization and nucleation.